الجمهورية الجزائرية الديمقراطية الشعبية

République Algérienne Démocratique et Populaire

Ministère de L'Enseignement Supérieur et de la Recherche Scientifique

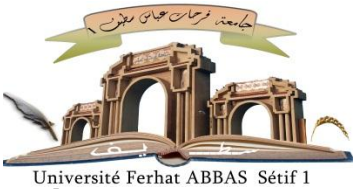

UNIVERSITÉ FERHAT ABBAS - SETIF1

FACULTÉ DE TECHNOLOGIE

THESE

Présentée au Département d'Electrotechnique

Pour l'obtention du diplôme de

DOCTORAT EN SCIENCES

Option: Réseaux Electriques

Par

MOUASSA Souhil

THÈME

Optimisation de l'écoulement de puissance par les méthodes non-conventionnelles dans les réseaux électriques intelligents (Smart Grid)

Soutenue le **01 Juin 2021**. devant le Jury**:**

GHERBI Ahmed	Professeur	Univ. de Ferhat Abbas Sétif 1	Président
SLIMANI Linda	Professeur	Univ. de Ferhat Abbas Sétif 1	Directeur de thèse
JURADO Francisco	Professeur	Univ. de Jaén Spain	Co-Directeur
RADJEAI Hammoud	Professeur	Univ. de Ferhat Abbas Sétif 1	Examinateur
BETKA Achour	Professeur	Univ. de Mohamed Khider Biskra	Examinateur
ARIF Salem	Professeur	Univ. de Amar Telidji Laghouat	Examinateur

Juin 2021

الجمهورية الجزائرية الديمقراطية الشعبية

PEOPLE'S DEMOCRATIC REPUBLIC OF ALGERIA

MINISTERY OF HIGHER EDUCATION AND SCIENTIFC RESEARCH

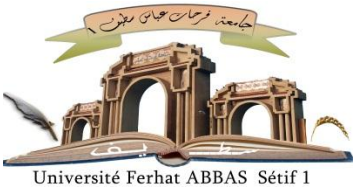

UNIVERSITY OF FERHAT ABBES - SETIF 1 – UFAS (ALGERIA)

FACULTY OF TECHNOLOGY

A thesis presented to the Faculty of Technology

Department of Electrical Engineering

in fulfilment of the requirement for the degree of

DOCTOR of SCIENCE

in Electrical Engineering

Presented by

MOUASSA Souhil

Thesis Title:

Optimal power flow solution with non-conventional methods in smart grids

Approved: **01 June 2021**

GHERBI Ahmed	Professor	Univ. of Ferhat Abbas Sétif 1	Chair of committee
SLIMANI Linda	Professor	Univ. of Ferhat Abbas Sétif 1	Supervisor
JURADO Francisco	Professor	Univ. of Jaén Spain	Co-Supervisor
RADJEAI Hammoud	Professor	Univ. of Ferhat Abbas Sétif 1	Examiner
BETKA Achour	Professor	Univ. of Mohamed Khider Biskra	Examiner
ARIF Salem	Professor	Univ. of Amar Telidji Laghouat	Examiner

June 2021

Certificate of Approval

This is to certify that the research work presented in this thesis, entitled "Optimal power flow solution with non-conventional methods in smart grids" was conducted by Mr. Souhil Mouassa, Univ/Setif 1 and Jaen/ISB under the supervision of Prof. Slimani Linda (Tarek Bouktir) and Francisco Jurado. No part of this thesis has been submitted anywhere else for any other degree. This thesis is submitted to the Department of Electrical Engineering, University Ferhat Abbas-Sétif 1, Algeria and Universidad de Jaén, Spain in the partial fulfilment of the requirement for the degree of Doctor of Science in the field of Electric Power System.

Souhil Mouassa Signature: _____

Examinations Committee

……	……..
Prof. Dr SLIMANI Linda Supervisor, University of Ferhat Abbas Setif 1 SETIF	Prof. Dr GHERBI Ahmed Chairman, University of SETIF
……	……..
Prof. Dr JURADO Francisco Co-Supervisor, University of Jaen SPAIN	Prof. Dr BETKA Achour Examiner, University of Mohamed Khider Biskra
……	……..
Prof. Dr RADJEAI Hammoud Examiner, University of Ferhat Abbas Setif 1 ALGIERS	Prof. Dr ARIF Salem Examiner, University of Amar Telidji Laghouat ALGIERS

Author's Declaration

This is to certify that M. Souhil Mouassa, Univ/Sétif-1June01,2021...../ISB under the supervision of Pr. SLIMANI Linda (Tarek Bouktir), conducted the research work presented in this thesis, entitled “Optimal power flow solution” with non-conventional methods in smart grids. No part of this thesis has been submitted anywhere else for any other degree. This thesis is submitted to the Department of Electrical Engineering, University Ferhat Abbas-Sétif 1, Algeria, in the partial fulfilment of the requirement for the degree of Doctor in Science in the field of Electric Power System.

Date: _____ Signature

Souhil MOUASSA

……

Certificate

It is certified that Souhil Mouassa, SET/.....-.....-...../ISB has carried out all the work related to this thesis under my supervision at the Department of Electrical Engineering, Ferhat Abbas University of Setif 1, Algeria and the work fulfils the requirement for award of PhD degree.

Date:_____ Supervisor

_____

Dr. SLIMANI Linda (Tarek Bouktir)

Associate Professor

DEDICATION

….dedicate

To the memory of my PhD Supervisor Pr., Dr. Tarek BOUKTIR, which I cannot forget him, his patience, motivation, immense knowledge and loving of scientific research.

*To my wonderful Parents **Tayeb** and **Taous** and to my beloved Wife with my daughter Meriem*
To my wonderful uncle Ahmed MOUASSA, Hydraulics Engineer
My Family members for their continuous support and encouragement

كَلِمَة وَفَاءْ

أهدي هذا العمل إلى روح أستاذي الغالي البروفيسور **طارق بوكثير** عليه رحمة الله الواسعة، الذي لم تكتحل للأسف عيناه بثمرة هذا المجهود، إذ وافته المنية والرسالة تشارف نهايتها. لقد كان خير سند لي في مسيرتي العلمية منذ كان هذا البحث مجرد فكرة تختمر إلى أن صار مشروعا مكتملا قائما على سوقه. حقا لقد كان نعم الأستاذ المُربِي الفاضِل تَعَلمنَا مِنهُ الكثير الكثير، فلم يذخر في ذلك جهدا بتقديم التوجيهات السديدة والتقْويمات المُفيدة. فَجَزاهُ اللهُ عني خير الجزاء، وجعل الله ثمرة هذا البحث في ميزان حسناته وغفر الله له بكل حرف منه. إِنَهُ سَمِيعً عليم وبالإجابة جدير.

الطالب: سهيل مــواســة

PREFACE

Due to the rapidly developing of electric power system across the world in response to technical, economic and environmental developments, modern power systems often operate proximate to their maximal limits, engendering voltage instability risks in electric grid. On the other hand, excessive penetration of renewable energy sources into electrical grids may lead to many problems and operational limit violations, such as over and under voltages, active power losses and overloading of transmission lines, power plants failure, voltage instability risks and users discomfort. These problems happen when the system exceeds maximal operational capability (MOC) limit. In this thesis, firstly, various meta-heuristic optimization techniques have been developed and implemented to deal with different power system problems, such as single and multi-objective optimal reactive power dispatch problem. Since the characteristics of optimal reactive power dispatch (ORPD) in nature non-linear and non-convex and are consisting of mix of discrete and continuous variables; some non-conventional optimization techniques are developed and adopted to deal with discrete ORPD problem in large-scale electric grids.

Technology advancement for green energy and its integration to the electric power system (EPS) has gathered substantial interest in the last couple of decades. Incorporating such resources has proven to reduce power losses and improve the reliability of electrical network. However, hyper-production or hypo-production of these resources in electric grid has imposed additional operational and control issues in voltage-regulation, system stability, and feasibility of solutions. Renewables incorporation into electric grid has led to significant changes in the types of consumption as well as dramatic and direct changes in the needs of optimal planning and operation of electric grids. To assess the suitability of the nonclassical optimization techniques for modern power systems, stochastic optimal power flow (OPF) problem with uncertain reserves from renewable energy sources was studied under different scenarios, including valve pointe effect and gas emission. Simulation results demonstrated that with hybrid generation system we could benefit with 2.4 % per hour cost reduction compared to traditional grid that based only on thermal generations as power sources. In addition, a new application of slim mould algorithm for practical optimal power flow with integration of renewables was conducted on Algerian electricity grid (DZA114-220/60 kV). Different cases were studied, where the feasibility of solutions and all control variables are

deeply discussed. Hence, hybrid generation system is more effective and viable than classical system.

In smart grid, efficient load management can help balance, reduce the burdensome on the electric network, and minimize operational electricity-cost. Robust optimization is a method that is used increasingly in the scheduling of household loads through demand side control. To this end, demand side management (DSM) scheme based on Meta-heuristic optimization techniques is proposed for home energy management system. The main objective behind this study is to adjust the peak demand and offering the total energy required at minimum cost with high quality. More precisely, in order to make consumers aware of their effective and essential contributions to helping the operator system during emergency cases (requests during peak hours). Simulation results showed that the proposed DSM scheme based meta-heuristic algorithms enrolling higher reduction in the total energy cost up to 26% compared to the base case and peak average ratio is curtailed by 55 %. In overall, the obtained results demonstrate significant improvement in energy quality, electric power system security, and notable reduction of peak demand in offering total energy required at minimum cost.

List of Publications

Journal Publications

1. Marcos Tostado-Véliz, **Souhil Mouassa**, Francisco Jurado, "A MILP Optimization Framework for Electricity Tariff-choosing Decision Process of Smart Consumers and Prosumers Considering 'Happy Hour' Tariffs" Accepted for Publication in International journal of electrical power & energy systems. 2021.

2. Fateh Slama, Hammoud Radjeai1, **Souhil Mouassa**, Aissa Chouder "New algorithm for energy dispatch scheduling of Grid-connected solar photovoltaic system with battery storage system" Electrical Engineering & Electromechanics Journal. Emerging source citation index. 2021.

3. **Souhil Mouassa**, F. Jurado, T. Bouktir, Muhammad AZ Raja "Novel Design of Artificial Ecosystem Optimizer for Large-scale Optimal Reactive Power Dispatch Problem with application to Algerian Electricity Grid", Neural Computing and Applications—2020.

4. **Souhil Mouassa**, T. Bouktir, F. Jurado "Scheduling of Smart Home Appliances for Optimal Load Management in Smart Grid Using an Efficient Harris-hawks Optimizer ".Optimization and Engineering—2020- DOI: 10.1007/s11081-020-09572-1.

5. **Souhil. Mouassa**, Tarek. Bouktir. "Multi-objective ant lion optimization algorithm to solve large-scale multi-objective optimal reactive power dispatch problem" COMPEL - The international journal for computation and mathematics in electrical and electronic engineering, October 2018, Vol. 38, Issue: 1, pp.304-324. DOI: 10.1108/COMPEL-05-2018-0208.

6. **Souhil Mouassa**, Tarek Bouktir "Ant lion optimizer for solving optimal reactive power dispatch problem in power systems" Engineering Science and Technology, an International Journal - Elsevier-May 2017 Vol. pp. 20 885–895.
   DOI: org/10.1016/j.jestch.2017.03.006.

7. **Souhil Mouassa**, Tarek Bouktir "Artificial Bee Colony Algorithm for Solving Economic Dispatch Problems with Non-Convex Cost Functions" International Journal of power energy and conversion. Inderscience. DOI.org/10.1504/IJPEC.2017.083211. Scopus-Elsevier.

Conference Proceedings

1. **Souhil Mouassa**, Tarek Bouktir " Artificial Bee Colony Algorithm for Discrete Optimal Reactive Power Dispatch" I4e2, International Conference on Industrial Engineering and Systems Management (IEEE IESM-2015), I4e2, Seville, Spain, October-2015. Doi: 10.1109/IESM.**2015**.7380228.

ACKNOWLEDGEMENT

First, thanks to Allah Almighty who give me strength and confidence to complete this thesis; by the bounty of ALLAH and mercy, I could to achieve this work. After that, I would like to express my sincere gratitude to my Supervisor, Professor **Tarek BOUKTIR** that has passed away in November 29, 2020. May Allah forgive him, raise his ranks, exalt his status, and grant him the highest degrees in Jannah, for invaluable direction and supervision work and his support, encouragement throughout my PhD studies. Really, I cannot forget him; he was very lively, friendly, smiley character and sympathetic person with all categories.

I would like to express my gratitude and thanks to Professor Francisco JURADO from Universidad de Jaén, who guided me with patience and dedication during last two years. He encouraged me to grow up and explore my potential. I really appreciate all the time he devoted to discussing all the topics of this dissertation. A special thanks to Dr. Lucian TOMA from Polytechnic University of Bucharest, for his invaluable discussion and bright comments on research Gate. I learned from him that research is a rigorous matter with a great breadth of applications and possibilities. I would like to pay a bundle of thanks to my colleague Professor, Hamza Houassine from Bouira University for his continuous support, bright advices and encouragements to realize this modest work. I am greatly thankful to the chairperson of the scientific committee of department Prof, Hamou Nouri for all administrative steps, his advices and assistance after death of supervisor to defending this thesis.

I am also thankful to my friends and colleagues here at the Department of Electrical Engineering, University of Sétif 1 and there at Bouira, Chlef and Jaén Universities.

I would like to thank committee members, Prof. Gherbi Ahmed and Prof. Hamoud Radjiea from University of Sétif 1, Prof. Arif Salem from University of Amar Telidji Laghouat, and Prof. Betka Achour from University of Biskra for their valuable and constructive comments. Finally, special thanks addressed to my parents, who encouraging me when everything seemed weak. Without their love and caring, I will be a drifting empty bottle.

Sincerely
Souhil Mouassa
2021

Table of Content

List of figures

List of Tables

List of Abbreviations

Acronyms

AEO	Artificial Ecosystem-Based Optimization
AGSO	Adaptive Group Search Optimization Algorithm
ALO	Ant Lion Optimizer
ANOVA	Analysis Of Variance
ARCBBO	Adaptive Real Coded Biogeography-Based Optimization
BA	Bat Algorithm
BBO	Biogeography-Based Optimization
BCS	Best Compromise Solution
CLPSO	Comprehensive Learning PSO
CPP	Critical-Peak-Price
CPVEIHBMO	Chaotic Parallel Vector Evaluated Interactive Honey Bee Mating Optimization
CSO	Chicken-Swarm-Optimization
DE	Differential Evolution Algorithm
DR	Demand Response
DSM	Demand Side Management
EC	Electricity cost
FA	Firefly Algorithm
GEM	Grenade Explosion Method
GSA	Gravitational Search Algorithm
GWO	Grey Wolf Optimizer
HEMS	Home−Energy Management−System
HHO	Harris Hawks Optimization
HNMSFA	Hybrid Nelder-Mead Simplex Based Firefly Algorithm
ICBO	Improved Colliding Bodies Optimization
IPGSPSO	Improved Pseudo-Gradient Search Particle Swarm Optimization
LoT	Length of operation time
MFO	Moth Flam Optimizer
MOALO	Multi-Objective Ant Lion Optimizer
Mod PSO	Modified Particle Swarm Optimisation
MOEPSO	Multiple objective Evolutionary Particle Swarm Optimization
MOORPD	Multi-Objective Optimal Reactive Power Dispatch

MOPSO	Multi-Objective Particle Swarm Optimization
NBA	Novel Bat Algorithm
NSGA-II	(Non-dominated Sorting Genetic Algorithm II)
OGSA	Opposition Gravitational Search Algorithm
OPF	Optimal Power Flow
ORPD	Optimal Reactive Power Dispatch
OSHA	Optimal Power Scheduling of Home Appliances
OTI	Operational Time Intervals
PAR	Peak Average Ratio
PDF	Probability Density Function
PSO	Particle Swarm Optimization
QOTLBO	Quasi-Oppositional Teaching Learning Based Optimization
RES	Renewable Energy Sources
RTP	Real-Time-Price
SG	Smart Grid
SKH	Stud Krill Herd Algorithm
SPSO-TVAC	Self-Organizing PSO with TVAC
SSA	Salp Swarm Algorithm
TLBO	Teaching–Learning-Based Optimization
UC	User Comfort
WCA	Water Cycle Algorithm
WOA	Whale Optimization Algorithm

Symbols

P	Active power
Q	Reactive power
S	Line resistance
V	Bus voltage magnitude
δ	Bus phase angle
R_l	Resistance reactance
X_l	Line reactance
Y	Admittance matrix
P_{loss}	Real Power loss / Active power losses
δ_{ij}	The voltage angle difference between bus i and bus j
θ_{ji} /V_{Gi}	The phase angle of term F_{ji} / voltage magnitude for generator at bus i

N_{PV}, N_{PQ}	The number of *PV* and *PQ* buses respectively
G_k	Conductance of k^{th} branch connected between bus *i* and *j*
$V_i, V_j / V_{L,N_{PQ}}$	Voltage magnitude of bus *i* and *j*/Voltage magnitude for load bus *i*
$\left\|Y_{ij}\right\| / \ S_i$	The elements of bus admittance matrix/apparent power flow of branch *i*
$P_{D,i} / Q_{D,i}$	The active/reactive, load consumption at bus *i*
P_{Gi} / Q_{Gi}	The active/reactive power generation at bus *i*
$P_{L,N_{PQ}}, Q_{L,N_{PQ}}$	The active and reactive power at each load bus
$V_i^{\max}, V_i^{\min}$	The maximum and minimum bus voltage magnitude at bus *i*
$Q_{Gi}^{\min}, Q_{Gi}^{\max}$	The minimum and maximum value of power generation at bus *i*
$T_k^{\max} / T_k^{\min}$	The maximum/minimum tap ratio of k^{th} tap changing transformer
$Q_{Ci}^{\min}, Q_{Ci}^{\max}$	The minimum and maximum VAR injection limits of shunt capacitor banks
$S_i^{\max}$	The maximum apparent power flow limit of branch *i*
NB / *NTL*	The number of buses in the test system/number of transmission lines
NLB / *NG*	The number of load buses/The number of generators buses
NT / *NC*	The number of the transformer taps /number of shunt capacitor banks
$\lambda_V, \lambda_Q, \lambda_I$	The penalty factors
$X_i^{\lim}$	The limit value of the dependent variables $V_i^{\lim}$, $Q_i^{\lim}$, and $S_i^{\lim}$
$X_i^{\max} / X_i^{\min}$	The maximum/minimum limit of state variables
$L(t)$	Energy-consumption of all appliances at time slot *t*,
$E_{a,t}^{price}$	Electricity-price at any time interval *t*,
$E_{interru}$	Energy consumed by interruptible appliances,
$E_{shiftable}$	Energy consumed by non-interruptible appliances,
E_{fixed}	Energy consumed by fixed appliances,
φ_{app}	Power rating of ( ) appliance,
t	Time-slot,
IN	Group of interruptible appliances,
$X(t)$	Status of appliances OFF\ON,
X_{fixed}^{app}	State of fixed appliances OFF\ON,
$X_{Shiftable}^{app}$	State of shiftable appliances OFF\ON,

X_{in}^{app}	State of interruptible-appliances OFF\ON,
φ_{in}^{t}	Power-rating of interruptible-appliances,
$\varphi_{Shiftable}^{t}$	Power-rating of shiftable appliances,
φ_{fixed}^{t}	Power-rating of fixed appliances,
L_{total}^{Sched}	Total-load scheduled per 24-h,
$L_{total}^{Unsched}$	Total-load unscheduled during 24-h,
C_{total}^{Sched}	Total-cost scheduled per 24-h,
C_{total}^{USched}	Total-cost unscheduled during 24-h,
X_{fixed}^{app}	State of fixed appliances OFF\ON,
$X_{Shiftable}^{app}$	State of shiftable appliances OFF\ON,
t_{α}	Start time of appliance
t_{β}	End time of appliance

Chapter 1

INTRODUCTION

1.1. Overview of the Thesis

Due to the constant expansion of the configuration of modern power systems (loads, lines, generators, etc.), and the urgent need to use more efficient elements and procedures and environmental concerns, the power system is currently subject a rapid transformation through the application of different types of strategies to reduce power losses in transmission lines. Optimal planning energy imports from multiple sources, increase energy efficiency in the presence of rapidly growing energy demand with the assurance of economic viability, and the reliability improvement against grid outages is a must, in modern power systems. Consequently, the traditional electric grid could no longer cope with this increase in global consumption, so it needs to evolve to become a smart electricity grid in order to correct some major shortcomings.

Smart Grid is a concept in which the infrastructure of pre-existing power grids is upgraded with the integration of several technologies such as distributed generation, dispatch loads, demand response programs, communication systems and storage devices operating in mode network-connected or isolated. These electric grids upgrades aim to improve energy quality and system security, and reduce the environmental impact, allowing consumers to play an important role in load balancing by their contribution to generate, transport, distribute and consume energy in efficient ways.

The smart grid is an electric grid that attempts to intelligently predict and respond to the behavior and actions of all consumers of electrical energy, providing reliable, economical and sustainable electrical services. In other words, it is a vision of future technology for the electrification of rural zones. In short, there is no universal definition of smart grid, but there are some concomitant features in the definitions or simply defined as an ‘intelligent’ grid [1].

The smart grid has three economic objectives: improve reliability, reduce peak demand and offering the total energy required at minimum cost with high quality. To achieve these objectives, various technologies have been developed and integrated into the electric grid.

Peak load is one of the main factors of risk in the AC transmission systems. Due to the untimely variation of energy demand throughout the day and year, it is more likely that some

generation plants will operate in extremely critical situations in an effort to meet the demand, which may affect: [2]

- Voltages instability in which in turn causes voltage collapse,
- Increase in active power losses,
- Increase in the total cost of production, (producer / consumers), which threatens the social and individual welfare of subscribers.
- Network security constraints.

In order to mitigate these risks, optimal power flow (OPF) analysis should be considered when planning and real-time operation of power grids. Unlike static planning, where the calculation of the static optimal power flow may no longer be important, in dynamic analysis, real-time tools are of great importance to cope with changing consumption.

OPF is one the important tools in the area of operation and control of modern power system, since with each variation in load demand, a set of optimal settings of control variables are updated with complying of grid constraints (hard and soft) to maintain a balance between supply and demand. Generally, that operation is performed each 15 minutes. Meanwhile, if the system constraints leave its allowable limits, emergency measures must be applied to drive the operating state of the network away from the points of insecurity.

In the last decade, with the emergence of unconventional optimization techniques (meta-heuristic techniques), and deregulation of electricity markets along with integration of renewable energy sources (RES), OPF studies becomes more complex and need a special effort to define optimal planning and operations management of electric power system. In this context, development new and efficient strategies to deal with this problem, is necessity. Further, this challenge has attracted wide attention in academia and research communities, especially with advent of computational intelligence which has also gained enormous popularity within the scientific and engineering communities due to its ability to solve hard problems.

This thesis is mainly based on the development of new and efficient artificial intelligence techniques for evaluating and continuous control of installed power in an effort to balance the load during peak hours and to improve the planning of the power generated from the whole electric system (thermal power stations, wind and solar generators (smart Grid). More importantly, the feasibility of findings obtained in this study may be recommended even with practical power system.

1.2. Problem statement

Optimal power flow calculation (automated load control) in the fields of modern power grid operation and planning is becoming increasingly more important. Classical optimal of power flow has been based only on thermal generators, which consume mainly fossil fuels. At this end, it is often difficult to use conventional optimization methods due to the lack of flexibility to cope with stochastic optimal power flow problem, especially in the practical electric grids. The calculus of optimal power flow with the presence of renewable energy sources (RES) is a very difficult problem due to their intermittent nature. The biggest issue facing operating with hybrid generation system is that renewable energy generators could not be scheduled in the same manner to the conventional ones due to their intermittent nature.

In addition, Large-scale integration of renewable energy sources (RES) into power grids is very challenging issue for system operators, since the climatic factors such as solar irradiation and wind speed are uncertain.

The fulfilling results are encouraging, but not very effective due to the complex nature of the OPF problem. Furthermore, these methods typically face the difficulties of identifying optimal solutions, especially when it comes to solve complex conflicting objectives in the large-scale or a real-sized electric power grid. In this context, choosing a right optimization approach for a specific problem is also a challenge. In addition, optimal planning energy via an optimal scheduling of a hybrid power generation system (Thermal generator+WG+PV) may effectively facilitate various missions of electric power system operator, brought many benefits to prosumer including the reliability against grid outages, quality and efficiency of the energy produced, ultimately reducing total generation electricity cost.

In the last two decades, many optimization methods have been employed to define the optimal control variables of the single / multi-objective dynamic problem of power flow with and without incorporation of RES, to obtain a good performance in the evaluation of the analysis and operation of power grids. The achieved results have been encouraged but not very effective due to the complex nature of the OPF problem. Furthermore, these methods typically face the difficulties of identifying optimal solutions, especially when it comes to solve complex conflicting objectives in the large-scale or a real-sized power grid particularly for large-scale power systems. In this context, choosing a right optimization approach for a specific problem is also a challenge.

Demand side management (DSM) is one of the most important aspects in smart grids and micro-grids which include programs of demand response (DR) and energy efficacy (EE). Also, it has an important part in minimizing the gap between supply and demand. This is can be adjusted by introducing load flexibility instead of only making adjustments on production levels, which reduces dependency on electricity expensive imports during peak hours. Consequently, the electricity prices requested will be very reasonable, which is keeping up consumers' loyalty. However, application of these programs for improving load control, while ensuring the security of system is still a challenge nowadays. Various optimization algorithms have been applied for demand side management schemes and the results exhibit better results due to its flexible nature allowing the implementation of load models according to the lifestyle of individuals in an effort to maximize comfort of users. At the end of this work, efficient power scheduling in smart homes using unconventional optimization techniques considering two pricing schemes is conducted.

1.3. Major contributions of the Thesis

The main contributions of this dissertation can be summarized in the following points:

- Different nature-inspired optimization algorithms were proposed to deal with different single aims optimal reactive power dispatch (ORPD) formulations in large-scale power systems. ALO and AEO algorithms are the two bright techniques that provide competitive results with other existing ones in the literature.

- The proposed non-conventional optimization methods have been extended to solve mixed-integer optimization problems with discrete variables, which reflect real nature of variables. We have also employed multi-objective ant lion optimization (MOALO) algorithm to solve large-scale multi-objectives optimal reactive power dispatch test system, (IEEE 300-bus).

  - Acknowledging the evolution of smart grid, some new approaches and formulations are proposed for solving OPF and ORPD problems incorporating stochastic renewable sources. To this end, a modified version of slime mould algorithm to solve optimal power flow problem incorporating stochastic wind and solar power is presented. Furthermore, superiority of feasible solutions constraint handling method is merged with artificial ecosystem optimization (AEO) algorithm.

- Unconventional optimization techniques based demand side management (DSM) scheme is developed for the home energy management system. The framework may define an optimal electric load curve which aims at minimizing the electricity bill while shift all peak-loads to off-peak hours.

1.4. Outline of the Thesis

The outline of this thesis is aptly listed with the chart in Figure 1.1 Chapter 2 introduces a thorough literature review on the meta-heuristic algorithms applied in the research work and optimization problems that have been resolved in electric power system. Chapter 3 describes the optimal reactive power dispatch (ORPD) study, followed by Single ORPD and muti-objective ORPD solutions using newly meta-heuristics optimization algorithms considering large-scale test system as well practical electrical network. Classical OPF study and a new version of slime mould algorithm to obtain OPF solutions with application to practical electric grid incorporating renewable generators sources are provided in Chapter 4. Efficient power scheduling in smart homes using a novel artificial ecosystem optimization technique considering two pricing schemes is described in Chapter 5**.** The conclusion and future-works are discussed in Chapter 6.

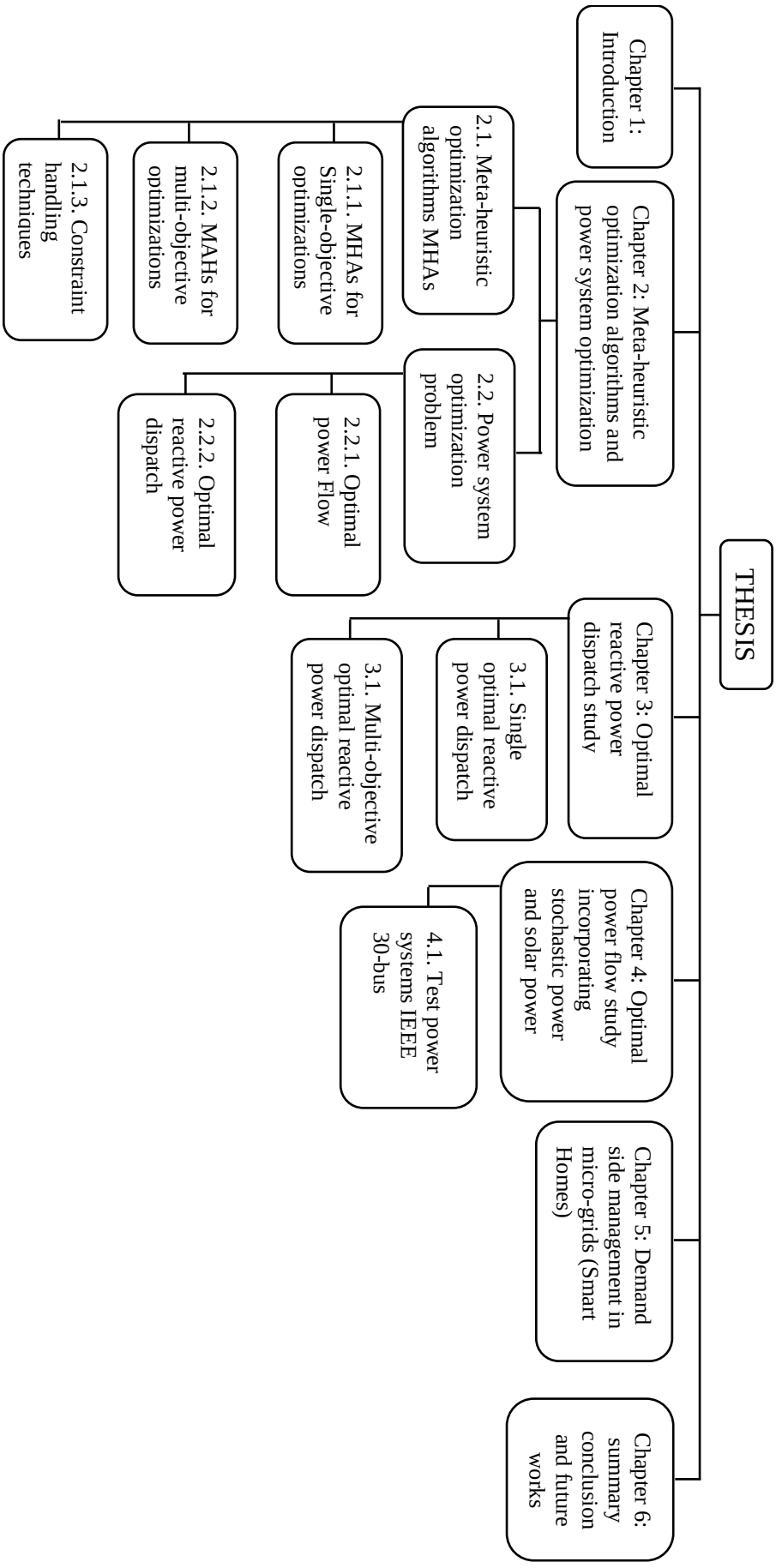

Figure 1.1 Outline of the thesis

Chapter 2

META-HEURISTIC OPTIMIZATION ALGORITHMS AND POWER SYSTEM PROBLEMS

2.1. Meta-heuristic optimization algorithms

"Optimization" is selecting inputs of a physical system that will lead to the best possible outputs. Its process is to find the best possible solution that corresponds to the maximum or minimum value of an objective-function (OF). Optimization is useful with the presence of limits or constraints restricting used variables. The need for optimization creates from the determination of making decisions in various applications so that are not costly, but efficient and optimal. The optimization has paramount importance in the topics of scientific research, engineering and finance as well is intrinsic software of human-life and activity. The optimization operation may cover a single-objective or multi-objectives. With single-objective optimization, the process is devoted to find only one optimal solution so that a defined objective function is minimized or maximized. However, in case of multi-objective optimization, optimization process is charged to find a set of optimal solutions instead of one solution.

Meta-heuristic algorithms (MHAs) have been very popular in last two decades for solving engineering optimization problems. These algorithms are inspired from evolution, swarm, biology and physics. In the last decade, numerous nature-inspired optimization algorithms have been applied to solve complex engineering works, we focuses only on recent published algorithms in this thesis such as ABC [3], BA [4], NBA [5], GWO [6], ALO [7], MFO [8], WOA [9], HHO [10], AEO [11] algorithms for single-objective function and on MOALO, MODA for multiple-objective function for optimization problems. The third section shows two famous constraint-handling methods are penalty method and superiority feasible solutions approach. The definitions and literature review on some power system optimization-problems are presented in the section 2.2.

2.2. Meta-heuristic algorithms for single-objective optimization

During of my preparation of this thesis, there is a huge exploration of characteristics nature-inspired optimizer techniques. Ant lion optimizer (ALO) [7] is one of these techniques, which considered as an efficient and powerful population-based stochastic search technique for solving constrained engineering optimization problems over continuous search-space. In short time, ALO algorithm was applied to a huge number of optimization problems due to its positive advantages: easy to implement, flexible, scalable, and has a good balance between exploration and exploitation. Recently, it has been applied to a huge number of optimization problems. It has many advantages: easy, scalable, flexible, and have a great balance between exploration and exploitation.

2.2.1. Ant Lion optimization (ALO) algorithm

In the last five years ago, ALO algorithm evolved as an efficient and powerful population based stochastic search technique for solving constrained engineering optimization problems. It has been applied to a large number of optimization problems in summary. A review study of ALO algorithm and its improved versions is presented at [12] [13].

The ALO algorithm mimics the hunting behavior of ant lions, i.e., the interaction between predator (ant lions) and prey (ant). The different steps that describe the relationship between ant-lions and ants are depicted in [14]. Like all other insects in nature, ants can easily detect the location of food by using a stochastic movement. This behavior is expressed mathematically by the following equations:

$$X\ (\mathrm{t}) = \left[0, cumsu\left(2r\left(t_1\right)-1\right), cumsu\left(2r\left(t_2\right)-1\right), ..., cumsu\left(2r\left(t_n\right)-1\right)\right] \qquad (2.1)$$

where $X\ (\mathrm{t})$ is the random walks of ants, n is the max_iterations, t is the step of random walk, and $r(t)$ is a function defined as follows:

$$r(t) = \begin{cases} 1 & if\ \ rand > 0.5 \\ 0 & if\ \ rand < 0.5 \end{cases} \qquad (2.2)$$

where, rand is a randomly generated number uniformly distributed in the range of [0, 1].
The following steps describe the five main phases in hunting technique of ant lions

a) random walk of ants

In every step of optimization, ants update their positions b_i to a random walk search equation 2.1. To ensure that all the positions of ants are inside the boundary of the search

space, they are normalized by using the following expression:

$$X_i^t = \frac{\left(X_i^t - a_i\right) \times \left(d_i^t - c_i^t\right)}{\left(b_i - a_i\right)} + c_i^t \tag{2.3}$$

Where a_i ,b_i are respectively the minimum and maximum of random walk corresponding of i^{th} variable. c_i^t, d_i^t : are respectively indicated the minimum and maximum of i^{th} variables at t^{th} iteration.

b) ***Trapping in ant-lions traps***

The following equations describe the effect of ant-lions traps on random walks of ants:

$$c_i^t = Antlion_j^t + c^t \tag{2.4}$$

$$d_i^t = Antlion_j^t + d^t \tag{2.5}$$

c) ***Building traps***

During optimization, the ALO use the roulette wheel selection operator, to choose antlions based on their fitness. This strategy gives more chance for antlions to traps prey.

d) ***Sliding ants against toward antlion:***

According to the aforementioned mechanisms, antlions are able to construct traps proportional to their fitness and the ants move near to the centre of pit. Once antlions catch an ant in trap, they will shoot the sand outward the middle of the trap. This mechanism mathematically modelled as follow.

$$c^t = \frac{c^t}{I} \tag{2.6}$$

$$d^t = \frac{d^t}{I} \tag{2.7}$$

I is a ratio, with $I = 10^{w\frac{t}{T}}$, t is the current iteration and w is the constant which is defined as follows:

w= 2 when $t > 0.1T$, w= 3 when $t > 0.5T$, w= 4 when $t > 0.75T$, w= 4 if $t > 0.9T$, w= 5 when $t > 0.95T$).

e) ***Catching preys and rebuilding the traps***

The catching the ants by predator and rebuilding the pit in order to catch new prey can be described with the following equations.

$$Antlion_j^t = Ant_i^t, \ \ if \ \ f\left(Ant_i^t\right) > f\left(Antlion_j^t\right) \tag{2.8}$$

where $Antlion_j^t$ is the j^{th} position of the selected antlion at iteration *t* and Ant_i^t is the position of the selected ant at iteration *t*.

f) *Elitism:*

Elitism is one of the most important characteristic of evolutionary algorithms. In ALO algorithm, at any iteration the best antlion obtained (solution) is saved as elite. Since the elite is the fittest antlion which is able to guide the movements of the remaining ants along the iterations. The elitism mechanism mathematically described as follows.

$$Ant_i^t = \frac{R_A^t + R_E^t}{2} \tag{2.9}$$

where R_A^t is the random walk around the ant-lion is selected by using the roulette wheel at t^{th} iteration, R_E^t is the random walk around the elite at t^{th} iteration, and Ant_i^t denote the position of i^{th} ant in t^{th} iteration.

In order to return ALO able to solve Multi-objective problem, equation 2.8, should be modified due to the nature of multi-objective problems by the following equation

$$Antlion_j^t = Ant_i^t, \ \ if \ \ f\left(Ant_i^t\right) \prec f\left(Antlion_j^t\right) \tag{2.10}$$

where $Antlion_j^t$ denotes the position of the selected j^{th} antlion at the t^{th} iteration and ant_i^t denotes the position of the i^{th} ant at the t^{th} iteration.

Another modification is for the selection of random antlions and elite. Authors utilized a roulette wheel and eq. 2.9 to select a non-dominated solution from the archive. The pseudo-code of MOALO is shown in Fig 2.1 below:

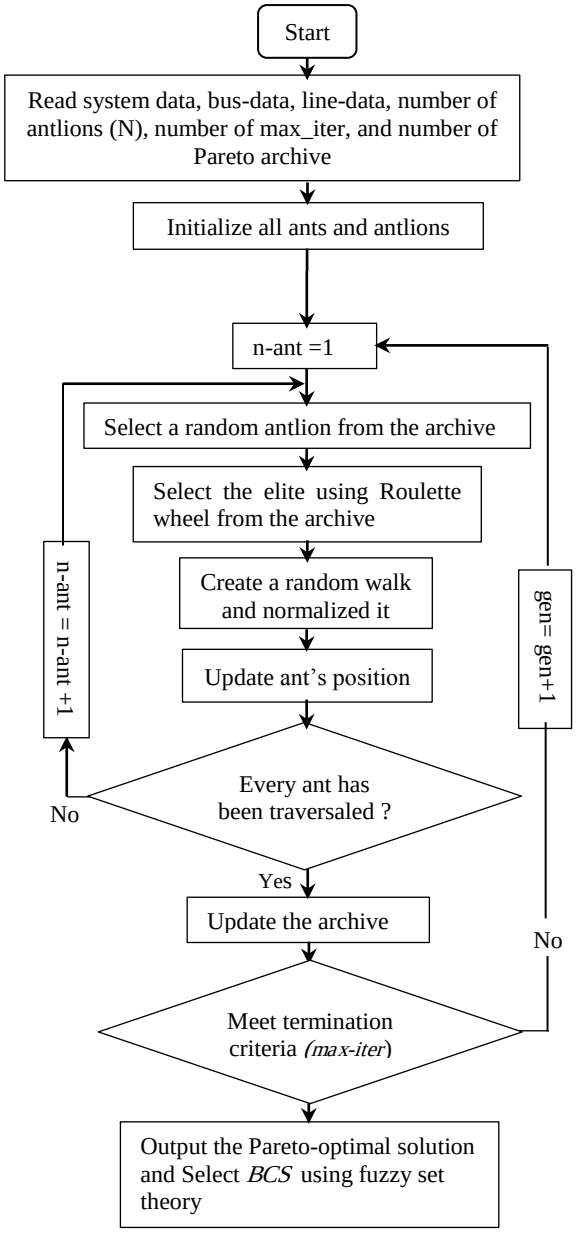

Figure 2.1 Flowchart MOALO

2.2.2. Artificial ecosystem optimization (AEO) algorithm

Artificial Ecosystem Optimization (AEO) algorithm is a novel nature-inspired technique was first proposed by *Weiguo Zhao* et al., in [11] to efficiently tackle engineering optimization problems. An ecosystem is a group of living organisms such as animals, people, and plants live together in a particular area and it explains the correlation between them. Ecosystem is first divided to two parts: (i) living and (ii) non-living organisms. The living organisms include people, animals, plants, and bacteria and the non-living organisms include water, lawn, and sunlight. AEO is a population-based algorithm that mimics the behaviors of living organisms in nature, production, consumption, and decomposition processes on the surface of earth. The principal effort to maintain ecological equilibrium in an ecosystem is the flow of

energy and the food resources. An ecosystem classifies the living elements into three distinct groups of organisms, namely, producers, consumers, and decomposers. The first group is the producer, which is the plants (An autotroph) since they produces its own energy through photosynthesis. The second is the consumer like animals, which depend on the other organisms which depend on one another either by its family or from the producer for gets energy. The third class of living organisms is the decomposers, which include most bacteria and fungi. Once an organism is died, the decomposers starts to break down the remain matter and converting them into a novel energy in form of water, minerals, and carbon dioxide. Then, these simple molecules serve as feeding source to the producers to again produce sugar and oxygen through photosynthesis and the process of cycle will be repeated.

The three kinds of living organism interact in many ways with each other in forming a food chain, which can guarantee a stable flow of energy within it. Some organisms feed from other ones proportional to the level of force and draws the path of energy in an ecosystem.

In an ecosystem, food web is made up of numerous interconnected and overlapping food chains, which describes a different ways of interconnections between them. These chains sorts the organisms based on their energy level. The producers are located usually at the up of the web food, whereas, the consumers are positioned at a higher level than what it consumes and they considered the most complicated one compared with others organisms. Figure 2.2 depicts the path of energy in an ecosystem. From the Fig 2.2 it can be seen that organism with higher energy is assigned at the top of food grid whereas the lower energy organism is located at the bottom of the food grid.

As noted earlier, main principle of operation of AEO algorithm is based on three phases, involving production, consumption, and decomposition. The first operator is the Producers. The first operator is carry to enhance the balance between the diversification and intensification abilities, while consumption was dedicated to exploitation process and the decomposition to ameliorate the exploitation process in this AEO. For each population, there is only one producer and one decomposer, while the remaining ones are the consumers. The fitness value is represented to the energy level of the each associated individual in a population. In other words, the individuals are sorted in a descending order according to their energy. Figure 2.3 show a graph theory of feeding behavior by omnivores.

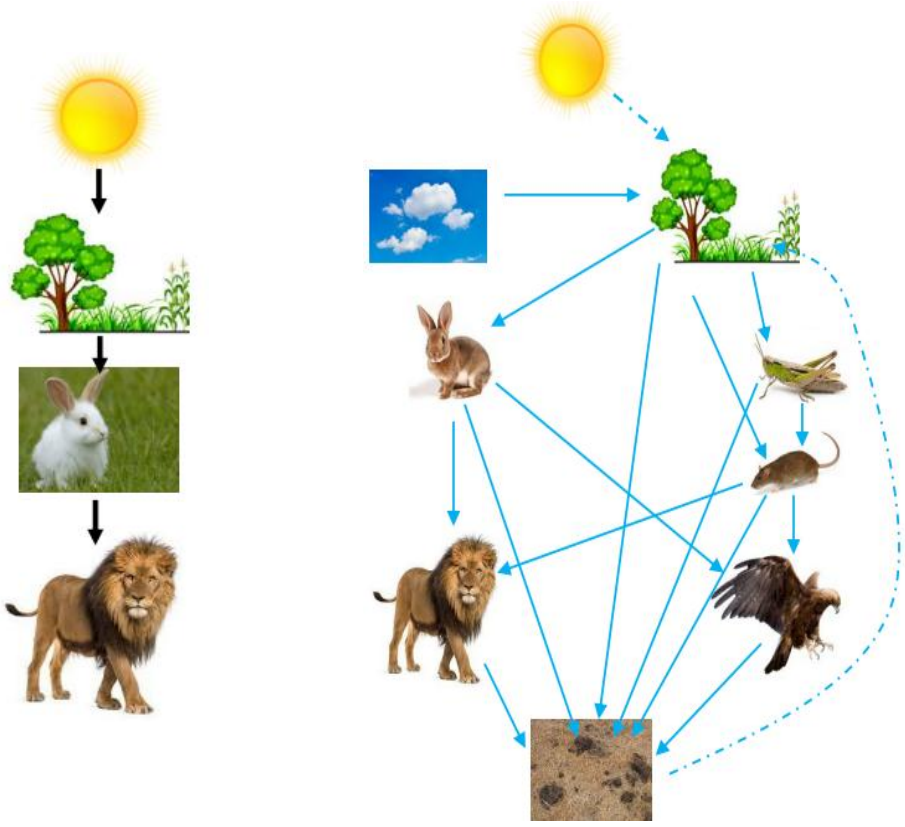

(A) (B)

Figure 2.2. Flow energy in an ecosystem; (a) food chain, (b) food web

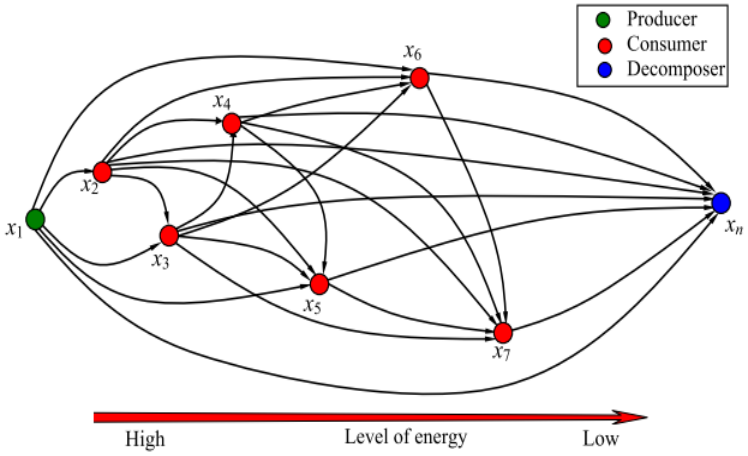

Figure 2.3. A graph theory for an ecosystem based on the AEO

A) **production**

In this ecosystem, the candidates that have worst value of the fitness function are classified as the best ones, while the worst candidates correspond to the higher fitness value. The worst candidate x_1 associates with the highest energy level (Producer), whereas the best candidate x_n attached with lowest level of energy (Decomposer). The rest of candidates of the population are consumers: x_2, x_5 defined by herbivores, x_3, x_7 omnivores and x_4 with x_6 are carnivores. [11]

The producer combines carbon dioxide, water, sunlight, and organic matter resulted from the decomposer to produce their food (energy) as sugar and oxygen. In this algorithm, the producer associated with lowest fitness value is updated according to their limits in search space. Based on this update, the other individuals in the population will try to update their positions. In AEO, the production operator generates a new individual to replace the old one between the better candidate (x_n) and a randomly generated candidate (X_{rand}) in the search space. Mathematically can be expressed as follows:

$$X_1(t+1)=(1-a)X_n(t)+a.X_{rand}(t) \tag{2.11}$$

$$a=\left(1-\frac{iter}{max\_iter}\right)r_1 \tag{2.12}$$

$$X_{rand}=lb+r(ub-lb) \tag{2.13}$$

where ub and lb are the upper and lower bounds of control variables, respectively.

B) **Consumption**

Once the production operator is attained, the consumers start to perform the consumption operator in order to obtain food energy. In this phase, the consumers eat other consumer of a low energy or a producer or the both together. Afterwards, the Levy flight concept is utilized in an effort to improve the exploration patterns. The Levy flight usually mimics the real searching mechanism of animals. A consumption parameter treated by the Levy flight concept is defined as follows:

$$C=\frac{1}{2}\frac{v_1}{|v_2|} \tag{2.14}$$

$$v_1 \sim N(0,1),\ \ v_2 \sim N(0,1) \tag{2.15}$$

Where $N(0,1)$ is a normal distribution of {mean = 0 and standard deviation (std =1)}. This consumption factor is mainly very helpful for each living consumers for gaining the food by utilizing the possible hunting techniques.

If a consumer is randomly picked as herbivore, it will eat only the producers. This behavior is expressed mathematically by eq. 2.16,

$$X_i(t+1)=X_i(t)+C.(X_i(t)-X_1(t)),\quad i\in[2,.....,n] \tag{2.16}$$

In case of a consumer is picked as a carnivore, then it will eat only consumers having lower fitness value. This behavior can be represented by eq. 2.17,

$$\begin{cases} X_i(t+1) = X_i(t) + C.\left(X_i(t) - X_j(t)\right), i \in [3,.....,n] \\ j = randi\left([2i-1]\right) \end{cases} \quad (2.17)$$

With the last case of consumption phase, when the consumer is considered as an omnivore, then it will be able to eat other consumers having higher energy level and producers too. This behavior is given by eq. 2.18,

$$\begin{cases} X_i(t+1) = X_i(t) + C.\left(r_2\left(X_i(t) - X_j(t)\right)\right) + (1-r_2)\left(X_i(t) - X_j(t)\right) \\ i \in [3,.....,n] \\ j = randi\left([2i-1]\right); \quad r2 = rand \end{cases} \quad (2.18)$$

c) **Decomposition**

Decomposition parameter is more important for the AEO, which act after each dies of any individual in the population to decay the residues of that individual. To gain an approximate mathematical model of this behavior, some parameters such as the decomposer factor D, weight variables e and h are considered.

To gain an approximate mathematical model of this behavior, some parameters such as the decomposer factor D, weight variables e and h are considered. Then, each individual X_i updates its coordinates based on the decomposer X_n and through predefined parameters: such as D, e, and h based on the following equations:

$$X_i(t+1) = X_n(t) + D.\left(e.X_n(t) - h.X_i(t)\right), \; i = 1,.....,n \quad (2.19)$$

$$D = 3u, \; u \sim N(0,1) \quad (2.20)$$

$$e = r_3.randi\left(2i-1\right) \quad (2.21)$$

$$h = 2.r_3 - 1 \quad (2.22)$$

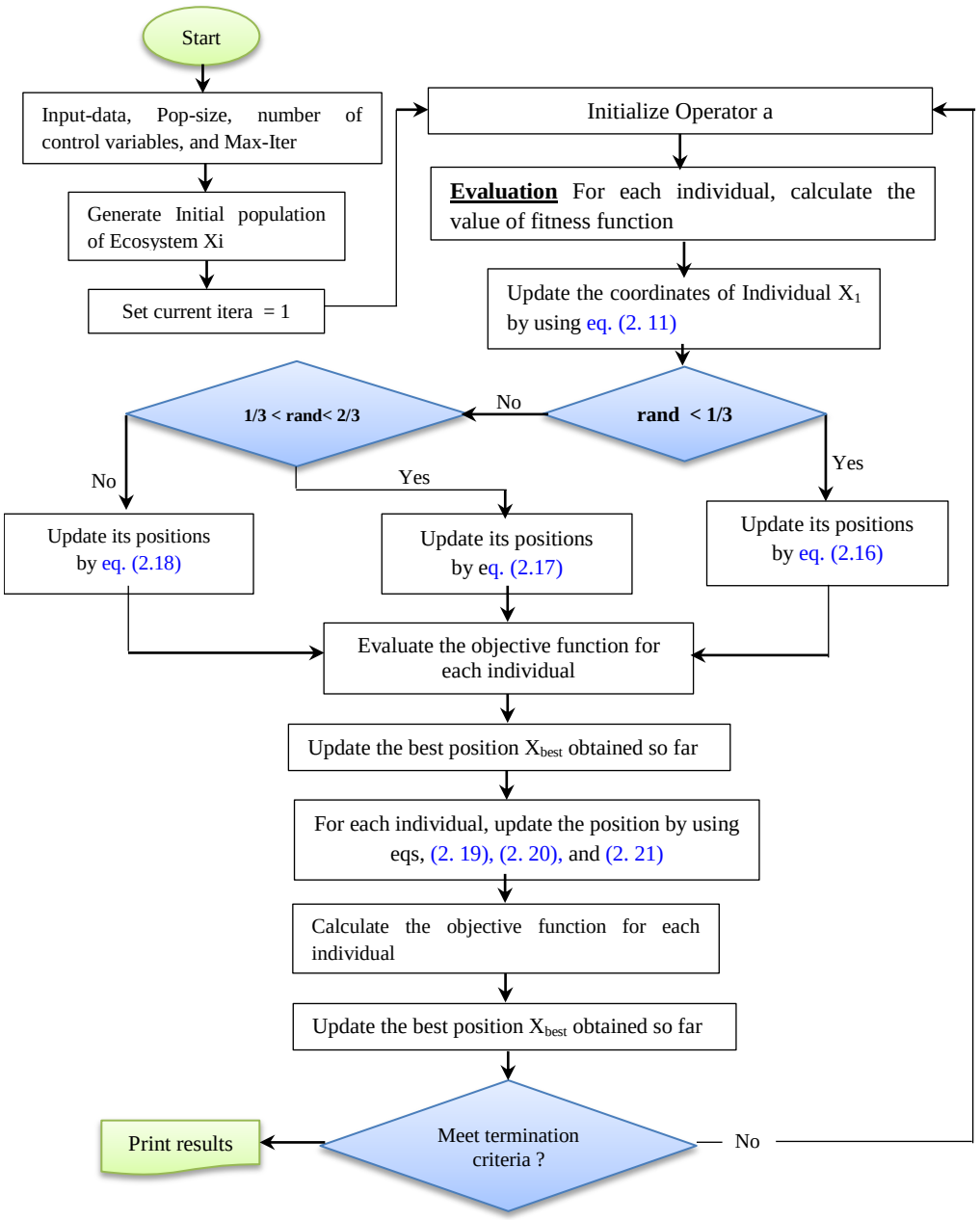

Figure 2.4. Flowchart of AEO algorithm

The optimization process in AEO starts with a population of individuals in which randomly generated into research space, then at each iteration the first individual (producer) updates its coordinates according to the eq. 2.11, while other candidates in the population will hence try to update their coordinates based on its own best consumer by using eqs. 2.12, 2.13, and 2.14, except in the case of the individual having a highest fitness value, then the position of that individual will be updated by using eq. 2.16. All aforementioned updates are repeated until a terminal criterion is satisfied. Finally, the optimal or near-optimal solution that corresponds to a best individual found so far is memorized.

2.2.3. Harris Hawks Optimization (HHO) Algorithm

HHO is a novel nature-inspired optimization algorithm proposed by *Ali Asghar Heidari* et al., in [9] to efficiently tackle engineering optimization problems. Harris' hawks are considered one of the most intelligent predators bird in the world. The collaborative behavior of Harris hawks is very noticeable because they can construct cooperative hunting during foraging activities in the open woodlands and semi-desert habitats. This behavior supports hawks in acquiring more energy throughout pursuing of the target prey. The idea of HHO algorithm is inspired through the hunting tactics and the cooperative behavior of hawks in nature. Furthermore, to that, this algorithm is motived by the hawks' intelligent updating mechanism in the hunting process, which can assist the local optima avoidance. In addition, HHO can always carry out a good balance between exploration and exploitation phases. However, the original algorithm occasionally fails to find a high- quality global solution in some real-world problems.

In HHO algorithm, the position vector of each Harris-hawk is defined for searching in a *D*-dimensional space, where *D* is number of control variables. The population of HHO X will defined of N_H hawks with *D*-dimensions. Therefore, the vector of population is made by an N × D-dimensional matrix, as given in eq. 2.23.

$$X_i = \begin{bmatrix} x_1^1 & x_2^1 & \cdots & x_D^1 \\ x_1^2 & x_2^2 & \cdots & x_D^2 \\ \vdots & \vdots & & \vdots \\ x_1^N & x_2^N & \cdots & x_D^{N_H} \end{bmatrix} \tag{2.23}$$

HHO consists of three searching phases. Firstly is the exploration-phase which is the process of observing and monitoring the desert site to explore the prey. In HHO, the prey is the target location of all Harris-hawks. Hence, the position of predator is recalculated through eq. 2.24,

$$\vec{X}(t+1) = \begin{cases} X_{rand}(t) - r_1 . \left| X_{rand}(t) - 2 r_2 . X(t) \right| & q \geq 0.5 \quad (a) \\ \left(X_{rabbit}(t) - X_m(t) \right) - r_3 . \left(lb + r_4 . (ub - lb) \right) & q < 0.5 \quad (b) \end{cases} \tag{2.24}$$

where $\vec{X}(t+1)$ indicates the position-vector of a predators in the next-iteration, $X_{rabbit}(t)$ is the position of prey (rabbit) and $X(t)$ indicates the current position vector of hawks, $r_1, r_2, r_3, r_4,$ and q are the random number between 0 to 1, which were updated in each iteration, $lb.$ and ub are respectively the lower and upper limits of variables. Although r_3 is determined randomly, it has to be different from r_4 to avoid the similar distribution schemes.

$X_{rand}(t)$ is the hawk which randomly selected from the novel-population, and $X_m(t)$ is the average position of the present-population of hawks.

Eq. 2.24 shows that the Hawks updates its position based in either respect of perching strategy that focuses on the position of other family members and rabbit, or on random position created inside group home range.

$X_m(t)$ is the average-position of the present-population of hawk which is expressed as follows:

$$X_m(t) = \frac{1}{N_H}\sum_{i=1}^{N} X_i(t) \tag{2.25}$$

Where the location of each hawk is denoted by $X_i(t)$ in the i^{th} generation and N_H is the total-number of hawks.

The second phase summarizes a passing from exploration- to exploitation-. It is evident that prey's energy will be decreased through the process of hunting. This behavior is modeled by eq. 2.26.

$$E_n = 2E_0\left(1-\frac{t}{T}\right) \tag{2.26}$$

where E_n denotes the escaping-energy of the rabbit, T indicates max-number of iterations, and E_0 is the primary-state to energy of prey. E_0 Randomly varies in [-1, 1].

The steps of transition can be briefly summarized by the following two points: For the condition of ($|E| \geq 1$) the exploration step occurs and for the condition of ($|E| < 1$), the exploitation step happens.

The last-step is that of exploitation-phase. The predators start to launch the surprise attacks using some tactics, whereas, the preys usually attempt to escape from such dangerous situations. Four steps are suggested to explain the attacking scheme. Here, r is refers to all possible chance of escape from hawks.

Step 1: Soft besiege is happened when $r \geq 0.5$ and $|E| \geq 0.5$. This behavior can be represented by eq. 2.27

$$\begin{cases} X(t+1) = \Delta X(t) - E.\left|J * X_{rabbit}(t) - X(t)\right| \\ \Delta X(t) = X_{rabbit}(t) - X(t) \\ J = 2\left(1-r_5\right) \end{cases} \tag{2.27}$$

where $\Delta X(t)$ indicates to available distance between the position-vector of prey and the present position in iteration t, J indicates the random leap-strength of the prey (rabbit) during the course of escaping procedure−which randomly changes with iteration to feign the real movement of rabbit, r_5 is a random number $\in[0, 1]$.

Step 2: Hard-besiege is occurred if r ≥ 0.5 and | E | < 0.5. In this step, the target-prey becomes wearied and its energy exhausted due to the intensive jumps during escapement process. Meanwhile, the Harris hawks encircle the target using a hard besiege. This behavior is expressed mathematically by eq. 2.28:

$$X(t+1)=X_{rabbit}(t)-E\left|\Delta X(t)\right| \tag{2.28}$$

Step 3: Soft-besiege with progressive prompt dive are realized if the following conditions are met: |E| ≥ 0 .5 and r <0.5. The target have enough energy to escape from claws of hawks, however, the hawk should persists to perform further move which is modeled by eq. 2.29.

$$Y = X_{rabbit}(t)-E\left|J * X_{rabbit}(t)-X(t)\right| \tag{2.29}$$

$$Z = Y + S \times LF(D) \tag{2.30}$$

where D is the problem dimension and S is a random vector of $1\times D$ size, LF define the levy-flight function, which is estimated by the following equation: [9]

$$LF(x)=0.01\times\frac{\mu.\sigma}{|\upsilon|^{1/\beta}},\quad \sigma=\left(\frac{\Gamma\left((1+\beta)\times sin\left(\frac{\pi\beta}{2}\right)\right)}{\Gamma\left(\frac{1+\beta}{2}\right)\times\beta\times 2^{\frac{\beta-1}{2}}}\right)^{\frac{1}{\beta}} \tag{2.31}$$

where μ and ν are two randomly values with a range of [0. 1], β is a constant equal to 1.5. Thus, as the last step used to update the positions of hawks in the present phase is executed by eq. 2.32

$$X(t+1)=\begin{cases} Y & if \quad F(Y)<F(X(t)) \\ Z & if \quad F(Z)<F(X(t)) \end{cases} \tag{2.32}$$

Step 4: Hard besiege with progressive rapid dives is done if | E | < 0 .5 and r < 0.5. In this stage, the prey exhausted all of its energy so that the chance for escaping becomes small or almost-null. This step is given by eq. 2.33.

$$X(t+1)=\begin{cases} X_{rabbit}(t)-E\left|J*X_{rabbit}(t)-X_{m}(t)\right|, & if \quad F(Y)<F(X(t)) \\ Y+S\times LF(D), & if \quad F(Z)<F(X(t)) \end{cases} \tag{2.33}$$

2.3. Multi-objective optimization problems

As mentioned earlier, multi-objective formulation framework is able to find the Pareto optimal set in just one run. The objectives in multi-objective optimization are often conflicting, which means one objective cannot be bettered without worsening one or more other objectives.

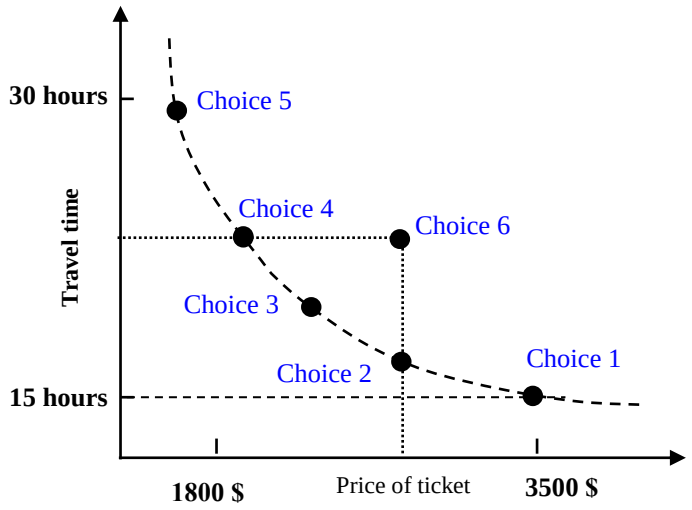

Figure 2.5. Presentation of decision-making process in buying flight-Ticket

In this schematic, the best solution (the extreme solution) for each objective functions required a compromise solution(s). Hence, chose of a solution based only on the one objective may be prohibitive. Herein, we present an experience of buying a flight-ticket for travel where the price of ticket and time of travel are decision-making criteria. The black points 1, 2, 3, 4, 5, and 6 in Fig. 2.5 represent different choices for flying between two cities: Kuala Lumpur and New York.

Its recognized generally in flight companies that a travel time is bind to the waiting time or connecting flight at transit, i.e., if the waiting time is long the price may be lower and vice versa. Choice "1" is the most expensive with ticket price of 3500 $, but with the least travel of 15 hours, meanwhile, the cheapest ticket of 1800 $ with travel time of 30 hours if one prefer choice "5". Here the decision making process of flight booking is not a single objective of either price or travel time.

The traveller has limited choice since he should compromise between price and travel time. If select "choice 2" instead of first choice, he will be affect his comfort by spending more time in transit but he saving a ticket price. Again, if the traveller selects fourth choice instead of third

one, he has to shell out more money for buying the ticket, but he gaining few hours. Then, if we move along available choices 1, 2, 3, 4, and 5, we cannot better one objective without worsening the other. However, the situation is not the same for sixth choice; this is because he is completely losing. In preference, he can select second choice at the same price with lesser travel time or fourth choice of same travel duration at a lesser price. Regarding to the choice six can be improved on both the objectives. The points 1, 2, 3, 4, and 5 are named as Pareto optimal front relative to the Italian scientist. Pareto-solutions are also known as non-dominated solutions where improvement of one objective leads to degradation of at least one other objective. The solution given by choice 6 is a dominated solution. This example is adopted only for two objective functions, but for multi-objective optimization problem, there are more than two objectives. The general mathematical formulation of multi-objective optimization is expressed as follows:

$$\text{Min } \mathbf{F} = \textit{Minimize}\left\{F_1(X),F_2(X),.....,F_n(X)\right\} \tag{2.34}$$

$$\text{Subject to: } \begin{cases} g_j(X)=0, & j=1,2,.....,M \\ h_j(X)\le 0, & j=1,2,.....,N \end{cases} \tag{2.35}$$

where **F** is vector of objective functions. *n* is the number of objective function, $g_j(X)=0$, $h_j(X)\le 0$ are equality and inequality constraints, respectively. The constraints denote the feasible region and vector *X* at feasible region reflects a feasible solution.

2.3.1. Pareto optimality

In multi-objective optimization (MOO) solution provides a set of control (decision) variables, $X=(X_1,X_2,X_3,.....,X_n)$, in the set of all vectors F which provides optimal objective functions eq. 2.34, while satisfying equality and inequality constraints eq. 2.35. We consider two vectors of solution X_1 and X_2, at least one dominates to other or no solution dominates the other. X_1 is said dominate X_2 if both of the following conditions are met:

$$\textit{(i)} \quad \forall i \in\{1,2\}: F_i(X_1)\le F_i(X_2) \text{ and } \textit{(ii)} \quad \exists j \in\{1,2\}: F_j(X_1)<F_j(X_2) \tag{2.36}$$

The solution X_1 is named the non-dominated solution and the set of the non-dominated solutions form the so-called Pareto front optimal, in which represents the trade-off between the conflicting objectives.

The Pareto optimality means that X is Pareto optimal solution if there is no feasible vector of control variables able to improve at least some objective function without deterioration at the

same time any. In other words, any improvement in a Pareto optimal solution in one objective function must lead to deterioration of at least one other objective.

2.4. Constraint handling (CH) methods

There are several and different constraint handling methods for meta-heuristic optimization in the literature, which can be classified into six categories, as follows:

1) ***Preserving feasible solution method***: The key concept of this approach is to place the solutions into feasible research-space and keeping within by updating process that produces only feasible ones.
2) ***Penalty function method:*** [16] In this technique a penalty terms is added to the objective function once any constraint violation happens.
3) ***Rejection of infeasible solutions***: Also called death penalty, in which rejects any infeasible solution as soon as they are generated. In addition, it has an efficient computational, because with any violate solution, it is assigned a fitness of zero.
4) ***Solution repair method***: in this approach, infeasible solution is repaired with feasible solution to become a valid one, but the approximation process consumes much time. In addition, the repaired solution may be considerably different from originally generated solution.
5) ***Superiority of feasible solutions method*** [17]: This approach is based on the assumption of the superiority of feasible points over infeasible ones.
6) ***Stochastic ranking method***: first introduced by *Runarsson* and *Yao* in 2000 [18]: In this technique a control factor Pf ($0 < P < 1$) is predefined by the user to check a balance between objective optimization value (feasibility) and whole of constraint violation (infeasibility points). The process is to determine whether the objective function value or the all constraint violation is used to rank a solution. The ranking process is performed as follow:

   If both solutions are feasible or rand < Pf , rank is performed only on the objective value. Otherwise, rank is conducted on the constraint violations only.

Since the selecting of the suitable constraint handling method is highly depending on the problem's nature. The problem formulation treating in this dissertation confirm that both of penalty function (PF) method and superiority of feasible solutions (SF) method are more appropriate than other ones. In other words, due to their relative success and the most commonly used ones in the power system optimization.[19] To this context, we give more

detail of these methods, and how to handling with different formulation of OPF and ORPD problems in guarantying the feasibility of solutions.

2.4.1. Penalty function method (PF)

Penalty function method is the simplest and oldest handling technique which transform a constrained problem into an unconstrained one throughout discarding infeasible solutions during the search process even after sufficient number of feasible solutions. Also known as static penalty function method, values of the penalty factors are chosen by trial and error process. Because this method requires proper adjustment of the penalty factors, a small penalty factors over-explores the infeasible region, thus delaying the process of finding feasible solutions, and may prematurely converge to an infeasible solution. On the other hand, large penalty factors may not explore the infeasible region properly, thereby resulting in premature convergence [20]. For this reason, it is preferable to choose the trial to start with the small values of factors until the suitable coefficients will be properly selected that ensure at the same time the convergence rate with feasibility of solution.

Among different formulations of the penalty method, the *Powell-Skolnik* [16] method where incorporates all the constraints with feasibility [21]:

$$\rho(x)=\begin{cases}1+\mu\left[\sum_{j=1}^{N}\max\{0,h_i(x)\}+\sum_{i=1}^{M}|g_i(x)|\right] & \text{if not feasible}\\ f(x) & \text{if feasible}\end{cases} \tag{2.37}$$

Where the constant $\mu>0$ is fixed, so this approach is a static penalty method.

The penalty-based method transforms the objective function $f(x)$ to a modified objective function $\mathrm{F}_{\mathrm{modi}}$ in the following from,

$$\mathrm{F}_{\mathrm{modi}}(x)=f(x)[\text{objective}]+P(x)[\text{Penalty}] \tag{2.38}$$

Where the penalty term $P(x)$ may take different forms, depending on the actual ways or variants of constraint handling techniques. For instance,

$$P(x)=\sum_{i=1}^{M}\mu_i g_i^2(x)+\sum_{j=1}^{N}k_j\max\{0,h_i(x)\}^2 \tag{2.39}$$

Where $\mu_i>0$ and $k_i>0$ are penalty factors. In order to avoid too many penalty factors, a single penalty constant $\lambda>0$ can be used as follows:

$$P(x)=\lambda\left[\sum_{i=1}^{M}g_i^2(x)+\sum_{j=1}^{N}\max\left\{0,h_i(x)\right\}^2\right] \tag{2.40}$$

Where λ is fixed factor, independent of iteration t, this basic form of penalty is the well-known static penalty method. Some studies show that it may be beneficial to vary λ over the course of iterations [22],

$$\lambda=(\alpha t)^{\beta} \tag{2.41}$$

Where $\alpha=0.5$ and $\beta=1.2$

In short, there are other forms of penalty approaches such as adaptive penalty and death penalty.

2.4.2. Superiority of feasible solutions (SF)

This approach was first proposed by Powell and Sklonick (1993) to deal infeasible solutions, afterwards Deb in [23] propose similar technique by eq. 2.42 and transform the equality constraints to inequality constraints with aid of a tolerance factor epsilon ε by using eq. 2.43. Mathematically described as follows:

$$\text{fitness}(x)=\begin{cases} f\left(\vec{x}\right) & \text{if } h_i\left(\vec{x}\right)\geq 0 \quad \forall i=1,2,.....,N \\ f_{worst}+\sum_{i=1}^{N}h_i(x) & otherwise, \end{cases} \tag{2.42}$$

$$\left|g_i(x)\right|-\varepsilon\leq 0 \tag{2.43}$$

where f_{worst} is the objective function value of the worst feasible solution in the population and if there are no feasible solutions in the population, then f_{worst} is set to zero. ε is a tolerance parameter for the equality constraints.

Other mathematical expression of SF method is presented as follows:

$$T_i(x)=\begin{cases} \max\left\{h_i(x),0\right\} & i=1,....,N \\ \max\left\{\left|g_i(x)\right|-\varepsilon,0\right\} & i=N+1,....,M \end{cases} \tag{2.44}$$

Therefore, the aim is to minimize a desired objective function $F_i(X)$ so that the optimal solution subjected to all inequality constraints $T_i(X)$. The overall constraint violation for an infeasible individual is a weighted mean for all the constraints, which is presented as,

$$v_i(x)=\frac{\sum_{i=1}^{N}w_i\left[T_i(x)\right]}{\sum_{i=1}^{N}w_i} \tag{2.45}$$

When we compare two solutions X_i and X_j, X_i is said superior to X_j under the following conditions:

a) A feasible point is preferred over an infeasible one

b) Between two feasible solutions, solution that has a smaller objective value in a minimization case (greater objective value in case of maximization) is preferred.

c) Between two infeasible solutions, the one that has a smaller constraint violation is chosen.

More detail on different constraint-handling techniques for meta-heuristic optimization can be found in [21,24].

2.5. Power system optimization problems

This research work titled as "Optimal power flow solution with non-conventional methods in smart grids". Over the last few decades, some power-system optimization problems have been solved using meta-heuristic methods. This section reports a survey on OPF and ORPD problems available in the literature, which attempted in our research work.

2.5.1. Optimal power flow problem (OPF)

Despite passing more than half of century from its inception, the optimal power flow (OPF) still one of crucial topic among power system research in academia and research communities across the globe due to the intriguing mixed challenges it poses. The OPF can be formulated as a single or a multi-objective problem, it main purpose is minimizing fuel cost, emission, voltage deviation, active power losses in transmission lines, etc. with constraints on generator capability, line capacity, bus voltage and power flow balance. OPF program runs in determining optimal control variables include generated active powers, generators output voltages, transformer tap settings, and VARs of compensation units while the physical system constraints involve load bus voltages, generated reactive powers, thermal limits in transmission line. In short, OPF involves multiple calculations with different variables, where determining optimal solutions while satisfying all imposed constraints at the same time is a challenge that one encounters.

Earlier, conventional optimization methods were used to solve the OPF problem such as Newton method, linear programming, non-linear programming, Quadratic programming and the interior point. The principal disadvantage of these optimization methods is that often trapped in local optima due to the gradient-based search method it utilises. Lack of flexibility

with respect to practical systems, i.e., each method is suit for a specific problem formulation in its proper objectives and/or constraints. They also encounter a huge difficult to set of uncertain and stochastic problems, such as OPF with insertion of renewable generation. A review of these classical methods can be found in *Refs* [25,26]. To overcome the above-mentioned shortages of conventional optimization techniques, several intelligence optimization techniques have been introduced in the field of numerical optimization in last two decades.

The stochastic search techniques of meta-heuristics can efficiently explore the search-space in pursuit of global optima. Intelligence optimization methods are inspired from multiple concepts such as evolution, swarm, biology and physics. Among the earliest stochastic population-based methods proposed to solve OPF were genetic algorithm (GA) [27], evolutionary programming (EA) [28]. In recent years, many meta-heuristic optimization techniques have been applied to the OPF problem. Some standard objectives of OPF were optimized in [29] for different IEEE test systems using moth swarm algorithm (MSA), an effective technique for real-complex optimization problems. Wenlei Bai *et. al.* [30] proposed an improvement on basic artificial bee colony (ABC) algorithm based on orthogonal learning to perform study on OPF. Chaib *et. al*. [31] applied backtracking search optimization algorithm (BSA) to perform OPF calculation with valve-point effect and multi-fuel options in thermal generators. Also, Improved colliding bodies optimization (ICBO) [32] algorithm was proposed to solve a variety of cases OPF problem with complex objective functions, security constraints, prohibited zones and different test systems. Ramzi *et. al* [33] proposed and applied ant lion optimizer (ALO) on different cases study of OPF for practical power system considering static VAR compensator to improve voltage profile. Powell's pattern search method was incorporated in invasive weed optimization (IWO) algorithm to improve exploitation ability of basic IWO technique in [34] and security-constrained OPF incorporating the FACTS device was solved. Proposed modified algorithm was applied on the medium-test systems IEEE 30-bus and IEEE -57 bus. To enhance convergence property and exploration capability of modified Jaya optimization algorithm (MJaya). A quasi-oppositional modified Jaya was suggested in [35] and applied to multi-objective OPF problem. Dynamic adjustment of control parameters in adaptive multiple teams perturbation-guiding Jaya (AMTPG-Jaya) technique [36] showed higher convergence speed and better accuracy than original Jaya for diverse single goal optimum power flow (OPF) forms. Again, however, it applied only on medium-sized test system IEEE 30-bus. Improved social spider optimization algorithm (ISSO) for solving OPF problem was introduced in [37] and applied to optimize

various objectives. Improved version has presented a new updating scheme for movement of spiders, and applied on a larger test system IEEE 118-bus. Salp swarm algorithm (SSA) [38] and its variant hybrid salp swarm (HSSA) algorithm [39,40] have also been popular in finding OPF solutions. Harris Hawks Optimization (HHO) [41] and hybrid Harrison hawk optimization based on differential evolution (HHODE) algorithm [42] have also show promising results for OPF as reported in respective papers. Modified imperialist competitive algorithm (MICA) and teaching learning algorithm (TLA) were hybridized (MICA-TLA) in [43] to improve local search and convergence of original ICA algorithm in finding OPF solutions. From this literature, we can see that either original or the improved version of an algorithm was tried. OPF problem is often solved for many different objective formulations and sometimes are contradicting. In this context, multi-objective formulations for OPF solutions are also available in the literature. One widely used approach to deal with multiple objectives OPF is the weighted sum method in which a predetermined weight point is assigned to each objective. While aforementioned references are mostly dealing with single objective cases. A few approaches based- weighted sum methods are summarized in the following: backtracking search optimization algorithm (BSA) [31], A black-hole-based optimization approach [44], An Enhanced Self-adaptive Differential Evolution [45], Adaptive group search optimization algorithm [46], and differential search algorithm (DSA) [47]. However, weighted sum approach leads to only Pareto solution with a set of weight factors in a full run of the algorithm. In point of view of accuracy, it is obvious a set of solutions with multi-objective algorithms is preferred to a single solution with weighted sum method. Moreover, the above references performed the optimization process with two or more objectives on single or multiple power systems, but they dealt with only thermal generators. However, a modern power system consisting of thermal and wind power and solar generators.

In studying OPF or MOOPF problem, in modern power system, i.e., with incorporation of intermittent sources, there are also a limited number of publications such as *Partha Biswas* et all [48] proposed success history based parameter adaptation technique of differential evolution (SHADE) to solve OPF problem in a system involving renewable power generators. Also, forecasting model is well designed to report renewable power generators outputs. In addition, the feasibility of results were discussed and checked that all control variables fell inside the allowed limits. Thus, findings clearly show the efficacy of the proposed model, but, unfortunately, it was applied only on medium-sized test system, IEEE 30-bus. In another publication [49], *Ehab E.Elattar* proposed modified version of the moth swarm algorithm to solve OPF problem of combined heat and power system with presence stochastic wind farm.

The model is well presented and results were discussion but only for IEEE 30-bus system in which feasibility of solution of large-scale test system IEEE 118-bus were not discussed. As well the application in a real power system is not realized. Zia Ullah et al [50] provide a new hybrid optimization algorithm PPSOGSA for OPF solution considering renewable energy generators. The model of stochastic behavior is based of PDF scheme. The results amply show the superiority of proposed hybrid method against basic PPSO and GSA. Again, however, the algorithm was not examined by applying it to real/ large-sized power system. In Yu-Cheng Chang et al [51], evolutionary particle swarm optimization (EPSO) algorithm was used for solving OPF problem in a wind-thermal power system. The suggested wind model is based on the up-spinning reserves and down-spinning reserves of the production units. Also, EPSO algorithm based proposed model was evaluated only on modified IEEE 30-bus system
A modified cuckoo search optimization technique employed for OPF solution incorporating wind power was proposed in *Chetan Mishra* el al in [52]. The proposed stochastic model of wind generation is based on the Weibull PDF. Again, however, the simulation was also conducted only on standard medium-sized test systems. In summary, optimal power flow study in a network consisting of thermal, wind power generators and photovoltaic (PV) needs further attention.

2.5.2. Optimal reactive power dispatch (ORPD)

Optimal reactive power dispatch (ORPD) solution is the principal key for modern electric grid control, as well as, operation. ORPD is a well-known complex combinatorial optimization problem with nonlinear characteristics. It is a sub-case of optimal power flow (OPF) problem. The principal mission of the ORPD solution is to determine steady condition operation parameters of all electrical equipment's of power system except the power of generators [48]. Efficient adjustment of control variables provide benefits advantages to Electric Power System Operators (EPSO) like help to convey energy to all existing loads at the network with a minimum loss of power while satisfying various physical and operational constraints imposed. Consequently, all electric elements operate under service voltage. Reactive power dispatch cannot be avoided in the system as most of system loads are inductive and elements such as transformers and transmission lines consume reactive power. Principal objective in ORPD is to minimize total real power losses with the basic concept that reactive power flow incurs active (real) power loss. In a typical network, can be achieved by identification of optimal solution of control variables, which consists of generator bus voltages as continuous variables, tap position of tap-changing transformers, and required number of shunt capacitors

as discrete variables. Total voltage deviation of load buses in the grid is also considered as an objective function in ORPD problem. This objective ensures that voltages at load buses are closed to the unit (1 p.u.) with control of reactive power flow. However, this objective does not ensure lowest real power loss of the system. Improvement of voltage stability index is also set an objective in ORPD problem. This objective ensures that provide the sufficient information's about the voltage instability and/or to quantify the vicinity of an electric grid of voltage collapse. This can be achieved by the minimization of voltage stability indicator L-index (L_j) at every bus of the electric network, and consequently the total power system (L-index), basing on information of normal load flow analysis of which the operating range of indicator L is set between 0-1 [53]. Several papers studied the ORPD problem for systems consisting of conventional thermal generators. The recently published of the last decade can be summarized in this section. Basic form stochastic fractal search (SFS) and its modified version (MSFS) [54,55] were applied to optimize ORPD objectives. Gravitational search algorithm (GSA) [56] was employed to propose solutions for ORPD on standard bus systems with conventional generators. The Gaussian bare- bones approach was incorporated in teaching–learning-based optimization (GBTLBO) in [57] in order to balance global searching and increase convergence speed. The hybrid algorithm applied to solve ORPD problem with discrete and continuous control variables in the standard IEEE power systems for reduction in power transmission loss. Gaussian bare-bones water cycle algorithm (GBWCA) in [58], the same philosophy of Gaussian bare bones was infused in water cycle algorithm (WCA). A Novel fuzzy adaptive configuration of PSO was applied in [59] to minimize single-objective functions of ORPD considering large-scale power systems. Also ant lion optimizer (ALO) was proposed in [11] to cope with different objectives of ORPD considering larger test system. A recently surfaced nature-inspired optimization technique called moth flame optimization (MFO) was applied in [12] to minimize single-objective functions of ORPD. *Mohd Herwan Sulaiman et. al*. [60] tried to establish efficacy and robustness of grey wolf optimizer to solve ORPD problem in a standard IEEE test systems. Novel design of fractional particle swarm optimization gravitational search algorithm (FPSOGSA) [61] showed competitive results for solutions of ORPD. Furthermore, a review study on meta-heuristic techniques applied to the ORPD field can be found in [62].

Multi-objective formulation and solutions of ORPD problem has also a part in literature review, in which many published algorithms have been proposed for solving the MOORPD problem. For example, in [63] the authors proposed a modified NSGA-II considering the strategies of controlled elitism and dynamic crowding distance to improve the diversity of

non-dominated solutions. The method was applied on the medium-sized test systems IEEE 30-bus and IEEE 118-bus, but voltage deviation and large-scale test systems were not taken into consideration when validating the technique. An enhanced version of multi-objective PSO to optimize power losses and voltage deviation in power systems was proposed in [64]. However, the reported control variables were outside admissible boundaries because the constraint handling method was not properly introduced. The authors in [65] proposed a new hybrid fuzzy multi-objective evolutionary algorithm (HFMOEA) to solve the complex nonlinear multi-objective ORPD problem. Again, however, the robustness of the algorithm was not tested on a large-scale test system. In [66], an improved version of the MOPSO method was proposed for MOORPD, but the solutions control variables were not discussed. In [67], the authors proposed a chaotic improved PSO-based multi-objective optimization to minimize power losses and the voltage stability index, but it was applied only on medium-sized systems, and in addition, almost all the results of the control variables fell outside the imposed limits. In [68] the authors derived a new multi-objective algorithm called chaotic parallel vector evaluated interactive honey bee mating optimization (CPVEIHBMO) algorithm to solve the MOORPD problem, but the feasibility of dependent variables was not satisfied. In [69] an improved version of the firefly algorithm to solve the multi-objective active/reactive ORPD problem was presented with load and wind generation uncertainties in a standard IEEE 30-bus system. This test system is insufficient however to confirm the consistency of the proposed algorithm. Again, the optimal control variables were not discussed. The formulation and solutions of single and multiple objectives of ORPD problem considering large scale test systems and practical power system are presented in Chapter 3.

2.6. Conclusion

This chapter has presented for the first time basic concepts of optimization term and three recent meta-heuristic optimization algorithms used to evaluate the common power system problems in this research work. Then, some constraints handling techniques employed for control variables treatment are presented. Afterwards, definition of OPF and ORPD problems and its important role in power system field are presented, following by literature review on the meta-heuristic algorithms applied to solve single and multi-objective formulations of optimal power flow (OPF) and optimal reactive power dispatch (ORPD) problems, with critical explanation.

Chapter 3

OPTIMAL REACTIVE POWER DISPATCH STUDY

3.1. Introduction to optimal reactive power dispatch

In recent years, Electric Power System Operators (EPSO) are constantly seeking out new strategies to meet operational planning challenges for reducing power losses and ensuring continuity of services with less damages on electrical equipment's. In the modern power system operation, each variation for demand-load, results a proper adjustment of reactive power generations for keeping the balance between supply and demand with minimum real power loss. Hence, the stability of electric grid is preserved. This is can be accomplished locally by proper reactive power management.

Optimization of reactive power flow in electric grid is a key factor for stable and secure operation as the reactive power supports grid voltage which needs to be maintained within allowable ranges for system reliability. This chapter presents a formulation and solution procedure for single / multi-objective optimal reactive power dispatch (ORPD/MOORPD) problem with practical and large-scale power systems. Active power losses and cumulative voltage deviation of load buses as well as voltage stability index in the electric grid are first independently set as the objective functions of optimization, and then, they are set as conflicting objective functions of optimization. The constraints in ORPD problem are handled using penalty function (PF) handling method. *M.S. Saddique* et. al.[70] assessed the performance of four meta-heuristic techniques like differential evolution (DE), particle swarm optimization (PSO), Novel bat algorithm (NBA) and sine cosine algorithm (SCA) with a status and technological review to ORPD solution considering penalty function method as handling method. We adopt ALO, AEO, NBA algorithms in this study. Simulations results are analysed in detail and the feasibility of solutions were fully verified and discussed.

The rest of the chapter is organized as follows: Section 3.2 covers the problem definition, objectives and mathematical formulation of ORPD problem with the constraints involved. The description of proposed method is presented in Section-2 of Chapter 2. Detailed analyses of results and comparison are performed in section 3.2.4 Section 3.2.5 reveals statistical results and the chapter ends with conclusion in Section-3.3.

3.2. Mathematical models for ORPD study

The mathematical formulation of the ORPD problem is amply described as objective functions and constraints, where these functions are minimized while fulfilling equality and inequality constraints. The general formulation of ORPD is:

$$\text{Min} \quad \text{F} = Minimize\ F_{Obj}\left(x,u\right) \tag{3.1}$$

$$\text{Subject to:} \begin{cases} g\left(x,u\right)=0 \\ h\left(x,u\right)\le 0 \end{cases} \tag{3.2}$$

where $F_{obj}\left(x,u\right)$ is the objective function, $g\left(x,\text{u}\right)$ equality constraints, $h\left(x,\text{u}\right)$ inequality constraints;

x : is the vector of dependent variables, consisting of load bus voltages, reactive power of generators, and transmission lines loading. Mathematically, it is written as follows:

$$x^T = \left[V_L ... V_{L,N_{PQ}}\,,\, Q_{g,1} ... Q_{g,N_{PV}}\,,S_1 ... S_{NTL}\right] \tag{3.3}$$

u: is the vector of control variables or independent variables, comprising the mixed control variables involving voltages of the PV-bus as (continuous variables), transformer tap settings and switching shunt capacitor banks as (discrete variables). Hence, u is written as follows:

$$u^T = \left[\overbrace{V_{g,1} .... V_{g,N_{PV}}}^{\text{continuous}}\,,\overbrace{T_1 .... T_{NT}\,,\, Q_{C1}\ .....,\, Q_{C,NC}}^{\text{Discrete}}\right] \tag{3.4}$$

In this chapter, three different objective functions are considered:

- Minimization of total real power losses;
- Minimization of total voltage deviation (TVD); and
- Minimization of voltage stability index (VSI)

3.2.1. Objective fonctions

In the ORPD, the active power of all generators are fixed and known, except that of the slack-bus. In the power flow study, total generation must be equal to the sum of all demand-loads connected and losses in the grid. Generator connected in the slack bus balances the active power and reactive power flow in the whole of grid.

a) Objective 1: minimization of total active power losses

In general, the ORPD aims to minimize the total real power losses via an optimal adjustment to the control variables of the power system [71]. Mathematically, it is characterized as follows**:**

$$\mathrm{F}_1(x,\mathrm{u}) = \min P_{\mathrm{Loss}} = \sum_{k=1}^{NTL} G_k \times \left(V_i^{\,2} + V_j^{\,2} - 2 \times V_i \times V_j \times \cos\delta_{ij}\right) \tag{3.5}$$

b) Objective 2: minimization of total voltage deviation (TVD)

This objective function is introduced for ensuring the security of electric power system. This case aimed to reduce the load-bus voltages gap resulting from specified value and those obtained from calculations.

$$\mathrm{F}_2(x,\mathrm{u}) = \min VD(x,\mathrm{u}) = Minimize \sum_{i=1}^{Npq} \left|V_i - 1.0\right| \tag{3.6}$$

c) Objective 3: Minimization of voltage stability index (VSI)

Liberalization of energy market lead to increasing demand for electricity, which makes operation of an electric power grids become close to their stability limits. Therefore, the continuous monitoring and control of power system via voltage stability enhancement is necessity in order to get more information on the voltage drops. The operating interval of index L was set in [0, 1] [72] The objective function to be minimized is defined as follow:
where L_j of the j^{th} bus is given by the following expression:

$$L_j = \left|1 - \sum_{i=1}^{N_{PV}} F_{ji} \times \frac{V_i}{V_j} \angle\left\{\theta_{ji} + \left(\delta_i - \delta_j\right)\right\}\right| \quad j = 1,2,...,N_{PQ} \tag{3.7}$$

$$\text{with} \qquad F_{ji} = \left|F_{ji}\right|\angle\theta_{ji}\,,\; V_i = \left|V_i\right|\angle\delta_i \;,\quad V_j = \left|V_j\right|\angle\delta_j \qquad F_{ji} = -\left[Y_1\right]^{-1} \times \left[Y_2\right] \tag{3.8}$$

Y_1, Y_2, Y_3, and Y_4 : are the sub-matrices of the system Y_{bus} obtained after rearranging the *PQ* and *PV*-bus bar parameters as shown in eq. 3.9.

$$\begin{bmatrix} I_{PQ} \\ I_{PV} \end{bmatrix} = \begin{bmatrix} Y_1 & Y_2 \\ Y_3 & Y_4 \end{bmatrix} \times \begin{bmatrix} V_{PQ} \\ V_{PV} \end{bmatrix} \tag{3.9}$$

3.2.2. System-Constraints

The equality and inequality constraints applied on ORPD problem are presented herein.

a) *Equality constraints*: are the power flow equations which are given below:

$$\begin{cases} P_{gi} - P_{di} - \sum_{j=1}^{NB} |V_i| \times |V_j| \times |Y_{ij}| \times \cos\times\left(\theta_{ij} - \delta_i + \delta_j\right) = 0 \\ Q_{gi} - Q_{di} - \sum_{j=1}^{NB} |V_i| \times |V_j| \times |Y_{ij}| \times \sin\times\left(\theta_{ij} - \delta_i + \delta_j\right) = 0 \end{cases} \tag{3.10}$$

b) Inequality constraints represent the limits applied on the following variables.

$$\begin{cases} V_{g,i}^{\min} \le V_{g,i} \le V_{g,i}^{\max}, & \\ Q_{g,i}^{\min} \le Q_{g,i} \le Q_{g,i}^{\max}, & i = 1,2.....Ng \\ V_i^{\min} \le V_i \le V_i^{\max} & i \in NPQ_{bus} \\ T_k^{\min} \le T_k \le T_k^{\max} & k \in NT \\ Q_{Ci}^{\min} \le Q_{Ci} \le Q_{Ci}^{\max} & i \in NC \\ S_l \le S_l^{\max} & l \in NTL \end{cases} \tag{3.11}$$

In this work, the concept of penalty functions is used, where only the violating variables such as $(V_i, Q_G, \text{and } S_l)$ are added to the F_{obj} in order to discard any unfeasible solution obtained during the optimization process. Then, the modified objective function is written as follows:

$$F = F_{obj}(x, \mathrm{u}) + \lambda_V \times \sum_{i=1}^{N_{PQ}} \Delta V_i + \lambda_Q \times \sum_{i=1}^{NG} \Delta Q_i + \lambda_l \times \sum_{i=1}^{NTL} \Delta S_i \tag{3.12}$$

where λ_V, λ_Q, and λ_l are the penalty factors; X_i^{limit} are the limit value of the dependent variables.

$$\Delta V_i = \begin{cases} \left(V_i^{\min} - V_i\right)^2 & \text{if } V_i < V_i^{\min} \\ \left(V_i - V_i^{\max}\right)^2 & \text{if } V_i > V_i^{\max} \\ 0 & \text{if } V_i^{\min} \le V_i < V_i^{\max} \end{cases} \tag{3.13}$$

$$\Delta Q_i = \begin{cases} \left(Q_i^{\min} - Q_i\right)^2 & \text{if } Q_i < Q_i^{\min} \\ \left(Q_i - Q_i^{\max}\right)^2 & \text{if } Q_i > Q_i^{\max} \\ 0 & \text{if } Q_i^{\min} \le Q_i < Q_i^{\max} \end{cases} \tag{3.14}$$

$$\Delta S_i = \begin{cases} \left(S_i - S_i^{\max}\right)^2 & \text{if } S_i > S_i^{\max} \\ 0 & \text{if } S_i^{\min} \le S_i < S_i^{\max} \end{cases} \tag{3.15}$$

3.2.3. Test systems

This chapter considers different test systems involving medium-sized and large-scale test systems to perform selected cases of ORPD and the compare the findings of those cases with previously reported results in the literature.

Table 3.1. A summary of IEEE 30 and IEEE 57 bus test systems

Items	**IEEE 30-bus system** [14]		**IEEE 57-bus system** [64]	
	Quantity	Details	Quantity	Details
Buses	30	See in **[**14]	57	See in **[**64**]**
Branch	41	See in [14**]**	80	See in **[**64**]**
Generator	6	Buses: **1 (swing)**, 2, 5, 8, 11 and 13	7	Buses: **1 (swing)**, 2, 3, 6, 8, 9 and 12
Shunt VAR compensation	9	Buses: 10, 12, 15, 17, 20, 21, 23, 24 and 29	3	Buses: 18, 25 and 53
Transformer with tap changer	4	Branches: 11, 12, 15 and 36	17	Branches: 19, 20, 31, 35, 36, 37, 41, 46, 54, 58, 59, 65, 66, 71, 73, 76 and 80
Control variables	19		33	
Connected load		283.4 MW, 126.2 MVAr		1250.8 MW, 336.4 MVAr
Allowable range for PV bus	24	[0.95 – 1.1] p.u	50	[0.94 – 1.06] p.u.
Base case for P_{Loss}, MW.		5.880		28.46
Base case for VD, p.u.		1.4942		1.2336
Base case for L-index		0.1798		0.3099

Table 3.2. A summary of IEEE 118 and DZ 114 bus test systems

Items	**IEEE 118-bus system** [73]		**DZ 114-bus system** [74]	
	Quantity	Details	Quantity	Details
Buses	118	See in [74]	114	See in [74]
Branch	186	See in [74]	175	See in [74]
Generator	54	Buses: **1 (swing)**, the rest see in Annex	15	Buses: **4 (swing)**, 5, 11, 15, 17, 19, 22, 52, 80, 83, 98, 100, 101, 109 and 111
Shunt VAR compensation	14	Buses: 5, 34, 37, 44, 45, 46, 48, 74, 79, 82, 83, 105, 107 and 110	7	Buses: 50, 55, 66, 67, 77, 89 and 93 [74]
Transformer with tap changers	9	Branches: 8, 32, 36, 51, 93, 95, 102, 107 and 127	16	Branches: 160 −175
Control variables	77		38	
Connected load		4242 MW, 1438 MVAr		3727 MW, 2070 MVAr
Allowable range for PV bus	109	[0.95 – 1.05] p.u	99	[0.90 – 1.10] p.u.
Base case for P_{Loss}, MW.		132.863		67.447
Base case for VD, p.u.		1.43933		3.82
Base case for L-index		0.0694		0.3421

Table 3.3. A summary of large test system IEEE 300

Items	**IEEE 300-bus system** [14]	
	Quantity	Details
Buses	300	See in [58]
Branch	411	
Generator	69	
Shunt VAR compensation	14	See in [75]
Transformer with tap changer	107	
Control variables	190	
Connected load		23525.8 MW, 7787.97 MVAr
Allowable range for load-bus voltage	231	
Base case for P_{Loss}, MW.		408.316
Base case for VD, p.u.		5.4286
Base case for L-index		0.4135

Table 3.4 Control variables settings for all power systems

Test system	**Variables**	**Lower**	**Upper**	**Step**
IEEE 30-bus [14]	V_{PV} and V_{PQ}	0.95	1.1	Continuous
	T	0.9	1.1	
	$Q\text{-}_{shunt}$ (9)	0	5	
IEEE 118-bus	V_{PV} and V_{PQ}	0.95	1.05	Continuous
	T	0.9	1.1	
	$Q\text{-}_{shunt}$ (14)	See in [73]		
IEEE 300-bus [76]	V_{PV} and V_{PQ}	0.9	1.1	Continuous
	T	0.9	1.1	
	$Q\text{-}_{shunt}$	See in [75]		
DZA 114-bus [74]	V_{PV} and V_{PQ}	0.9	1.1	Continuous
	T	0.9	1.1	0.01
	$Q\text{-}_{shunt}$	See in [74]		Discrete

3.2.4. Numerical Results and Discussions

An empirical study was conducted to select the population size, i.e., we study the effect of population size on the performance of the AEO technique, in which 30 trial runs have been performed under different population sizes like 20, 30, 40, and 70. The results of this study not introduced, but we only indicate that 30 individuals of population give best results for all case studies. For that reason, in all simulation cases, population size is specified as 30 individuals and maximum number of iteration is fixed 100 for IEEE 30-bus, 200 for DZA 114-bus, IEEE 118-bus and IEEE 300-bus test systems. For the purpose of comparison, in all

simulation cases, we considered all control variables as continuous except those of Algerian power system DZA 114-bus.

3.2.5. IEEE 30-bus test system [58][77]

This test system has 6 generators (PV buses) at buses 1, 2, 5, 8, 11, 13 while the rest are the load buses (PQ buses), 4 Transformers with off nominal tap ratio at the branches 11, 12, 15, and 36, as well as 9 shunt compensators at bus bars 10, 12, 15, 17, 20, 21, 23, 24, and 29 taken from [78]. The load demand is (2.834+j 1.262) p.u; its full data is given in [79]. In IEEE 30-bus test system, the upper and lower voltages bounds of all buses are chosen to be 1.1 p.u. and 0.95 p.u., respectively. The limits for other decision variables are taken from [54][80].

In this part, the adopted objective function is the real power loss minimization by means of the AEO, ALO, and NBA algorithms. Figure 3.1 shows the convergence curves of the considered optimizers and, as noticeably, the AEO algorithm converges to high quality solutions in the first quarter of iterations. Based on the convergence plot presented in Figure 3.1, it can be seen that AEO algorithm achieve the global optimal power losses in only 35th iteration.

In addition, it can be seen that the AEO technique outperforms the NBA and ALO methods in terms of convergence characteristic as well as solution merit. The best settings of the control variables obtained via the implemented techniques AEO, NBA, and ALO are reported in Table 3.5. In the 30 independent runs performed, proposed AEO found the best solution. It can be seen that the real power loss achieved via AEO, NBA, and ALO algorithms are is 4.5262 MW, 4.5529 MW and 4.5919 MW, respectively. Figure 3.2 illustrates the performance of AEO for 30 independent run of executions. It can be observed that the best and worst solutions are very close, with a difference of 0.3%. Noticeably, it was explored that a number of optimizers published seem to have violated the feasibility boundaries, rendering the solutions infeasible.

Compared recalculated results with obtained ones provided in Table 3.5, It clearly appears that all of implemented algorithms such as ALO, NBA, and proposed AEO gives exact values and insure the feasibility of solutions by keeping all state variables within the specified limits. The voltage profile at load buses-(PQ buses) for IEEE 30-bus is illustrated in Figure. 3.3.

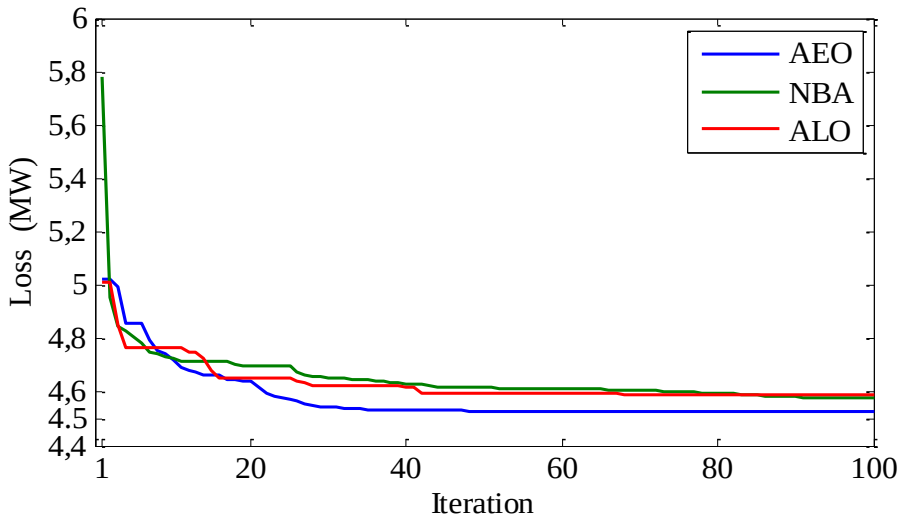

Figure 3.1. Convergence characteristic of IEEE 30-bus system for P_{Loss} minimization

Table 3.5. Solution of minimum power losses (MP) for IEEE 30-bus test system

Control variables	**FA** [77]	**DE** [71]	**QOTLB** [81]	**TLBO** [81]	**BBO** [82]	**ALO** [80]	**GSA** [77]	**MFO** [60]	**NBA**	**ALO**	**AEO**
Generator Voltage (p.u)											
$\mathbf{V_1}$	1.1000	1.1000	1.1000	1.1000	1.1000	1.1000	1.0999	1.1	1.1	1.1000	1.1000
$\mathbf{V_2}$	1.0644	1.0931	1.0942	1.0936	1.0944	1.0953	1.0743	1.0943	1.0951	1.0953	1.0944
$\mathbf{V_5}$	1.0745	1.0736	1.0745	1.0738	1.0749	1.0767	1.0749	1.0747	1.0775	1.0764	1.0751
$\mathbf{V_8}$	1.0869	1.0756	1.0765	1.0753	1.0768	1.0788	1.0768	1.0766	1.0792	1.0787	1.0770
$\mathbf{V_{11}}$	1.0916	1.1000	1.1000	1.0999	1.0999	1.1000	1.0999	1.1	1.0960	1.0916	1.1000
$\mathbf{V_{13}}$	1.0999	1.1000	1.0999	1.1000	1.0999	1.1000	1.0999	1.1	1.0998	1.0862	1.1000
Tap ratio (p.u)											
$\mathbf{T_{11}}$	1.00	1.0465	1.0664	1.0251	1.0435	1.01	1.00	1.0433	1.0313	1.0333	1.0392
$\mathbf{T_{12}}$	0.94	0.9097	0.9000	0.9439	0.9011	0.99	0.93	0.9	0.9424	1.0004	0.9000
$\mathbf{T_{15}}$	1.00	0.9867	0.9949	0.9992	0.9824	1.02	0.98	0.9791	1.0009	1.0361	0.9729
$\mathbf{T_{36}}$	0.97	0.9689	0.9714	0.9732	0.9691	1.000	0.97	0.9647	0.9854	0.9976	0.9632
Capacitor Banks (MVAR)											
$\mathbf{Q_{C\text{-}10}}$	3	5.0000	5.0000	5.0000	4.9998	4	3.7	5	4.2055	4.9477	4.9948
$\mathbf{Q_{C\text{-}12}}$	4	5.0000	5.0000	5.0000	4.987	2	4.3	5	5	4.8343	4.9963
$\mathbf{Q_{C\text{-}15}}$	3.3	5.0000	5.0000	5.0000	4.9906	4	3.7	4.8055	3.3446	4.5170	4.8409
$\mathbf{Q_{C\text{-}17}}$	3.5	5.0000	5.0000	5.0000	4.997	3	2.2	5	5	4.7030	4.9985
$\mathbf{Q_{C\text{-}20}}$	3.9	4.4060	4.45	4.57	4.9901	2	3.1	4.0623	4.3974	3.5384	4.2895
$\mathbf{Q_{C\text{-}21}}$	3.2	5.0000	5.00	5.00	4.9946	4	3.9	5	4.9844	4.5841	5
$\mathbf{Q_{C\text{-}23}}$	1.3	2.8004	2.83	2.86	3.8753	3	4.2	2.5193	4.8984	4.8054	2.6464
$\mathbf{Q_{C\text{-}24}}$	3.5	5.0000	5.00	5.00	4.9867	5	4.4	5	3.7526	4.9123	4.9998
$\mathbf{Q_{C\text{-}29}}$	1.42	2.5979	2.56	2.58	2.9098	5	2	2.1925	2.8649	2.8453	2.2293
$\mathbf{P_{Loss}}$ (MW)	**4.5691**	**4.5550**	**4.5594**	**4.5629**	**4.5511**	**4.59**	**4.54**	**4.534**	**4.55293**	**4.5919**	**4.5262**
$\mathbf{P_{Loss}}$ **Calculated**		**4.532**	**4.535**	**4.538**	**4.532**	**4.590**	**4.952**[(a)]	**4.527**	**4.553**	**4.592**	**4.526**
VD	1.7752	1.9589	1.9057	1.8760	NA	NA	1.92	NA	1.5270	1.2210	**1.83**
L-index	NA	0.5513	0.1273	0.1278	NA	0.1307	NA	NA	0.1285	0.1323	**0.1250**
CPU (s)	NA	NA	NA	NA	110	98	NA	NA	65	85	**116**

Bold results are the Best one achieved by AEO

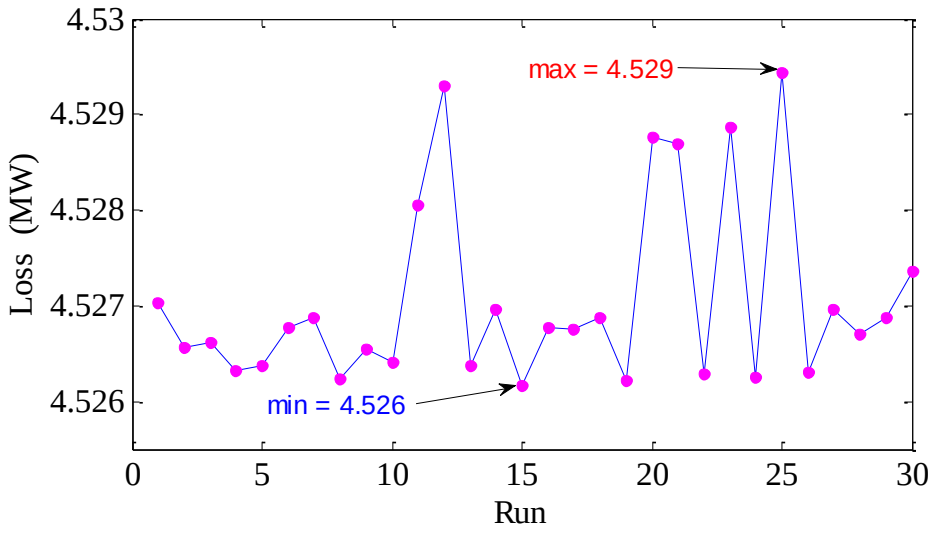

Figure 3.2. Performance of 30 individuals for 30 independent execution runs

3.2.6. IEEE *118*-bus test system [79]

IEEE 118-bus test system consists of one hundred eighty-six branches, fifty four generators, sixty four load buses, nine branches under load tap-changing transformers and fourteen reactive power sources. The load demand is (42.42+j 14.38) p.u., under base power of 100 MW. The complete data can be found in [76]. The minimum and maximum limits of variables can be found in [60]. Two cases are considered as follows:

Case 1: minimization of P_{Loss}.
Case 2: minimization of *VD*.
Case 1: Minimization of active power losses

Table 3.6 shows the obtained findings of active power losses minimization case and the corresponding control variables settings for IEEE 118 bus test system. The results confirm that the proposed AEO is able to provide the best result than other optimization techniques listed, both with respect of the solution quality and validity. From the results of this case, AEO reduces the power losses to 115.302 MW, i.e., 3.78 % less than ALO, 6.14 % less than NBA 0.97 % less than MFO, 4.63 % less than GWO, 10.13 % less than OGSA, 13.57 % less than PSO, 10.81 % less than GSA. These significant values reflect substantial improvement in the achieved findings. Figure 3.3 shows the bus voltage profiles for the best obtained solutions. Remarkably, the magnitude of voltages is exactly inside the defined range which affirm the feasibility of solutions the AEO algorithm. The convergence curves of real power loss for IEEE 118-bus system for three implemented algorithms AEO, NBA and ALO is presented in Figure. 3.4. According to the Figure. 3.4, it is clearly that proposed algorithm

converges to optimal real power loss after 80th iteration. Moreover, the proposed AEO takes lesser execution time as compared to CPVEIHBMO, GSA, PSO, OGSA, GWO, and MFO. However, ALO and NBA solvers require less time to complete the simulation. Figure 3.5 discloses the performance of AEO for 30 independent execution runs. It observed that the best and worst results are **115.3027** MW and 116.938 MW, respectively in which difference between them is no longer than 1.64 MW.

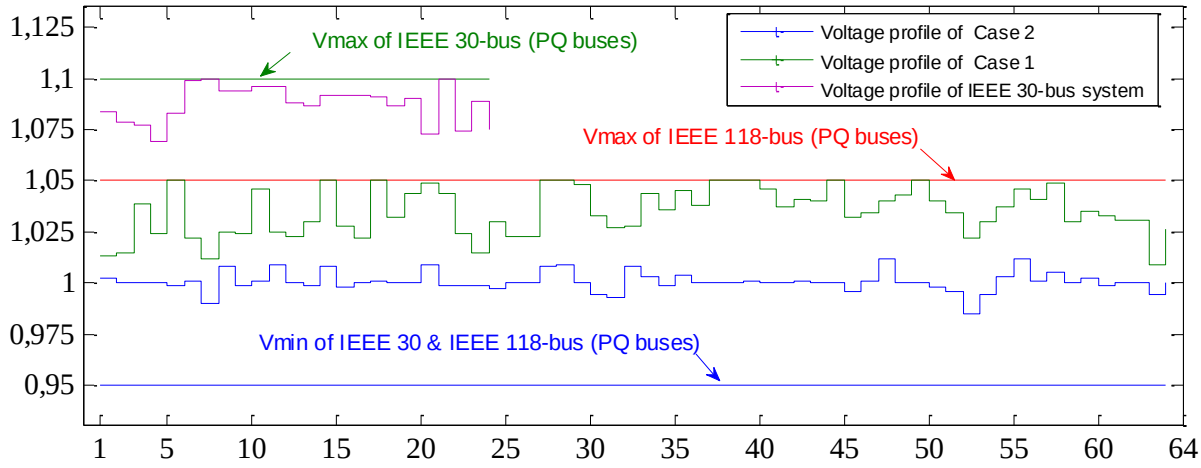

Figure 3.3. Voltage profile at load buses-(PQ buses) for IEEE 30 & 118-bus systems

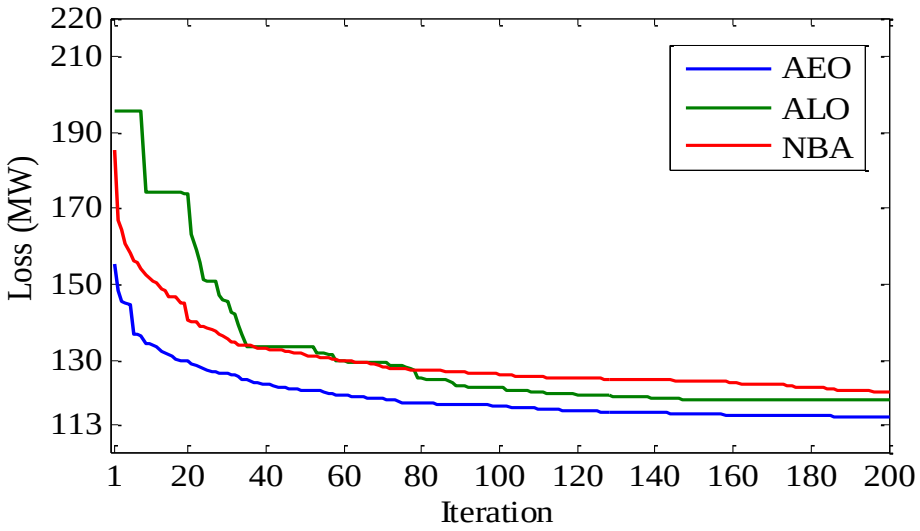

Figure 3.4. Comparative convergence curves for P_{Loss} minimization of the 118-bus

Table 3.6. Solution of minimum power losses for power system 118-bus system

Cont varia	CPVEIH BMO[83]	GSA [79]	PSO [83]	OGSA [83]	GWO [73]	MFO [60]	NBA	ALO	AEO
Generator Voltage (p.u)									
V_1	0.9926	0.9600	1.0332	1.035	1.0204	1.0173	1.0429	1.0242	1.0090
V_4	1.0108	0.9620	1.055	1.0554	1.0257	1.0402	1.0415	1.0439	1.0388
V_6	1.0037	0.9729	0.9754	1.0301	1.0208	1.0292	1.0495	1.0349	1.0248
V_8	0.9976	1.0570	0.9669	1.0175	1.0419	1.0600	1.0457	1.0269	1.0366
V_{10}	1.0215	1.0885	0.9811	1.025	1.0413	1.0374	1.0313	1.0608	1.0419
V_{12}	1.0093	0.9630	1.0092	1.041	1.0232	1.0250	1.0429	1.0348	1.0241
V_{15}	1.0075	1.0127	0.9787	0.9973	1.0207	1.0268	1.0317	1.0363	1.0313
V_{18}	1.0259	1.0069	1.0799	1.0047	1.0270	1.0298	1.0406	1.0530	1.0363
V_{19}	0.9943	1.0003	1.0805	0.9899	1.0204	1.0275	1.0337	1.0402	1.0338
V_{24}	1.0179	1.0105	1.0286	1.0287	1.0137	1.0483	1.0388	1.0500	1.0469
V_{25}	1.0177	1.0102	1.0307	1.06	1.0270	1.0600	1.0453	1.0664	1.0768
V_{26}	0.9990	1.0401	0.9877	1.0855	1.0386	1.0600	1.033	1.0465	1.0858
V_{27}	1.0084	0.9809	1.0157	1.0081	1.0188	1.0267	1.0298	1.0365	1.0403
V_{31}	0.9838	0.9500	0.9615	0.9948	1.0138	1.0101	1.0408	1.0352	1.0229
V_{32}	0.9827	0.9552	0.9851	0.9993	1.0135	1.0226	1.0479	1.0302	1.0325
V_{34}	1.0065	0.9910	1.0157	0.9958	1.0261	1.0556	1.0284	1.0409	1.0453
V_{36}	1.0190	1.0091	1.0849	0.9835	1.0261	1.0548	1.0336	1.0374	1.0442
V_{40}	1.0267	0.9505	0.983	0.9981	1.0125	1.0419	1.0239	1.0215	1.0210
V_{42}	0.9865	0.9500	1.0516	1.0068	1.0233	1.0429	1.0322	1.0147	1.0228
V_{46}	1.0084	0.9814	0.9754	1.0355	1.0272	1.0450	1.042	1.0367	1.0419
V_{49}	1.0035	1.0444	0.9838	1.0333	1.0401	1.0589	1.0413	1.0582	1.0567
V_{54}	0.9806	1.0379	0.9637	0.9911	1.0230	1.0284	1.046	1.0179	1.0431
V_{55}	0.9969	0.9907	0.9716	0.9914	1.0221	1.0289	1.0438	1.0111	1.0459
V_{56}	0.9881	1.0333	1.025	0.992	1.0226	1.0283	1.0501	1.0147	1.0456
V_{59}	1.0197	1.0099	1.0003	0.9909	1.0379	1.0512	1.0466	1.0494	1.0548
V_{61}	0.9956	1.0925	1.0771	1.0747	1.0241	1.0534	1.0467	1.0526	1.0459
V_{62}	1.0064	1.0393	1.048	1.0753	1.0199	1.0506	1.0446	1.0505	1.0474
V_{65}	0.9883	0.9998	0.9684	0.9814	1.0465	1.0596	1.0529	1.0436	1.0532
V_{66}	1.0101	1.0355	0.9648	1.0487	1.0378	1.0600	1.0389	1.0669	1.0626
V_{69}	0.9931	1.1000	0.9574	1.049	1.0501	1.0600	1.0417	1.0568	1.0717
V_{70}	1.0127	1.0992	0.9765	1.0395	1.0243	1.0600	1.0338	1.0185	1.0462
V_{72}	1.0145	1.0014	1.0243	0.99	1.0187	1.0526	1.049	1.0462	1.0480
V_{73}	1.0174	1.0111	0.9651	1.0547	1.0397	1.0600	1.0467	1.0090	1.0437
V_{74}	1.0025	1.0476	1.0733	1.0167	1.0170	1.0600	1.032	1.0230	1.0395
V_{76}	0.9842	1.0211	1.0302	0.9972	1.0080	1.0390	1.0316	1.0272	1.0269
V_{77}	0.9914	1.0187	1.0275	1.0071	1.0192	1.0502	1.0407	1.0316	1.0465
V_{80}	1.0257	1.0462	0.9857	1.0066	1.0329	1.0600	1.0413	1.0372	1.0535
V_{85}	0.9876	1.0491	0.9836	0.9893	1.0224	1.0600	1.0421	1.0421	1.0499
V_{87}	1.0213	1.0426	1.0882	0.9693	1.0361	1.0599	1.0519	0.9965	1.0555
V_{89}	1.0069	1.0955	0.9895	1.0527	1.0558	1.0600	1.0427	1.0657	1.0679
V_{90}	1.0298	1.0417	0.9905	1.029	1.0290	1.0431	1.0385	1.0289	1.0378
V_{91}	0.9839	1.0032	1.0288	1.0297	1.0127	1.0496	1.0266	1.0353	1.0341
V_{92}	1.0021	1.0927	0.976	1.0353	1.0360	1.0600	1.0369	1.0576	1.0552
V_{99}	0.9853	1.0433	1.088	1.0395	1.0297	1.0551	1.0262	1.0453	1.0454
V_{100}	1.0281	1.0786	0.9617	1.0275	1.0360	1.0584	1.0445	1.0507	1.0523
V_{103}	0.9802	1.0266	0.9611	1.0158	1.0232	1.0442	1.0404	1.0425	1.0461
V_{104}	1.0187	0.9808	1.0125	1.0165	1.0180	1.0333	1.0314	1.0430	1.0467
V_{105}	1.0209	1.0163	1.0684	1.0197	1.0176	1.0281	1.0345	1.0459	1.0389
V_{107}	1.0234	0.9987	0.9769	1.0408	1.0201	1.0161	1.0517	1.0848	1.0271
V_{110}	0.9842	1.0218	1.0414	1.0288	1.0207	1.0215	1.0313	1.0366	1.0326

V_{111}	1.0000	0.9852	0.979	1.0194	1.0261	1.0280	1.0419	1.0591	1.0418
V_{112}	0.9930	0.9500	0.9764	1.0132	1.0066	1.0042	1.0311	1.0185	1.0190
V_{113}	1.0200	0.9764	0.9721	1.0386	1.0251	1.0350	1.0476	1.0398	1.0410
V_{116}	1.0016	1.0372	1.033	0.9724	1.0342	1.0484	1.0372	1.0261	1.0522
Tap ratio setting of transformers									
$\mathbf{T_8}$	1.0255	1.0659	1.0045	0.9568	1.0208	1.0136	1.032	0.9700	0.9933
$\mathbf{T_{32}}$	0.9891	0.9534	1.0609	1.0409	1.0279	1.1000	0.99874	1.0217	1.0999
$\mathbf{T_{36}}$	0.9932	0.9328	1.0008	0.9963	1.0323	1.0038	0.99845	1.0035	0.9896
$\mathbf{T_{51}}$	0.9873	1.0884	1.0093	0.9775	1.0209	0.9826	1.0059	0.9642	0.9762
$\mathbf{T_{93}}$	0.9868	1.0579	0.9922	0.956	1.0091	0.9843	0.97775	0.9696	0.9641
$\mathbf{T_{95}}$	1.0235	0.9493	1.0074	0.9956	1.0366	1.0139	0.99487	1.0059	1.0145
$\mathbf{T_{102}}$	1.0090	0.9975	1.0611	0.9882	1.0301	1.1000	1.0052	1.0204	0.9569
$\mathbf{T_{107}}$	1.0075	0.9887	0.9307	0.9251	1.0234	1.1000	0.99449	0.9827	0.9464
$\mathbf{T_{127}}$	0.9872	0.9801	0.9578	1.0661	1.0211	0.9683	1.0055	1.0440	0.9792
Reactive power of shunt resources (MVAR)									
$\mathbf{Q_{C\text{-}5}}$	0	0	0	−33.19	−39.76	0	−17.747	−3.2410	−8.9587
$\mathbf{Q_{C\text{-}34}}$	6.0111	7.4600	11.714	4.8	13.7900	0	1.8726	1.7198	6.4884
$\mathbf{Q_{C\text{-}37}}$	0	0	0	−24.9	−24.73	−0.0312	−5.5757	−12.8228	−8.8591
$\mathbf{Q_{C\text{-}44}}$	6.0057	6.0700	9.8932	328	9.9571	10	0	0.4357	5.6581
$\mathbf{Q_{C\text{-}45}}$	3.0001	3.3300	9.4169	3.83	9.8678	0	8.5929	1.4848	7.0815
$\mathbf{Q_{C\text{-}46}}$	5.9838	6.5100	2.6719	5.45	9.9186	0	5.6952	3.2751	4.9572
$\mathbf{Q_{C\text{-}48}}$	3.9920	4.4700	2.8546	1.81	14.8900	0.00084	7.3115	6.3305	7.0284
$\mathbf{Q_{C\text{-}74}}$	7.9862	9.7200	0.5471	5.09	11.9720	0.22054	5.0436	1.1433	1.8367
$\mathbf{Q_{C\text{-}79}}$	13.9892	14.2500	14.853	11.04	19.6490	20	15.242	10.8565	16.778
$\mathbf{Q_{C\text{-}82}}$	17.9920	17.4900	19.427	9.65	19.8900	0	16.258	1.1730	14.582
$\mathbf{Q_{C\text{-}83}}$	4.0009	4.2800	6.9824	2.63	9.9515	10	6.6489	1.4741	4.9715
$\mathbf{Q_{C\text{-}105}}$	10.9825	12.0400	9.0291	4.42	19.9680	0	5.6212	16.9174	0.0077
$\mathbf{Q_{C\text{-}107}}$	2.0251	2.2600	4.9926	0.85	5.9136	6	3.8228	3.5582	2.7109
$\mathbf{Q_{C\text{-}110}}$	2.0272	2.9400	2.2086	1.44	5.8834	6	3.0696	0.3696	2.3012
$\mathbf{P_{loss}}$	124.098	127.76	130.96	126.99	120.65	116.4254	122. 391	119.6645	**115.3027**
L-max	NA	NA	NA	NA	NA	NA	0.06540	0.06466	**0.06373**
CPU(s)	1053	1198	1472	1101.2	1372	1419	417	568	**886**

-Bold results denote best results

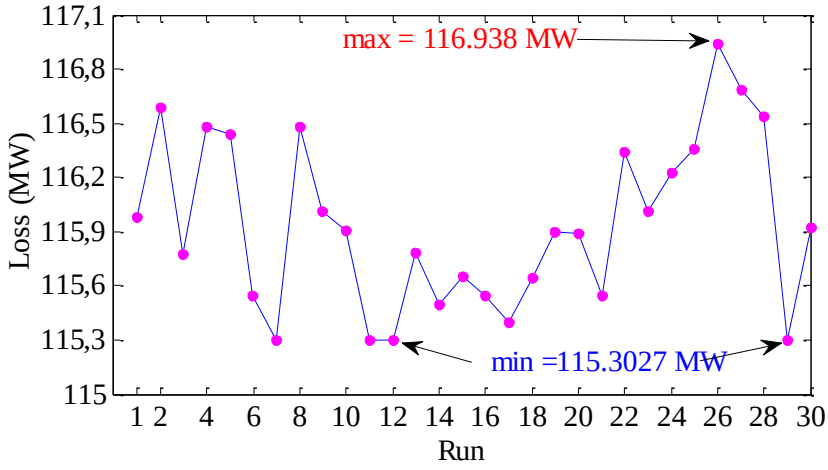

Figure 3.5. Performance of 30 individuals for 30 independent execution runs10

Table 3.7 reveals comparison results of AEO and a number of optimizers reported in the literature and the corresponding percentages of power losses reduction. The greatest reduction is achieved by AEO algorithm which is 13.21 % with regard to the base case and better than those reported by other algorithms. Thus, simulation results confirm that AEO

algorithm can define the optimal solution or near-optimal solution, even with large-scale test system.

Table 3.7. Comparison of loss reduction percentage for IEEE 118-bus test system

Algorithms	**Case 0**	**PSO**	**WCA**	**CLPSO**	**GSA**	**OGSA**	**CPVEIH-BMO**	**DE**
P_{Loss} MW	132.86	131.99	131.83	130.96	127.76	126.99	124.098	122.36
Loss reduction (%)	–	0.66	0.77	1.43	3.84	4.42	6.60	7.90
Algorithms	**WOA**	**NGBWCA**	**ABC**	**GWO**	**ALO**	**GA**	**MFO**	**AEO**
P_{Loss} MW	122.39	121.47	120.42	120.65	119.77	119.30	116.42	**115.30**
Loss reduction (%)	7.88	8.57	9.33	9.19	9.85	10.95	12.37	**13.21**

Case 2: Voltage deviation minimization

In this case, the minimum, average, and maximum results of active power losses achieved by AEO, NBA and ALO and some other algorithms reported in the literature are tabulated in Table 3.8. Due to the space reasons, the corresponding optimal control variables of this case are not listed here. The value of VD for AEO is better than other optimizers. From Table 3.8, it can be pointed that proposed AEO is able to reduce the voltage deviation index by 86.8% with respect to initial losses, compared to 86.7 % with QOTLBO, 84.1 % with TLBO, 72.7 % with PSO-TVAC, 85.5% with SPSO-TVAC, and 83.6 % with PGSWT-PSO. The voltage profiles of all load buses-(PQ buses) for this case are depicted in Figure. 3.3. It is clear from this figure that the voltage profile has been significantly improved. In case 2, the active power loss is slightly increased to 155.94 MW, while the VD is reduced from 3.41 to 0.1898 p.u, compared with case 1.

Table 3.8. Comparison of voltage deviation minimization percentage for IEEE 118-bus system

Algorithms	**PSO-TVIW** [84]	**PSO-TVAC** [84]	**SPSO-TVAC** [84]	**PGSWT-PSO** [84]	**TLBO** [81]	**QOTLBO** [81]	**AEO**
Min VD	0.1935	0.3921	0.2074	0.2355	0.2237	0.1910	**0.1898**
Average VD	0.2291	0.4724	0.2498	0.2755	0.2306	0.2043	**0.2122**
Max VD	0.2809	0.5407	0.3012	0.3239	0.2543	0.2267	**0.2346**
Standard deviation	0.0206	0.0316	0.0215	0.0205	0.0384	0.0356	**0.0117**
P_{Loss}	176.45	179.79	146.81	150.5609	NA	NA	**155.94**
L-max	0.0672	0.0667	0.0650	0.0671	NA	NA	**0.0672**

Bold result denote the best findings

3.2.7. Large-scale test system IEEE 300-bus [14]

To examine the scalability of the proposed AEO algorithm in solving large-scale ORPD problem, the IEEE 300-bus has been also analyzed [75,76]. This system consists of sixty-nine generators, forty hundred eleven transmission-lines of which hundred-seven branches with off nominal tap ratios, and fourteen parallel reactive power sources [14]. The total load is (235.258 + j77.8797) p.u. The limits of the control variables are given in Table 2 and from [85]. This test system exhibits very large voltage drops [86], making it harder to ensure the feasibility of solutions. Two cases are considered with this test system:

Case 3: minimization of P_{Loss}; Case 4: Voltage Deviation (VD).

Due to numerous variables and/or for sake of brevity, only the optimal solutions of reactive powers of the best results of three implemented algorithms are presented in the Table 3.9. From this table, it can be observed that reactive powers of parallel compensators are within admissible limits. The results demonstrate that applying AEO algorithm has led to highest reduction of power loss up to 10.62% compared with that achieved by other solvers, which is to 5.19% with ALO and 3.45% with NBA. Figure 3.6 illustrates comparison between voltage profiles of case 3 and case 4. It is clear from this figure that voltage profile has been significantly improved while guarantying the feasibility of solutions. The convergence plots of the algorithms are shown in Figure. 3.7, AEO algorithm has better convergence rate compared with NBA and ALO algorithms. Hence, it can be concluded that AEO algorithm has the best performance among all rival techniques.

Table 3.9 Reactive power outputs of reactive power sources for IEEE 300-bus system

Reactive power	Q_{min} MW	Q_{max} MW	ALO	NBA	AEO
Q_{96}	0	450	156.1047	310.5364	265.9470
Q_{99}	0	59	42.3299	46.6332	56.0155
Q_{133}	0	59	43.1910	13.6233	13.7380
Q_{143}	-450	0	-366.3272	-213.1504	-138.9393
Q_{145}	-450	0	-313.4199	-22.31805	-0.011484
Q_{152}	0	59	26.7216	24.8115	27.3465
Q_{158}	0	59	1.7599	29.6067	50.6618
Q_{169}	-250	0	-43.947	-65.5245	-190.8406
Q_{210}	-450	0	-441.0207	-206.2088	-171.7650
Q_{217}	-450	0	-125.9645	-242.5776	-144.7891
Q_{219}	-150	0	-17.3397	-26.4242	-52.5704
Q_{227}	0	59	11.8801	52.9413	43.0150
Q_{268}	0	15	10.4662	2.5657	2.8092
Q_{283}	0	15	7.7908	3.8356	7.37052
min P_{Loss} MW	P_{Loss}^{0} = 408.316		387.1207	394.2322	**364.9162**
L-index (p.u)	L_{-index}^{0} = 0.4135		0.40816	0.3900	**0.38952**

Table 3.10. Comparison of the results for case 3 and 4 of IEEE 300-bus system

Algorithms	**MVMO** [31]	**DEEPSO** [31]	**SOS** [85]	**A-CSOS** [85]	**GM** [85]	**ALO**	**NBA**	**AEO**
Case 3: P_{Loss} minimization								
Min P_{Loss} (MW)	385.62	394.434	409.964	367.1255	372.26	384.922	394.2322	364.9162
L-index	NA	NA	NA	NA	NA	0.3663	0.3900	0.3895
Reduction *(%)*	5.55	3.4	–0.40	10.08	8.83	5.72	3.44	11.32
Case 4: VD minimization								
	SOS [85]		**A-CSOS** [85]		**NBA**	**ALO**		**AEO**
Min VD (p.u)	4.5420		2.7113		3.8929	3.5033		1.9718
P_{Loss} (MW)	NA		NA		553 .168	469.533		423.243
L-index	NA		NA		0.4177	0.3945		0.4045
Reduction *(%)*	16.33		50.05		28.28	35.46		63.67

Table 3.10, summarizes the comparison results of optimum power losses and voltage deviation obtained by employing different algorithms for both cases. From Table 3.10 we can see that proposed AEO achieves high quality solutions compared to other approaches. Again, according to numerical findings, lower voltage deviation value by AEO in comparison with other algorithms is observable which achieved to 1.97 (p.u), i.e., minimized by 63.7% compared to the initial value, whereas, is minimized up to 50% with A-CSOS, 16.3% [85] with SOS, 35.4% [85] with ALO, and 28.28% with NBA. Consequently, the proposed AEO algorithm not only benefits from high quality solutions, but also by guarantee the feasibility of solutions of both cases for large-scale test system.

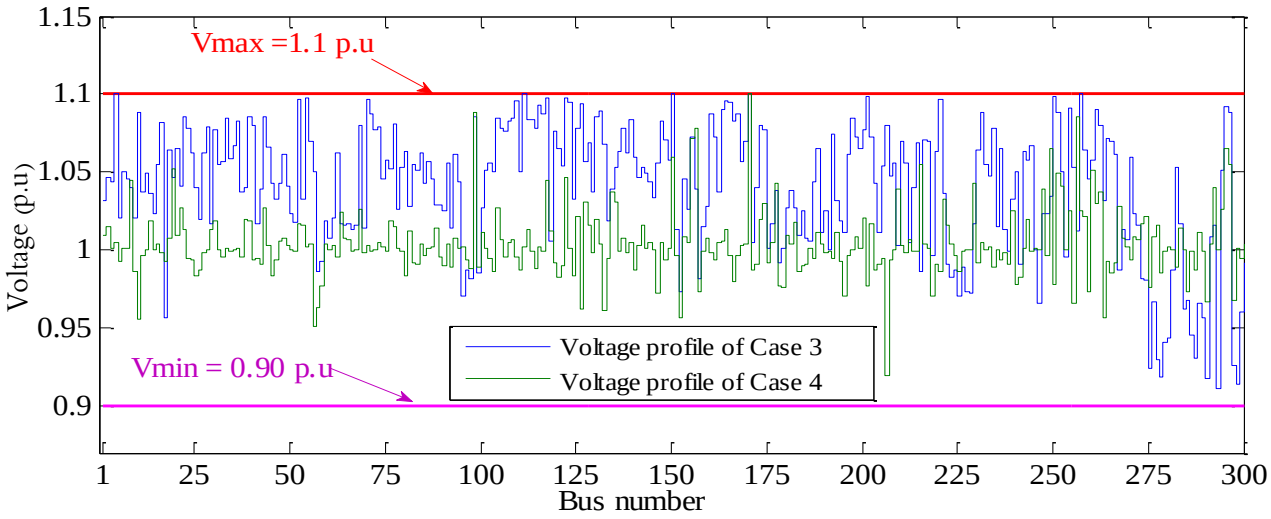

Figure 3.6. Voltage profile for both cases of IEEE 300-bus test system

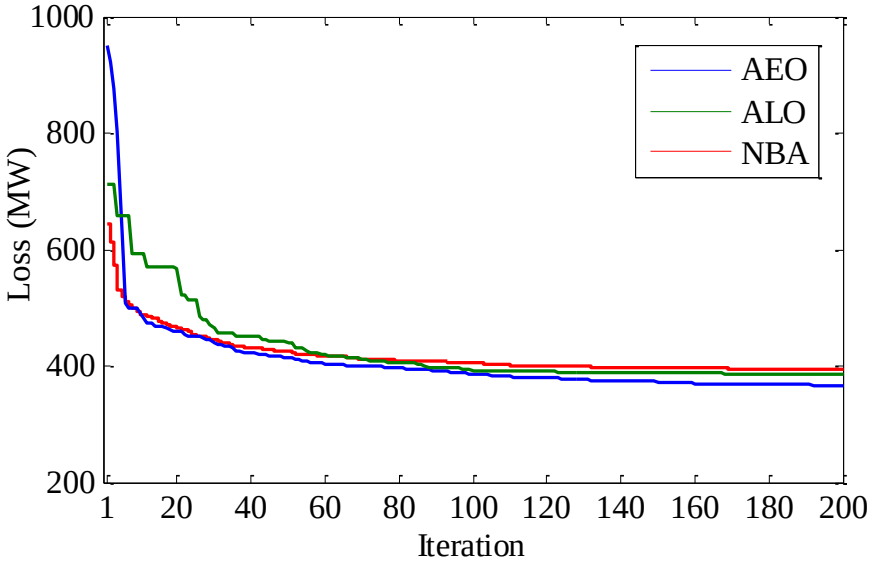

Figure 3.7. Comparative convergence curves for P_{Loss} minimization of the 300-bus

3.2.8. Algerian power grid DZA 114-bus

In order to give a practicability aspect, the Algerian power system DZA 114-bus [74] has been considered as test system. The Algerian electricity grid topology is depicted in Figure A in the Annex. This system comprises 175 transmissions lines, 15 generators, and 16 branches with off-nominal tap ratio. In addition, buses nos. 50, 55, 66, 67, 77, 89 and 93 have been selected as reactive power sources. The total load demand is (37.27+ j 20.70) p.u at 100 MVA base. Bus 4 is selected as the slack-bus. Therefore, the system has a total of 38 variables to be optimized, including fifteen generators, 16 transformers and seven reactive power sources. Also, this power system presents undesirable voltage drops. The upper and the lower operating limits of the control variables are given in Table 3.2.

a) Case 5: minimization of P_{Loss}

Table 3.11 summarizes the optimal control variables of DZA 114-bus, obtained by AEO, NBA and ALO. From the results, the smallest active power losses are obtained using the AEO technique. The proposed algorithm can find the losses as 53.204 MW in continuous variables case and 53.244 MW with discrete variables case. The results confirm that the AEO algorithm is able to find the best solution for both kinds of control variables (continuous and discrete) in comparison to the results of NBA and ALO algorithms. The evolution of losses across iterations for three algorithms are given in Figure 3.8. The performance of AEO for 30 independent execution runs is shown in Figure 3.9. From this figure, it can be seen that the difference between worst and best solution doesn't exceed 1.61

MW. It can be noted that best, worst solutions for all test systems after 30 runs are extremely close, which clearly reflects the stability and robustness of AEO algorithm in terms of exploring the optimal solution in each trial.

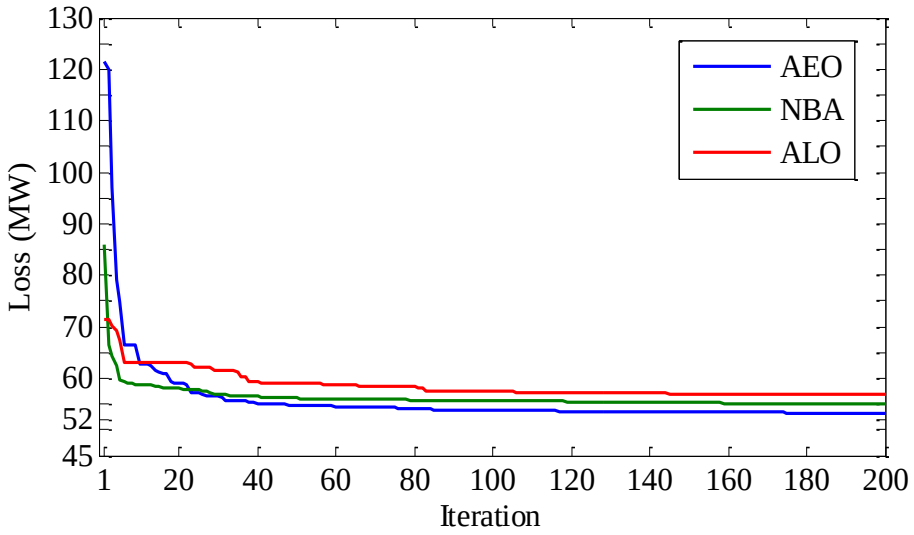

Figure 3.8. Comparative convergence curves for P_{Loss} minimization of the 114-bus

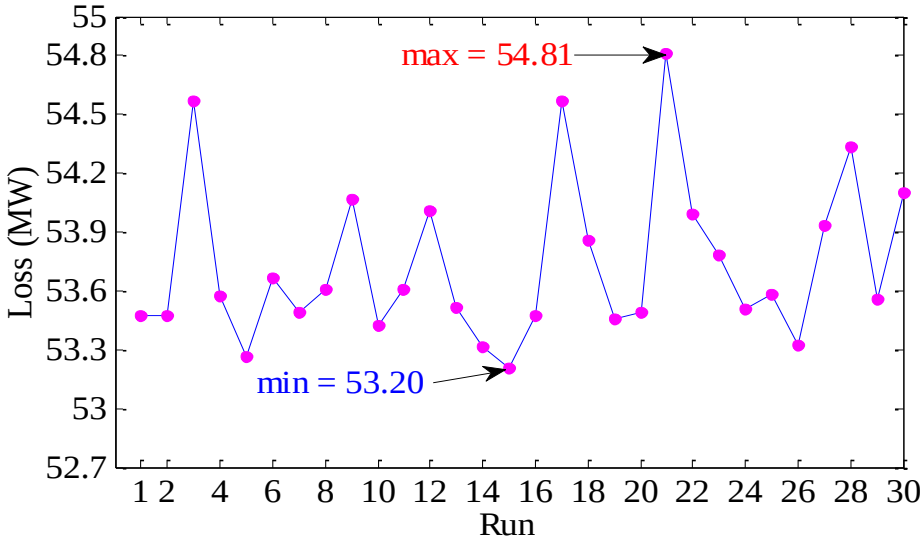

Figure 3.9. Performance of 30 individuals for 30 independent execution runs

Table 3.11. Solution of minimum P_{loss} for Algerian Electricity Grid- DZA 114-bus

Control variables	Continuous variables				Discrete variables		
	ALO	**NBA**	**AEO**		**ALO**	**NBA**	**AEO**
Case 5							
Generator Voltage (p.u)							
$\mathbf{V_4}$	1.099960	1.1	1.099999		1.1	1.099994	1.1
$\mathbf{V_5}$	1.099750	1.1	1.099833		1.099999	1.099562	1.0997
$\mathbf{V_{11}}$	1.096232	1.1	1.099999		1.099981	1.099991	1.1
$\mathbf{V_{15}}$	1.093981	1.098069	1.091310		1.098029	1.092537	1.0935
$\mathbf{V_{17}}$	1.1	1.1	1.099999		1.1	1.1	1.0999
$\mathbf{V_{19}}$	1.055576	1.066200	1.082310		1.017579	1.022780	1.0936
$\mathbf{V_{22}}$	1.062448	1.071543	1.087102		1.023613	1.020059	1.0985
$\mathbf{V_{52}}$	1.042803	1.050259	1.087556		1.023684	1.032393	1.0932
$\mathbf{V_{80}}$	1.093085	1.091932	1.091039		1.098850	1.091589	1.0926
$\mathbf{V_{83}}$	1.099997	1.099171	1.099837		1.1	1.1	1.0999
$\mathbf{V_{98}}$	1.0995280	1.099086	1.099271		1.099999	1.1	1.1
$\mathbf{V_{100}}$	1.1	1.1	1.099995		1.1	1.099999	1.0999
$\mathbf{V_{101}}$	1.1	1.1	1.1		1.1	1.099745	1.0999
$\mathbf{V_{109}}$	1.0998462	1.1	1.099947		1.1	1.099999	1.1
$\mathbf{V_{111}}$	1.0975876	1.1	1.099976		1.1	1.099286	1.1
Tap ratio (p.u)							
$\mathbf{T_{80\text{-}81}}$	1.0074685	1.039184	0.901745		1.03	0.99	0.90
$\mathbf{T_{81\text{-}90}}$	1.0581378	1.029146	0.946162		1.04	1.04	0.96
$\mathbf{T_{86\text{-}93}}$	1.0735973	1.015320	0.963416		1.05	1.06	0.99
$\mathbf{T_{42\text{-}41}}$	1.0668528	1.013559	0.980564		1.04	1.08	0.98
$\mathbf{T_{58\text{-}57}}$	1.0716278	0.993079	0.965906		1.07	1.02	0.97
$\mathbf{T_{44\text{-}43}}$	1.0878220	1.022719	0.974318		1.05	1.06	1.00
$\mathbf{T_{60\text{-}59}}$	1.0518370	1.044176	0.989930		1.08	1.03	0.98
$\mathbf{T_{64\text{-}63}}$	1.0938053	0.973303	0.959374		1.03	1.02	0.97
$\mathbf{T_{72\text{-}71}}$	1.0395981	0.982745	0.955683		1.01	1.06	0.96
$\mathbf{T_{17\text{-}18}}$	1.0023307	0.994556	0.989024		1.05	1.03	0.98
$\mathbf{T_{21\text{-}20}}$	1.0379620	1.022736	0.998976		1.09	1.05	0.99
$\mathbf{T_{27\text{-}26}}$	1.0416436	0.975391	0.961404		1.09	1.03	0.96
$\mathbf{T_{28\text{-}26}}$	1.0933018	1.050337	1.029924		1.06	1.06	1.02
$\mathbf{T_{31\text{-}30}}$	1.0676910	1.027098	0.989257		1.04	1.05	0.99
$\mathbf{T_{48\text{-}47}}$	1.0972839	1.024613	0.984472		1.09	1.1	0.99
$\mathbf{T_{74\text{-}73}}$	1.0648045	0.948207	1.014127		1.08	1.07	1.08
Capacitor Banks (MVAR)							
$\boldsymbol{Q_{C\text{-}50}}$	22.509200	16.09386	24.35864		13	24	25
$\boldsymbol{Q_{C\text{-}55}}$	14.801860	12.77946	10.15448		23	15	10
$\boldsymbol{Q_{C\text{-}66}}$	24.509874	24.32149	19.44356		18	23	22
$\boldsymbol{Q_{C\text{-}67}}$	21.278427	20.83231	25		19	25	25
$\boldsymbol{Q_{C\text{-}77}}$	23.289257	20.41054	14.309846		24	25	16
$\boldsymbol{Q_{C\text{-}89}}$	21.607676	8.110358	7.539387		21	15	7
$\boldsymbol{Q_{C\text{-}93}}$	24.973281	25	24.95138		13	25	25
$\mathbf{P_{Loss}}$ **(MW)**	57.02444	55.122041	**53.2043026**		57.412317	55.9677	**53.244609**
L-index	0.312056	0.31199	**0.278219**		0.315175	0.302761	**0.278153**
$\mathbf{P_{save}}$ **(%)**	15.4	18.27	**21.11**		14.8	17	**21**
Case 6							
Algorithms	**ALO**	**NBA**	**AEO**		**ALO**	**NBA**	**AEO**
VD (p.u)	1.2179	1.28439	**1.04515**		1.2183	1.43166	**1.07067**
$\mathbf{P_{Loss}}$ **(MW)**	65.611	74.478	**71.779**		66.710	75.592	**72.679**
L-index	0.3233	0.3177	**0.31822**		0.31817	0.319307	**0.31791**

b) Case 6 Voltage deviation minimization

In this case, the proposed algorithm is also applied to minimize the total voltage deviation. Case 6 of Table 3.11 gives the simulation results obtained by three algorithms with either discrete or continuous variables. The VD value obtained by the AEO algorithm is better than those accomplished by the NBA and ALO algorithms for both kinds of variables. It can be seen that also with discrete control variables AEO converge to the optimal solutions. In case 6, the active power losses is slightly increased, while the voltage deviation VD is reduced from 7.024 to 1.045 with continuous variables and from 6.84 p.u to 1.07067 p.u with discrete variables compared with case 5, respectively. For ALO and NBA algorithms the optimized voltage deviation is 1.2179 and 1.28439 p.u, for continuous variables and 1.2183 and 1.43166 p.u., for discrete variables. Hence, it can be drawn that AEO algorithm is better than all other listed algorithms in terms global search capacity and efficacy to solve large-sized and nonlinear optimization problems. Fig. 3.10 presents a comparison between voltage profiles of case 5 and case 6 for Algerian electricity grid DZA 114-bus. It can be seen that all bus voltage magnitudes are within the admissible limits.

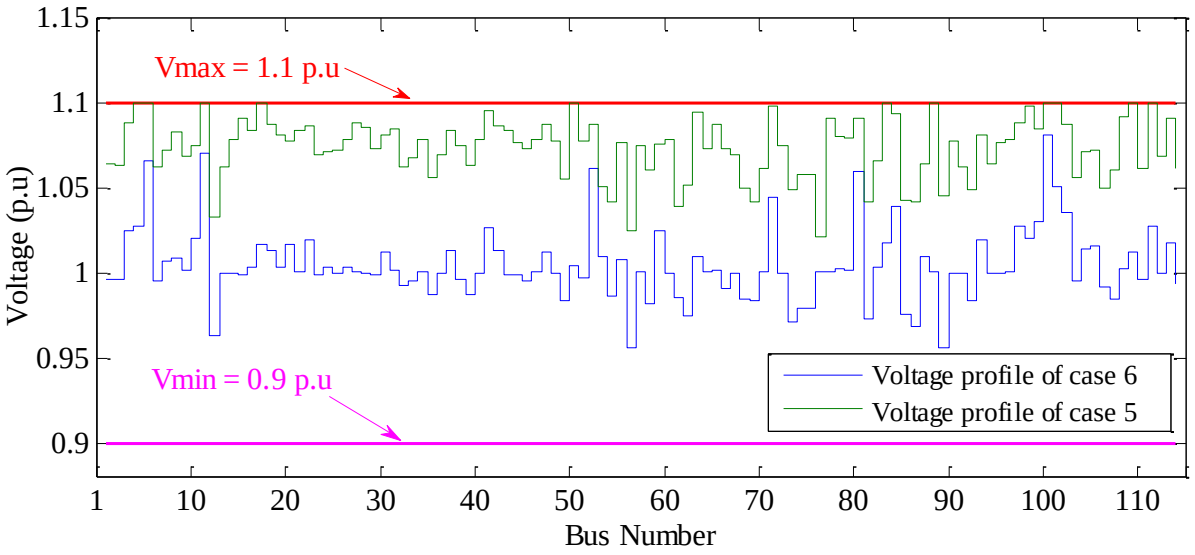

Figure 3.10**.** Voltage profile for DZA 114-bus power system

3.2.9. Statistical test of one-way ANOVA

Due to the stochastic nature of meta-heuristic optimization algorithms, it is evident must be run each technique several times on the same objective function in an effort to get the best result values, which probably vary to each execution. Instead of relying on the statistics of the aforementioned results in terms of best, worst solution and standard deviation, one-way analysis of variance (ANOVA) has been performed to observe the statistical significance of the difference between the performance of AEO algorithm and other implemented

approaches. This study gives certain level of confidence to the present work 95% and to evaluate which techniques could be potentially suitable to cope with ORPD problem in large-scale systems. The one-way ANOVA results obtained from experimented algorithms on three test systems (IEEE 30-bus, IEEE 118-bus and DZA 114-bus) are listed in Table 3.12. In this experiment, assumption of homogeneous variances is considered, it can be seen that the p-value is less than significance level of 0.05. It can be declared that the null hypothesis can be rejected. There is statistically significant difference between the means of the different groups. Thus, it is strong evidence that the mean values in the groups differ. Hence AEO is statistically different from ALO and NBA.

Table 3.12 One way ANOVA stats for active power losses of IEEE 30-bus system

Null hypothesis	All means are equal
Alternative hypothesis	At least one mean is different
Significance level	$\alpha = 0.05$

Test ANOVA IEEE 30-bus

Source of variance	SS	df	MS	F	P-value	F-crit
Between groups	0.18868	2	0.09434	136.23	1.5785 e-27	3.1012
Within groups	0.06025	87	0.00069			
Total	0.24893	89				

Test ANOVA IEEE 118-bus

Source of variance	SS	df	MS	F	P-value	F-crit
Between groups	956.14	2	478.07	205.69	1.0604 e-33	3.1012
Within groups	202.21	87	2.324			
Total	1158.35	89				

Test ANOVA DZA 114-bus

Source of variance	SS	df	MS	F	P-value	F-crit
Between groups	209.827	2	104.914	77.18	5.2785 e-20	3.1012
Within groups	118.256	87	1.359			
Total	328.083	89				

3.3. Multi-objective optimal reactive power dispatch (MOORPD)

In the section 3.1 of this Chapter, many single objective cases of ORPD are solved. In present, the electric power is facing increasing substantial developments due to fundamental changes in both supply and demand, which increase the total power losses in affecting the security-constraints. These developments oblige transmission system operators to modify their applied

optimization strategies in order to ensure both economic scheme and guarantee the satisfaction of all security constraints. Therefore, consideration of more than one objective in ORPD formulation and solution becomes necessary. Statutory developments of modern power system regarding quality of service have increased importance of guarantee the satisfaction of all security constraints. Maintaining high level of power quality requires minimal voltage deviation from the rated value and reduction of transmission loss to any extent signifies commercial benefit to the utilities.

The ORPD is formulated as a non-linear multi-objective optimization problem, which aims at simultaneously minimizing either the active power losses and index of voltage stability (L-index) or the active power losses and the total voltage deviation. Solution of multi-objective ORPD necessitates effective optimization techniques, as the objectives are often highly conflicting. In the vast majority of published papers, however, the ORPD problem is dealt with as a single-objective optimization problem [58–60,80,88] using various conversion methods, such as the weight sum method, epsilon-constraint method and others. These are popularly known as a priori methods. Single-objective optimization approaches are recognized as useful for finding only one best solution to the problem in one program execution or multiple executions to generate a set of Pareto-optimal solutions [89]. However, these optimization methods generally encounter some difficulties in identifying the complete or exact Pareto-optimal solutions, especially when it comes to solving complex conflicting objectives (Deb and Saxena, 2006). Furthermore, they are often computationally costly. These difficulties make these methods unsuitable for solving multi-objective optimization problems. In contrast, posterior methods can easily identify a set of Pareto optimal solutions in a single execution and are always capable of determining any kind of Pareto front. However, they are also computationally expensive. On the basis of the detailed literature surveys in [90,91], the multi-objective particle swarm optimization (MOPSO) algorithm, the Non-dominated sorting genetic algorithm (NSGA) and their improved versions are the most widely used ones for solving the MOORPD problem.

In recent years, the ORPD problem has attracted considerable attention in the research community in an effort to ensure the stable and secure operation of electric power systems. At the present time, many published algorithms have been proposed for solving the MOORPD problem [63][69]. Accordingly, the major impediment of these algorithms resides in the inability of dominance to converge to the Pareto frontier while maintaining sufficient diversity. Moreover, due to the complexity of the objective functions used (ORPD problem), they continue to converge towards the local optimum. On the other hand, it obvious to note

that is not only interesting to find optimal solution or near optimal solution of such problem, but the most important is to assure the safety constraints and to guarantee that the control variables are within the admissible limits. In this study of MOORPD, multi-objective algorithm based on the ALO technique is applied on several multi-objective cases of standard IEEE 30-bus and IEEE 57-bus test systems as well as large-scale test system IEEE 300-bus. The algorithm is discussed in detail in Chapter 2, Section 2.2.1. The computation complexity of MOALO is less than multi-objective particle swarm optimization (MOPSO) and non-dominated sorting genetic algorithm-II (NSGA-II).

The contribution reported in this section is as follow:

The ALO algorithm was originally developed for unconstrained multi-objective ORPD problem. Constraints in MOORPD have been handled by penalty function method. Thereafter, results of study cases and feasibility of the obtained and reported outcomes are analyzed, discussed and compared with MOPSO and NSGA II. Furthermore, results of all cases study are fully verified with the use of power flow calculations.

The MOALO algorithm is used to solve MOORPD problem, which aims to find the set of optimal solutions of controlled variables by which the solutions found correspond to a minimum value of the selected objective function. The following steps describe the computational procedure for solving the MOORPD problem using the MOALO algorithm and the flowchart of proposed algorithm is shown in Figure.2.1. In the proposed algorithm, the solution vectors are *antlions* and *ant* and their positions represent the output of each control variables at the MOORPD problem.

Step 1: Define input power system data (line data + bus data) and identify the control variable limits, number of variables, number of search agent, maximum number of iterations, number of Pareto archive.

Step 2: Initialize random values of *ants* and *antlions* populations i.e. for each search agent in population is a randomly generating a string of real values within their control variable limits. Set the generation count (gen = 1).

Step 3: Run power flow algorithm based on the Newton Raphson method for each search agent (*ant* and *antlion*) in an effort to evaluate fitness values corresponding to both objective function (P_{loss} and *VSI* or P_{loss} and *VD*) as well as constraint violations.

Step 4: Find the best *antlion* and store it as an elite.

Step 5: For each *ant*, select an *antlion* by using Roulette wheel mechanism

Step 6: Search space coverage, i.e., limit of ORPD control variables towards selected *antlion*

Step 7: Create random walk for *ants* (the position of ants here, indicates the control variables of MOORPD problem) in order to promote the control variables.

Step 8: Update the control variables (position of *ant*).

Step 9: Check if a limit of promoted control variables is within the admissible limit (search space); if so, go to step 11; otherwise go to step 5.

Step 10: Run power flow algorithm based on the Newton-Raphson method by utilizing the set of promoted variables to calculate of both objective function values (P_{loss} and *VSI* or P_{loss} and *VD*).

Step 11: Replace *antlion* with better *ant* than current *antlion*.

Step 12: Update elite and archive maintenance to realize best Pareto optimal front.

Step 13: Check the stop criterion, i.e., if gen= max generation count, then stop; otherwise increment generation count (gen=gen+1) and go to step 3.

Step 14: Generate the Pareto optimal front and extract the best compromise solution from the Pareto optimal front using fuzzy set theory.

3.4. Objectives, case studies for MOORPD and input for MOALO

In order to assess the performance of MOALO, standard IEEE 30 and IEEE 57-bus test systems as well as large-scale IEEE 300- bus test system are selected and several case studies with multi-objectives have been performed. The summaries of systems data along with real power losses, Voltage deviation, and voltage stability index in the initial conditions have already been provided in Tables 3.1–3.3.

The multi-objective cases are formulated with two objectives. The case studies are summarized as follows: summarized as follows:

- Case 1: minimization of P_{Loss} and *VD* in IEEE 30-bus [64].
- Case 2: minimization of P_{Loss} and *VD* in IEEE 57-bus [64].
- Case 3: minimization of P_{Loss} and *VSI* in the IEEE 57-bus [67].
- Case 4: minimization of P_{Loss} and *VD* in the IEEE 300-bus;
- Case 5: minimization of P_{Loss} and *VSI* in the IEEE 300-bus.

The algorithm were developed in MATLAB 7.10 programming language and the simulation conducted on a computer Core (TM) i5 a 1.90 GHz with 4 Go RAM.

Table 3.13 Control parameter settings of MOALO algorithm for test power systems

Parameter	**Setting Value**		
	IEEE 30-bus	IEEE 57-bus	IEEE 300-bus
No of search agents (NSA)	50	50	60
No of iterations	100	100	200
Search domain (rand)	[0 1]		
Number of Pareto archive	50	50	100

3.4.1. Results and comparisons of MOORPD case studies

a) Best Pareto front and the best compromise solution

Each case study is run 20 times independently. Thereafter, from 20 Pareto fronts, we select the best Pareto front. Once having the set of Pareto optimal solutions has been obtained, fuzzy set theory is implemented to extract so-called the best compromise solution that will satisfy the different goals to some extent. In this approach, the membership function μ_i^j for i^{th} objective function F_i of non-dominated solution j is calculated by using the equation below: [92,93].

$$\mu_i^j = \begin{cases} 1 & F_i \le F_i^{\min} \\ \dfrac{F_i^{\max} - F_i}{F_i^{\max} - F_i^{\min}} & F_i^{\min} < F_i < F_i^{\max} \\ 0 & F_i \ge F_i^{\max} \end{cases} \tag{3.16}$$

where $F_i^{\max}$ and $F_i^{\min}$ are respectively the maximum and the minimum values of the i^{th} objective function among all the non-dominated solutions. The membership function reflects the degree of achievement of the original objective function as a value within [0, 1], i.e., with μ^j = 1 wholly satisfactory and with μ^j = 0 as not satisfactory. For each non-dominated solution j, the membership function is normalized as follows:

$$\mu^j = \frac{\sum_{i=1}^{N_{obj}} \mu_i^j}{\sum_{j=1}^{M} \sum_{i=1}^{N_{obj}} \mu_i^j} \tag{3.17}$$

where N_{obj} is the number of objective functions, and M is the number of non-dominate solutions. The solution with the maximum membership can be considered as the best compromise solution.

b) IEEE 30-bus and IEEE 57-bus test systems

In first two cases (cases 1, 2), two competing objective functions, i.e., active power losses and voltage deviation are optimized simultaneously using MOALO algorithm. The best solution of control variables with results of minimum power loss, minimum voltage deviation, and power loss reduction in percentage, as well as CPU time, are listed in Tables 3.14– 3.16. In addition, under the same variable limits and constraints, the results obtained using MOALO are compared with those reported with the MOPSO and MOEPSO algorithms. From this comparison, it can be seen that MOALO is much more efficient than MOPSO and MOEPSO in terms of solution quality and computation time: with MOALO, the active power losses and voltage deviation for case 2 decreased by about 0.7198 MW and 0.0352 (p.u) compared to those reported with the MOEPSO algorithm. The distribution of the Pareto optimal front for the IEEE 30-bus test system is shown in Fig. 3.11.

Table 3.14 Comparison of simulation results of MOPSO and MOALO for case 1

Variables	**MOPSO** [64]			**MOALO**		
	Min P_{Loss}	Min *VD*	BCS	Min P_{Loss}	Min *VD*	BCS
V_{G1}	0.900	0.9003	1.0957	1.0984	1.0560	1.0802
V_{G2}	1.100	1.1000	1.1000	1.0914	1.0350	1.0719
V_{G5}	1.100	1.1000	1.1000	1.0683	1.0152	1.0438
V_{G8}	1.100	1.1000	1.1000	1.0766	0.9964	1.0481
V_{G11}	1.100	1.1000	1.1000	1.0703	1.0356	1.0614
V_{G13}	1.100	1.1000	1.1000	1.0398	1.0139	1.0304
$T_{6\text{-}9}$	1.04	1.10	1.08	1.0963	1.0272	1.0759
$T_{6\text{-}10}$	0.90	0.90	0.90	1.0368	0.9487	1.0140
$T_{4\text{-}12}$	0.98	1.10	1.04	1.0928	1.0007	1.0677
$T_{28\text{-}27}$	0.96	0.98	0.98	1.0310	0.9630	1.0085
Q_{C10}	5.00	0.50	0.00	4.6403	4.6017	4.6279
Q_{C12}	5.00	5.00	5.00	3.2946	3.7432	3.4322
Q_{C15}	5.00	5.00	5.00	4.1006	4.2643	4.1182
Q_{C17}	5.00	5.00	5.00	2.9287	3.1922	2.9951
Q_{C20}	5.00	5.00	5.00	4.9652	4.9082	4.9045
Q_{C21}	5.00	5.00	5.00	3.3647	3.6315	3.4059
Q_{C23}	5.00	5.00	5.00	3.4841	3.6185	3.4882
Q_{C24}	5.00	5.00	5.00	3.2282	3.5834	3.2965
Q_{C29}	3.50	2.50	2.50	4.9953	4.9441	4.9157
P_{Loss} (MW)	5.1089	5.2069	5.1450	**4.7633**	5.4267	**4.9201**
VD (p.u)	0.6130	0.1885	0.2821	0.6371	**0.1599**	**0.3880**
% P_{save_loss}	10.10	8.37	9.46	16.81	4.50	13.42
CPU (s)	53.2			**56.1**		

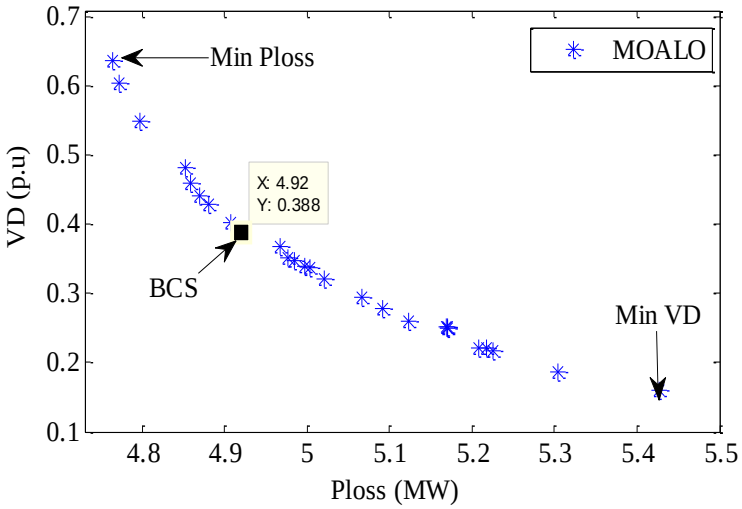

Figure 3.11 Pareto optimal front of MOALO, Case 1

Table 3.15 Comparison of simulation results of MOEA and MOALO for case 2

Variables	MOEA [94]	VEPSO [94]	MOALO
V_{G1}	1.050	1.0403	1.0759
V_{G2}	1.044	1.1000	1.0638
V_{G5}	1.023	1.0231	1.0395
V_{G8}	1.022	0.9500	1.0434
V_{G11}	1.042	1.0551	1.0415
V_{G13}	1.043	0.9500	1.0386
$T_{6\text{-}9}$	1.090	1.0329	1.0442
$T_{6\text{-}10}$	0.905	0.9913	1.0377
$T_{4\text{-}12}$	1.020	0.9974	1.0431
$T_{28\text{-}27}$	0.964	1.0165	0.9892
Q_{C10}	Fixed at 19.0	15.056	21.957
Q_{C24}	Fixed at 4.3	3.7842	9.6227
P_{Loss} (MW)	5.1995	5.0941	**4.9818**
VD (p.u)	0.2512	**0.1374**	0.3742

For case 3, the optimum values of power losses and voltage stability index (L-index) obtained with MOALO were 26.3952 MW and 0.2854, i.e. 16% and 1.02% less than those reported with MOPSO.

Table 3.16 Comparison of simulation results of MOEPSO and MOALO for case 3

Objectives	**MOEPSO** [64]			**MOALO**		
	Min P_{Loss}	Min *VD*	BCS	Min P_{Loss}	Min *VD*	BCS
P_{Loss} (MW)	27.3128	27.7258	27.4268	**26.593**	27.967	**27.2131**
VD (p.u.)	1.0724	0.8459	0.89635	1.1039	**0.8107**	**0.8909**
CPU (s)	531.07			115.02		

Furthermore, the computational time for MOALO was less than for the MOPSO and MOEPSO algorithms for case 2 and case 3, but a little worse for case 1. The reactive power outputs of generators corresponding to the MOORPD solution obtained by the proposed MOALO for cases 2, and 3 are presented in Figs 3.12–3.13. Figure 3.14 depicts the voltage profile of case 2. These results amply confirm the capability of the proposed algorithm to handle the equality and inequality constraints of the MOORPD problem.

Table 3.17 Comparison of simulation results of MOPSO and MOALO for 57-bus system

Variables	**MOPSO** [67]			**MOALO**		
	Min P_{Loss}	Min *VSI*	BCS	Min P_{Loss}	Min *VSI*	BCS
V_{G1}	1.10000	1.10000	1.10000	1.0638	1.0456	1.0550
V_{G2}	0.90000	0.90000	0.90000	1.0486	1.0298	1.0381
V_{G3}	1.10000	1.10000	1.10000	1.0510	1.0297	1.0383
V_{G6}	1.10000	0.99771	1.05681	1.0570	1.0336	1.0424
V_{G8}	0.90000	0.90000	0.90000	1.0967	1.0764	1.0830
V_{G9}	1.08959	0.96893	1.05494	1.0666	1.0462	1.0552
V_{G12}	1.10000	1.10000	1.10000	1.0805	1.0642	1.0701
$T_{4\text{-}18}$	0.90000	0.90000	0.90000	1.0195	0.9978	1.0053
$T_{4\text{-}18}$	0.97000	1.00000	1.01000	1.0340	1.0112	1.0210
$T_{21\text{-}20}$	1.01000	1.10000	1.04000	1.0990	1.0952	1.0983
$T_{24\text{-}25}$	0.90000	0.90000	0.90000	0.9909	0.9642	0.9735
$T_{24\text{-}25}$	1.10000	1.10000	1.10000	1.0128	0.9844	0.9934
$T_{24\text{-}26}$	1.10000	1.10000	1.10000	1.0998	1.0947	1.0977
$T_{7\text{-}29}$	0.91000	0.91000	0.91000	0.9973	0.9693	0.9799
$T_{34\text{-}32}$	0.90000	0.90000	0.90000	1.0305	1.0029	1.0136
$T_{11\text{-}41}$	0.90000	0.9000	0.90000	1.0260	1.0057	1.0138
$T_{15\text{-}45}$	0.92000	0.9200	0.92000	0.9904	0.9642	0.9737
$T_{14\text{-}46}$	0.90000	0.9000	0.90000	0.9828	0.9579	0.9672
$T_{10\text{-}51}$	0.90000	0.9000	0.90000	0.9963	0.9759	0.9853
$T_{13\text{-}49}$	1.10000	1.1000	1.10000	1.0084	0.9902	0.9988
$T_{11\text{-}43}$	0.91000	0.9100	0.91000	0.9987	0.9738	0.9825
$T_{40\text{-}56}$	1.10000	1.1000	1.10000	1.0291	1.0038	1.0140
$T_{39\text{-}57}$	0.97000	1.0300	1.01000	0.9995	0.9765	0.9864
$T_{9\text{-}55}$	0.92000	0.9200	0.92000	1.0650	1.0421	1.0525
Q_{C18}	7.500	18.50	17.50	5.8080	5.8077	5.8632
Q_{C25}	0.000	0.000	0.000	8.6317	8.3751	8.4914
Q_{C53}	0.000	0.000	0.000	13.5386	13.3489	13.4402
P_{Loss} (MW)	31.424	31.595	31.462	**26.3952**	27.2634	**26.7477**
VSI (p.u)	0.29123	0.28834	0.28952	0.2994	**0.2854**	**0.2885**
CPU (s)	424.59			151.55		

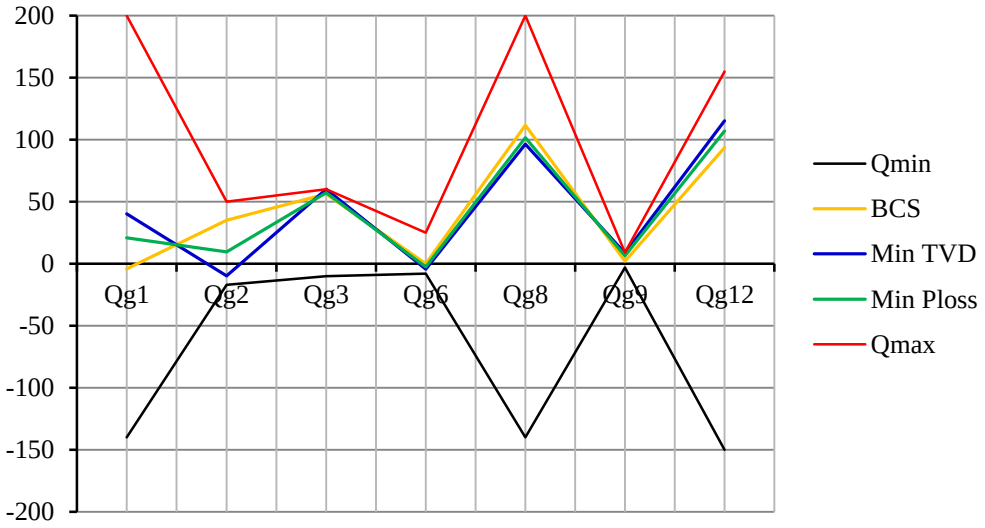

Figure 3.12. Reactive power outputs at generators for Case 2, IEEE-57 bus system

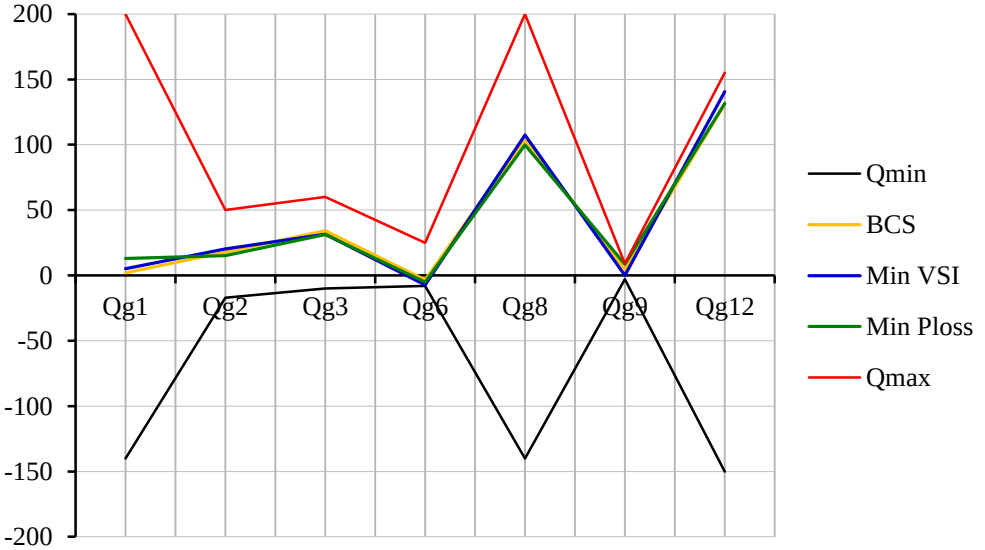

Figure 3.13. Reactive power outputs at generators for Case 3, IEEE-57 bus system

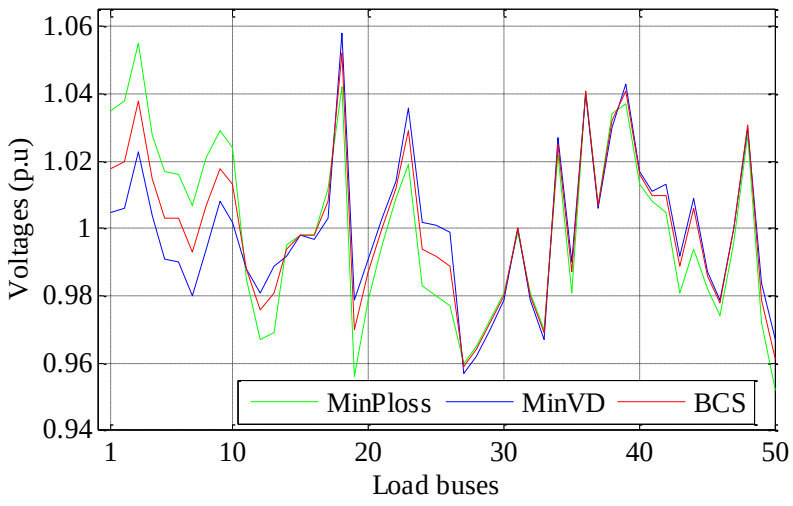

Figure 3.14 Voltage profile for IEEE 57-bus system, case 2, Ploss and VD

In order to further assess the results obtained and to highlight the value of the MOALO algorithm in solving the constrained MOORPD problem, the accuracy of the results reported with the MOPSO and MOEPSO algorithms as well those obtained with the MOALO algorithm were checked, specifically those of the dependent variables (reactive power outputs of generators and load bus voltages). The outcomes were recalculated by using the corresponding optimal control variables of each simulation case as input data of the MATPOWER load flow program.

The exact results of P_{Loss}, *VD*, and *L-index* obtained from the power flow program for the three cases are summarized in Table 3.18. A meticulous observation of these results reveals a violation of the dependent variables' limits, rendering the solutions infeasible. An in-depth critical analysis of the reported results was carried out on the IEEE 30-bus and IEEE 57-bus test systems and can be summarized as follows:

- ***Case 1***− *min* P_{Loss}: The reactive power of generators at buses 1, 2, and 8 violates their limits by 95.14 %, 95.26 %, and 31.81 % respectively. Also, all the voltage magnitudes at the load buses except buses 3 and 4 exceed the fixed limits [0.94−1.06] p.u.
- ***Case 2***− *min VD*: The reactive power of generators in all PV buses except 12 violates their limits by 79.26 %, 95.51 %, 94.71, 42.92, and 99.67 % respectively. Also, almost all voltage magnitudes at the load buses exceed the upper and lower limits [0.94−1.06] p.u. In addition, the exact values of power loss and voltage deviation are 134.634 MW and 3.8182 (p.u) respectively. Therefore, there are significant differences between reported and recalculated results.
- ***Case 3***− *min VSI*: The reactive power of generators at all buses 1, 2, 3, 6, 8, 9, and 12 violates their limits by 73.26 %, 97.77 %, 86.78 %, 60.93%, 39.20%, 78.46%, and 41.16% respectively. Furthermore, the voltage magnitudes at the load buses 7, 8, 16–18, 43–48, 51 exceed the voltage limits [0.94 − 1.06] p.u.

The same verifications were performed for all the remaining cases, and significant differences between the obtained power flow outcomes and the corresponding results reported in references [67] and [64] were found (see Tab. 3.18). These solutions are therefore judged to be infeasible due to the undesirable violation of dependent variables. On other hand, just a glance at Fig 3.14 and Table 3.17 is sufficient to confirm the consistency of the proposed algorithm of finding the best solutions while satisfying the power flow equations, system security, and equipment operating limits.

Table 3.18 Results of power flow for control variables given in Tables 3.14−3.16

Algorithms		**Calculated**		**Violating constraints**	
		P_{Loss} (MW)	VD (p.u)	Load buses	Q_G
min P_{Loss}	**Case 1** MOPSO	36.993	2.137	all buses except 3 and 4	1,2, and 8
min VD		36.971	1.54	4, 6, 10, 17, 25, 27, 28, 29	1, 2, 3
BCS		4.836	2.027	all buses	1
min P_{Loss}	**Case 2** MOEPSO	123.78	2.976	12-20, 24,26, 27, 30, 31,34-39, 55, 57	1-3, 6, 8, 9,12
min VD		134.63	3.818	4, 5, 13-28, 30-44, 55	all except 12
BCS		149.62	2.964	4, 5, 11-17, 19-26, 30-40, 55	all except 12
min P_{Loss}	**Case 3** MOPSO	117.98	***VSI*** 0.249	4, 5, 11, 13-25, 32, 33, 36-51, 54-57	all except 12
min ***VSI***		105.44	0.273	7, 8, 16-18, 43-48, 51	1-3, 6, 8, 9,12
BCS		109.52	0.256	4, 8, 13,15-24, 32, 33, 38, 41,43-48, 50,	all except 12

c) Large-scale test system, IEEE 300-bus

In order to examine the capability of MOALO algorithm to solve the MOORPD problem in a large-scale power system, the IEEE 300-bus [76] was used as the test system. The min/max of the control vector were taken from [80]. Moreover, it is important to note that this test system exhibits very large voltage drops [86], making it harder to ensure the feasibility of solutions.

Discussion

Under the constraints used here, the P_{loss} and *VD* were optimized simultaneously as multi-objective functions on a large-scale IEEE 300-bus system. The Pareto optimal front obtained using MOALO is depicted in Figure 3.15. The optimal values of reactive power sources as well as the P_{Loss}, *VD*, and best compromise solution (*BCS*) are listed in Table 3.19 that also satisfies system security. Power losses and voltage deviation were reduced by 3.63% and 4.76 % respectively with respect to the base case. The average computation time required to attain a near-optimal solution for the large-scale power system was 23.8 seconds per iteration. In addition, from Figure 3.15, it can be seen that the optimal Pareto front has a good distribution of the non-dominated solutions, thus validating the potential of MOALO algorithm to solve the nonlinear multi-objective problem.

Table 3.19 Reactive power outputs of parallel compensators for IEEE 300-bus, case 4

IEEE 300-bus system								
Variables	Limits		Case 4			**Case 5**		
	Q_{min}	**Q_{max}**	Min P_{Loss}	Min *VD*	BCS	Min P_{Loss}	Min *VSI*	BCS
Q_{96}	**0**	**4.5**	3.661	3.614	3.638	1.991	1.915	1.962
Q_{99}	**0**	**0.59**	0.4218	0.4176	0.4188	0.509	0.500	0.506
Q_{133}	**0**	**0.59**	0.3108	0.3087	0.3085	0.444	0.433	0.440
Q_{143}	**-4.5**	**0**	-4.3382	-4.2047	-4.251	-2.574	-2.621	-2.59
Q_{145}	**-4.5**	**0**	-2.4711	-2.3514	-2.4021	-3.377	-3.428	-3.95
Q_{152}	**0**	**0.59**	0.1534	0.1471	0.1503	0.1721	0.1629	0.1685
Q_{158}	**0**	**0.59**	0.5589	0.5539	0.5543	0.5325	0.5163	0.5274
Q_{169}	**-2.5**	**0**	-1.2811	-1.2306	-1.2443	-2.231	-2.262	-2.238
Q_{210}	**-4.5**	**0**	-3.036	-2.935	-2.989	-4.194	-4.214	-4.201
Q_{217}	**-4.5**	**0**	-3.991	-3.904	-3.938	-3.305	-3.386	-3.328
Q_{219}	**-1.5**	0	-0.6356	-0.5987	-0.6115	-0.8038	-0.8135	-0.807
Q_{227}	0	0.59	0.5059	0.4957	0.4983	0.375	0.362	0.369
Q_{268}	0	0.15	0.1143	0.1125	0.1131	0.1180	0.1157	0.1170
Q_{283}	0	0.15	0.0868	0.08560	0.0860	0.0847	0.0825	0.0839
P_{Loss} (MW)			**393.4646**	408.899	**398.852**	**384.5104**	392.7140	**386.24**
VD (p.u)			8.5482	**5.1702**	**6.0169**			
L-index						0.2058	**0.1983**	**0.2010**

Q_g in p.u,

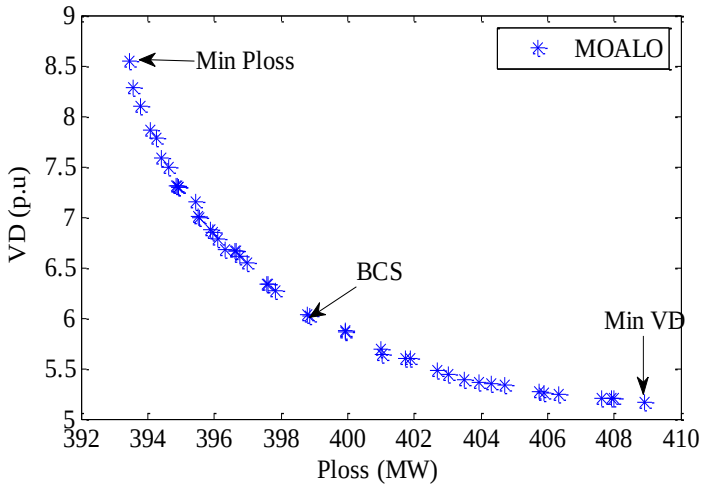

Figure 3.15 Pareto optimal front of MOALO, Case 4

For case 5, the optimum values for power losses and voltage stability index obtained with the MOALO algorithm were 384.51 MW and 0.1983 respectively, i.e. a reduction of 5.83% and 52% respectively compared with the base cases. It is necessary to note that the voltages magnitudes at all of load buses are inside the imposed boundaries. Therefore, according to Table 3.19, the reactive powers of the parallel compensators are within the admissible limits, confirming the efficiency of the proposed algorithm to obtain the feasible solutions. Figure 3.16 shows the distribution of non-dominant solutions that correctly represent the Pareto optimal front.

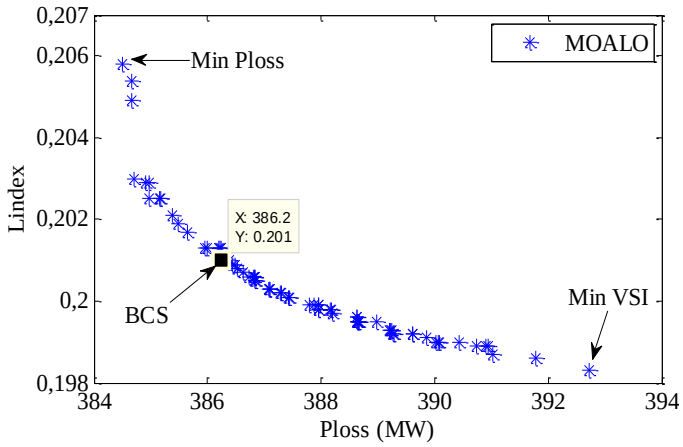

Figure 3.16 Pareto optimal front of MOALO algorithm, Case 5

As a result, even with the large-scale test system, the MOALO algorithm gives the best adjustment of control variables and converges well to the Pareto front with a good diversity of solutions. In other words, it has been also proven that the proposed MOALO algorithm is more suitable to solve MOORPD than the other algorithms of which it can not only benefit from good distributions of the non-dominated solutions, but also guarantee the feasibility of solutions obtained for three test power systems.

3.5. Conclusion

In this chapter, a newly introduced optimization paradigm namely AEO, has been proposed to cope with the nonlinear ORPD problems in the practical and large-scale power systems. Among these algorithms are ALO, and its version multi-objective (MOALO), WOA, NBA, and AEO. These optimization techniques have been extended to solve mixed integer optimization problems with discrete variables. Also, adopted as search strategies to define optimal control variables, so that desired objective functions are optimized. Medium-size and large scale as well as Practical Algerian power system are selected as test systems. The conflicting objectives, namely real power loss, voltage deviation, and voltage stability index were successfully minimized under various constraints. An in-depth analysis on the both obtained and reported results was presented, verified and approved the feasibility of solutions. The comparison indicates that the proposed approaches are much more effective than others algorithms in terms of the quality of obtained optimal solutions and simulation time required. At the end, on the light of detailed information given in this article, it is concluded that the suggested algorithm is the more suitable choice of coping optimal reactive power dispatch problems where it proves its efficiency even with large-scale and real power systems.

Chapter 4

OPF STUDY INCORPORATING STOCHASTIC WIND AND SOLAR POWER

4.1. Introduction

Recently, the Optimal Power Flow solution in large-scale systems under uncertainties of intermittent energy sources has attracted considerable attention. However, despite the huge efforts conducted in this area since half-a-century ago, this issue is still an open subject nowadays. In this context, determination of the optimum operating parameters of electric grid with optimal scheduling of different energy sources is very important. In this chapter, we propose artificial ecosystem optimization (AEO) algorithm to cope with stochastic optimal power flow (OPF) problem in presence of renewable energy sources. The problem is formulated as large-scale constrained optimization problem with non-linear characteristics. Its degree of complexity increases with incorporation of intermittent and uncertain renewable sources, making it harder to be solved using conventional optimization techniques. However, it can be efficiently resolved by using nature-inspired optimization algorithms and solvers without any modification or approximation into the original-formulation. The Weibull and lognormal probability-distribution-functions (PDF) are used to forecast wind power and solar photovoltaic production, respectively. The objective function is the overall cost of system, including reserve cost for over-estimation and penalty cost for under-estimation of both PV-solar and wind energy. Several numerical results of IEEE 30-bus test system and Algerian electricity grid DZD114-bus (220/60 kV) serve to show the performance of the proposed algorithm. A comparative study of the experimental results confirms that proposed AEO performs better than other optimizers in all studied cases for both electric grids.

4.2. Overview and literature of stochastic OPF problem

OPF is one of primordial tools of electric power systems, offering the electric power at minimum cost with high quality. In short, is therefore the backbone of electric grids due to the important role that its plays in facilitating operation and planning functions. Its master objective is to specify the optimal adjustment of control variables so that a selected objective function is optimized while satisfying various physical and operational constraints imposed by electric power grids (equality and inequality constraints). The most commonly treated objective function is the minimization of the overall generation cost. However, other

functions are minimization of gas emission, active power loss, voltage stability index, and bus voltage deviation [19].While the used control variables are active power of generators outputs, generator voltages magnitudes, positions of the transformer taps, and amount of reactive power sources injected by parallel compensators. These variables are a mix between discrete and continuous ones, the parallel compensators and tap changer transformer are discrete variables, whereas the remaining ones are continuous.

In traditional electric grids, the study of OPF considers conventional power generators run on fossil-fuels. However, with electricity market liberalisation, and integration of renewable energy sources (RES), study of OPF becomes more complicated leading to increase the complexity of objective function significantly. This is due to the diverse functions based on the variability and uncertain used in its problem formulation. The prime objective behind incorporation of wind power and solar PV generators in the grids is to reduce the transmission line losses and improving the reliability and quality of electric grids. Also they reduce environmental pollution [95]. In addition, with increasing of injected power from RES, specifying optimal contribution of each generator in the system is necessity. Thus, energy management and optimal scheduling of different resources can effectively help diverse missions of electric power system operator, ultimately reducing total generation electricity cost.

In the few past decades, numerous conventional optimization techniques have been applied to solve different versions of OPF problem. The conventional solvers are the Newton method [96] [97], non-linear programming (NLP) [98] and interior point methods [99]. Despite the fact that some of abovementioned methods have excellent convergence characteristics and some of them are usually suitable for industry applications. However, they have some weaknesses, which are summarized as follows:

1) Sensitivity to the initial search point, i.e., they might converge easily to local solutions as may converge to global ones.
2) Lack of flexibility with respect to practical systems, i.e., each method is suit for a specific problem formulation in its proper objectives and/or constraints.
3) Besides the inflexibility aspect, they also encounter a huge difficult to set of uncertain and stochastic problems, such as OPF with application of renewable generation.

Therefore, developing new and effective optimization methods is necessity in effort to overcome the shortcomings of the traditional optimization techniques'[100]. Thanks to the computational intelligence, schemes and open access to optimization techniques have

liberated considerable researches in the field of meta-heuristic algorithms to solve complex optimization problems during first decade. These optimizers have ability to provide near-global solutions and capability to escape local ones, avoiding in premature convergence. Many meta-heuristic optimization algorithms have been implemented to cope with classical OPF problem like improved version of PSO [101], moth swarm algorithm (MSA) [29], improved bacterial forging method (IBF) [102], teaching-learning-based optimization (TLBO) technique [103], backtracking search optimization algorithm (BSA) [31], improved colliding bodies optimization (ICBO) [32], and adaptive multiple teams perturbation-guiding Jaya (AMTPG-Jaya) algorithm [36]. While aforementioned references are limited on the thermal power generators only. In the few past years, a system with mixed resources involving thermal, wind and solar generators have been studied in quest of provide electrical energy at minimum generation-cost with high-quality. As mentioned earlier, electricity market allows the incorporation of renewable sources to be connected into the electric grid in order to minimize the environmental problems and relief transmission lines loading as well enhancing bus voltage profile by power losses curtailment. In that context, a few works has been published in literatures. For instance in [104] modified Jaya algorithm is applied to solve OPF incorporating RES considering four different objective functions to improve recorded results against other optimizers while the RES is modeled as a negative load, but any forecasting technique was not employed to forecast wind and solar photovoltaic power output. The results show outperforms of MJAYA on the basic Jaya as well on other existing algorithms. *Partha Biswas* et all [48] proposed success history based parameter adaptation technique of differential evolution (SHADE) to solve OPF problem in a system involving renewable power generators. Also, forecasting model is well designed to report renewable power generators outputs. In addition, the feasibility of results were discussed and checked that all control variables fell inside the allowed limits. Thus, findings clearly show the efficacy of the proposed model. In another publication [49], Ehab E.Elattar proposed modified version of the moth swarm algorithm to solve OPF problem of combined heat and power system with presence stochastic wind farm. Zia Ullah et al [50] provide a new hybrid optimization algorithm PPSOGSA for OPF solution considering renewable energy generators. The model of stochastic behavior is based of PDF scheme. In Yu-Cheng Chang et al [51], evolutionary particle swarm optimization (EPSO) algorithm was used for solving OPF problem in a wind-thermal power system. The suggested wind model is based on the up-spinning reserves and dow-spinning reserves of the production units. A modified cuckoo search optimization technique employed for OPF solution incorporating wind power was proposed in Chetan

Mishra el al in [52]. The proposed stochastic model of wind generation is based on the Weibull PDF. Again, however, the simulation was also conducted only on standard medium-sized test systems.

From the aforementioned works point of view, the results are promising and encouraging, however, OPF in an electric-grid consisting thermal generators and renewable energy generators (wind power + solar PV) needs further attention. Despite these optimization methods have realised satisfactory results, but still suffer from some limitations and shortcomings as far as their susceptibility of falling into local optima and the difficulty of tuning the main intrinsic parameters. Moreover, the diversity of sub-functions used to formulate the objective function for OPF problem in presence of renewable energy sources give an opportunity to solve complex-problems by suggesting or developing effective meta-heuristic techniques able deal different OPF formulations.

4.3. OPF study with stochastic wind and solar power

Traditional grid consists only of thermal-generators, wherein the study OPF is a complex problem with non-linear characteristics. Incorporating stochastic-nature of wind and solar power significantly increase the complexity of the problem. This work presents a formulation and solution procedure for sole-objective OPF problem incorporating RES. Total generation cost, total voltage deviation of load buses and voltage stability index in the electric grid are optimized independently as single objective functions. Case studies with valve-point loading effect and emission of thermal units are also considered.

In this study, ALO, AEO, and WOA algorithms are adopted to cope with OPF problem merging stochastic wind energy and solar power with conventional thermal units in the system. The standard IEEE 30- test system is selected as test system. Herein, superiority of feasible solutions (SF) method is more suitable one to handle constraints of stochastic OPF problem, due to some limitations of static penalty function method mentioned in chapter 2. Simulations results are analysed in detail and the feasibility of solutions were critically discussed.

The rest of the chapter is organized as following way. Mathematical formulation of OPF problem with different objective functions is presented in section 4.3.1. Modeling of uncertainties in wind and solar power is highlighted in section 4.3.2, followed by a detail on the data of test systems for all cases study is provided. Sections 4.3.3-4.3.5 discussed the feasibility of obtained results followed by its comparison with those reported in the recent published papers. The conclusion of this chapter is drawn in section 4.3.4.

4.3.1. Mathematical models of OPF involving stochastic wind and solar power

Table 4.1 abridges basic data of the modified IEEE 30-bus test system. This system consists in overall on six thermal generators, but the modified one consists of three conventional thermal units attached at buses 1, 2 and 8; two wind generators in the buses 5 and 11 and one PV array installed in the bus 13. Figure 4.2 shows the diagram of this test system. There are two case studies, of which first, one has 11-control variables for the optimization and the second has 15 variables. In addition, since the outputs of wind and solar generators are variables, the fluctuation in power output must be balanced by merging outputs from all the generators and the reserve.

Table 4.1. Summary of modified IEEE 30-bus test system

Items	**Quantity**	**Details**
Buses	30	
Branches	41	
Thermal generators TG_1, TG_2, TG_3	3	Buses: 1 (swing), 2 and 8
Wind generator (WG_1, WG_2)	2	Buses: 5 and 11
PV unit (PV)	1	Bus: 13
Connected load	283.4 +j126.2	
Allowable limit for load-bus voltage	24	[0.95 – 1.05] p.u.

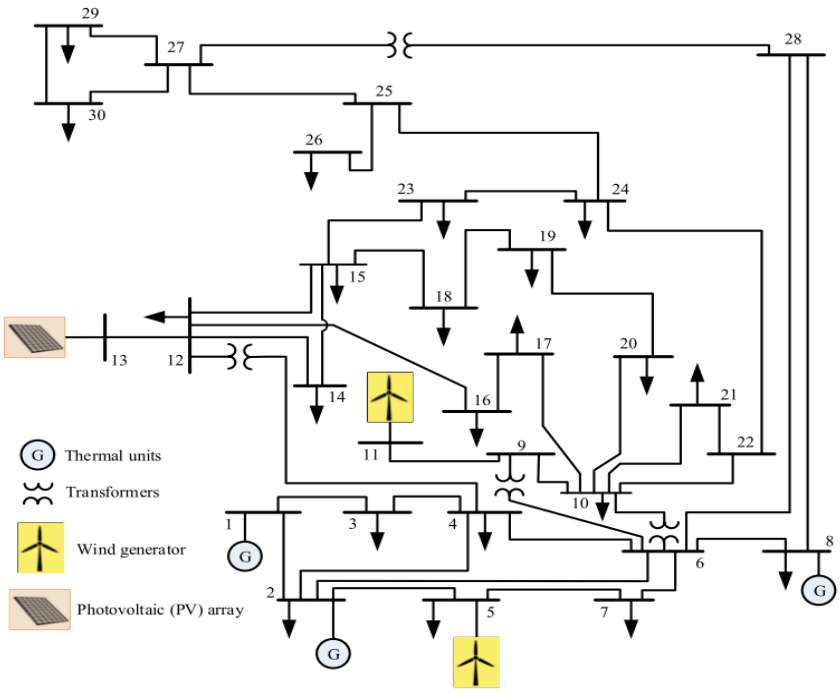

Figure 4.1. Modified IEEE 30-bus system for OPF study with intermittent sources

a) Cost model of thermal power plants

The fuel cost of thermal power generators can be described as:

$$C_{\mathrm{T0}}\left(P_{TG}\right)=\sum_{i=1}^{N_{TG}} a_i+b_i P_{TGi}+c_i P_{TGi}^2 \tag{4.1}$$

For more realistic pattern and precise modelling valve-point effect scheme is considered. The cost function C under valve-point loading rewritten as follows:

$$C_{\mathrm{T}}\left(P_{TG}\right)=\sum_{i=1}^{N_{TG}} a_i+b_i P_{TGi}+c_i P_{TGi}^2+\left|d_i \times \sin\left(e_i\left(P_{TG}^{\min}-P_{TG}\right)\right)\right| \tag{4.2}$$

Where $a_i, b_i, c_i, d_i,$ and e_i are the cost coefficients of the i-th thermal generators producing power output P_{TGi}, N_{TG} is the number of thermal generating and $P_{TG}^{\min}$ is the minimum of power of conventional thermal generator. The cost and emission gas coefficients for the conventional units used here are provided in Table 4.3.

b) Direct cost of wind energy and photovoltaic power

Wind and solar generators require no fuel like conventional thermal generators. Therefore, if the installation of wind/solar power units are private, i.e., independent system operator (ISO), the direct cost parameter may not exist. However, in case of the renewable power plants is owner for private party, ISO pays a price proportional to the scheduled power contractually agreed. A direct cost assigned with wind power from j-th plant can be modelled as a follows:

$$Cost_{w,j}\left(P_{ws,j}\right)=g_j P_{ws,j} \tag{4.3}$$

where g_j is the coefficient of direct-cost attached with j-th wind power plant and $P_{ws,j}$ represent the scheduled power from the same plant

Also, direct cost pertaining to k-th PV power plant can be expressed as follows:

$$Cost_{s,k}\left(P_{ss,k}\right)=h_k P_{ss,k} \tag{4.4}$$

where h_k is the coefficient of direct-cost attached with k-th solar power plant whereas $P_{ss,k}$ represent the scheduled-power from the same plant.

c) Cost due to the underestimation power of wind farm (penalty-cost)

The situation of underestimation power happens when actual power delivered by the wind farm is higher than the estimated value, reason to the uncertain source. This cost named penalty-cost, which mathematically can be expressed as follows:

$$C_{RW,j}\left(P_{wav,j}-P_{ws,j}\right)=K_{PW,j}\left(P_{wav,j}-P_{ws,j}\right)$$
$$=K_{PW,j}\int_{P_{ws,j}}^{P_{wr,j}}\left(p_{w,j}-P_{ws,j}\right)f_w\left(P_{w,j}\right)dp_{w,j} \quad (4.5)$$

where $K_{PW,j}$ is the penalty cost coefficient for the *j*-th wind power plant, $P_{wav,j}$ is the actual available power from the same plant. $f_w\left(P_{w,j}\right)$ is the wind power probability density function for *j*-th wind power plant.

d) Cost due to overestimation on power of wind farm (Reserve cost)

The overestimation of wind power happens when actual power delivered by the wind farm is less than the estimated value. In this situation, the utility operator needs to have a spinning reserve. So, the spinning reserve cost is written with following equation:

$$C_{RW,j}\left(P_{wsj,j}-P_{avj,j}\right)=K_{RW,j}\left(P_{ws,j}-P_{wav,j}\right)$$
$$=K_{RW,j}\int_{0}^{P_{ws,j}}\left(p_{ws,j}-P_{w,j}\right)f_w\left(P_{w,j}\right)dp_{w,j} \quad (4.6)$$

where $K_{RW,j}$ is the reserve cost coefficient pertaining to wind power plant, $P_{wav,j}$ is the actual available power from the same plant.

e) Cost evaluation of uncertainties in photovoltaic power

Like wind power generators, PV power units also have intermittent and uncertain output. Reserve cost for the k-th solar PV plant is:

$$C_{Rs,k}\left(P_{ss,k}-P_{sav,k}\right)=K_{Rs,k}\left(P_{ss,k}-P_{sav,k}\right)$$
$$=K_{Rs,k}*f_s\left(P_{sav,k}<P_{ss,k}\right)*\left[P_{ss,k}-E\left(P_{sav,k}<P_{ss,k}\right)\right] \quad (4.7)$$

where $K_{Rs,k}$ is the reserve cost coefficient relative to *k*-th solar power plant, $P_{sav,k}$ is the actual available power from the same plant. $\left(P_{sav,k}<P_{ss,k}\right)$ is the probability of solar power shortage i.e. actual power below the scheduled power $(P_{ss,k}), E\left(P_{sav,k}<P_{ss,k}\right)$ is the expectation of PV power below $P_{ss,k}$

Penalty cost for the underestimation of *k*-th solar power plant is:

$$C_{Ps,k}\left(P_{sav,k}-P_{ss,k}\right)=K_{Ps,k}\left(P_{sav,k}-P_{ss,k}\right)$$
$$=K_{Ps,k}*f_s\left(P_{sav,k}>P_{ss,k}\right)*\left[E\left(P_{sav,k}>P_{ss,k}\right)-P_{ss,k}\right] \quad (4.8)$$

where $K_{Ps,k}$ is the penalty cost coefficient pertaining to k-th solar power plant, $f_s\left(P_{sav,k} > P_{ss,k}\right)$ is the probability of solar power surplus i.e. actual power above the scheduled power ($P_{ss,k}$), $f_s\left(P_{sav,k} > P_{ss,k}\right)$ is the expectation of solar power above $P_{ss,k}$.

f) Emission and carbon tax

Conventional thermal generators emit harmful and greenhouse gases, such as SO_X, and NOx, and CO_2 into the environment, which pollute the atmosphere. The objective function of emission is written as follows:

$$E = \sum_{i=1}^{N_{TG}}\left[\left(\alpha_i + \beta_i P_{TGi} + \gamma_i P_{TGi}^2\right)\times 0.01 + \omega_i \exp\left(\mu_i P_{TGi}\right)\right] \tag{4.9}$$

$$\text{Emission cost, } C_E = C_{TAX} \times E \qquad C_{TAX} = 20 \tag{4.10}$$

where α_i, β_i, γ_i ω_i, μ_i are the emission coefficients corresponding to the i-th generator given in Table 4. 2

Table 4.2. Cost and emission coefficients for thermal generators of IEEE 30-bus

Gen	Bus	a	b	c	d	**e**	α	β	γ	ω	μ
TG1	1	0	2	0.00375	18	0.037	4.091	-5.554	6.49	0.0002	2.857
TG2	2	0	1.75	0.01750	16	0.038	2.543	-6.047	5.638	0.0005	3.33
TG3	8	0	3.25	0.00834	12	0.045	5.326	-5.554	3.38	0.002	2

g) Objectives of optimization

All objective functions of OPF are formulated considering all the aforementioned cost functions. The first objective functions minimize the generation cost without including emission cost.

$$\begin{aligned} F_{Obj}^1 = C_T\left(P_{TG}\right) + &\sum_{j=1}^{N_{WG}}\left[C_{w,j}\left(P_{ws,j}\right) + C_{Rw,j}\left(P_{ws,j} - P_{wav,j}\right) + C_{PW,j}\left(P_{wav,j} - P_{ws,j}\right)\right] \\ &+ \sum_{k=1}^{N_{SG}}\left[C_{s,k}\left(P_{ss,k}\right) + C_{Rs,k}\left(P_{ss,k} - P_{sav,k}\right) + C_{Ps,k}\left(P_{sav,k} - P_{ss,k}\right)\right] \end{aligned} \tag{4.11}$$

Where N_{WG} and N_{SG} are the numbers of wind generators and solar PVs in the grid, respectively. All the remaining cost components are given in eqs. 4.2 – 4.8

Second objective function Minimize-

$$F_{Obj}^{2} = F_{Obj}^{1} + C_{tax} \times E \tag{4.12}$$

h) Constraints

Equality constraints include the typical load flow equations, which are given below:

$$\begin{cases} P_{Gi} - P_{Di} - \sum_{j=1}^{NB} |V_i| \times |V_j| \times |Y_{ij}| \times \cos\times\left(\theta_{ij} - \delta_i + \delta_j\right) = 0 \\ Q_{Gi} - Q_{Di} - \sum_{j=1}^{NB} |V_i| \times |V_j| \times |Y_{ij}| \times \sin\times\left(\theta_{ij} - \delta_i + \delta_j\right) = 0 \end{cases} \tag{4.13}$$

where $\theta_{ij} = \theta_i - \theta_j$, is the difference of voltage angles of bus *i* and *j*, *NB* is the total number of buses, P_{Di} and Q_{Di} are active and reactive load demands, respectively at bus *i*, P_{Gi} and Q_{Gi} are active and reactive power generation respectively from all sources.

Inequality constraints: include the power flow equations, which are given below:
These constraints reflect the system operational and the security limits in the power system. They are described below:

a) Generator constraints

$$P_{TGi}^{\min} \le P_{TGi} \le P_{TGi}^{\max}, \qquad i = 1,2.....N_{TG} \tag{4.14}$$

$$P_{wsj}^{\min} \le P_{wsj} \le P_{wsj}^{\max}, \qquad j = 1,2.....N_{WG} \tag{4.15}$$

$$P_{ss,k}^{\min} \le P_{ss,k} \le P_{ss,k}^{\max} \qquad k = 1,2.....N_{SG} \tag{4.16}$$

$$Q_{TGi}^{\min} \le Q_{TGi} \le Q_{TGi}^{\max}, \qquad i = 1,2.....N_{TG} \tag{4.17}$$

$$Q_{wsj}^{\min} \le Q_{wsj} \le Q_{wsj}^{\max}, \qquad i = 1,2.....N_{WG} \tag{4.18}$$

$$Q_{ss,k}^{\min} \le Q_{ss,k} \le Q_{ss,k}^{\max} \qquad k \in N_{SG} \tag{4.19}$$

$$Q_{Ci}^{\min} \le Q_{Ci} \le Q_{Ci}^{\max} \qquad i \in N_C \tag{4.20}$$

$$V_{Gi}^{\min} \le V_{Gi} \le V_{Gi}^{\max}, \tag{4.21}$$

$$V_{Li}^{\min} \le V_{Li} \le V_{Li}^{\max} \qquad i \in NL \tag{4.22}$$

b) Security constraints

$$T_k^{\min} \le T_k \le T_k^{\max} \qquad k \in NT \tag{4.23}$$

$$S_i \le S_i^{\max} \qquad i \in NTL \tag{4.24}$$

Eqs. 4.14 − 4.16 represent the active power generation limits of thermal, wind and solar power generators, respectively. Eqs. 4.17 − 4.20 define the reactive power capabilities of thermal, wind, solar power generators and shunt reactive power sources. Eq. 4.21 present the constraint on voltage of PV buses, while eq. 4.22, defines the voltage limits imposed on load buses (PQ buses) with *NL* being the number of load buses. Constraints security of tap changing transformer and line capacity constraints are given by eqs, 4.23 and 4.24 respectively. *NTL* is the number of lines in the electric grid.

Convergence of power flow to a solution ensures when the equality constraints of power balance equations are satisfied. In addition, a feasible solution is directly depending on the controlling decision variables, i.e., if all decision (control) variables without exception are within allowable limits, then this solution is feasible; otherwise, the solution is infeasible. Therefore, it is worth mentioning that feasibility of generators reactive power capability is an important factor in OPF study.

In the last years, the reactive power capability of wind turbines has considerably been enhanced. Wind turbines (WTs) featuring full reactive power capability are available already in market. Furthermore, authors in [105] discusses dependence of reactive Power capability of wind turbines based on doubly fed induction generators (DIFG) on several factor for a certain active power. However, the reactive power range is found to be approximately between –0.8 p.u. and 0.8 p.u. Similarly, Ref. [106] also analyses reactive power capability of PV including converter and controller models. In this study the reactive power capability of the solar power generator is approximately considered between –0.4 p.u. and 0.5 p.u. [106].

In this context, active power losses in the grid and cumulative deviation of voltages of PQ buses are also important objectives to be optimized. The power loss in transmission lines is unavoidable as lines have inherent-resistances. The objective function of grid loss is calculated through the following equation:

$$\begin{aligned} \mathrm{F}_2(x,\mathrm{u}) = \min P_{\mathrm{Loss}} &= \sum_{k=1}^{NTL} G_k \times \left(V_i^{\,2} + V_j^{\,2} - 2 \times V_i \times V_j \times \cos\delta_{ij}\right) \\ &= \sum_{i=1}^{NTL}\sum_{j\neq i}^{NTL} G_{ij} \times \left(V_i^{\,2} + V_j^{\,2} - 2 \times V_i \times V_j \times \cos\left(\delta_i - \delta_i\right)\right) \end{aligned} \tag{4.25}$$

where $\delta_{ij} = \left(\delta_i - \delta_j\right)$ is difference in voltage angles between bus *i* and bus *j* and G_k is the conductance of transfer.

Voltage quality in the grid is measured by voltage deviation level. The voltage deviation indicator is modeled as result of voltage magnitudes minimization of all load buses in the electric grid around nominal value of 1 p.u. Expressed as follows:

$$\mathrm{F}_3(x,\mathrm{u}) = \min VD(x,\mathrm{u}) = Minimize\left(\sum_{i=1}^{Npq} |V_{Li} - 1|\right) \tag{4.26}$$

The equations 4.25 – 4.26 to be used are same as eq. 3.5 – 3.6 and re-written here for easy reference.

4.3.2. Stochastic wind/ solar and uncertainty models

Since wind speed is a random variable, its distribution is obtained by Weibull Probability Density Function (PDF) with shape factor (k) and scale factor (c). Mathematically given by:

$$f_{\upsilon}(S) = \left(\frac{k}{c}\right)\left(\frac{S}{c}\right)^{(k-1)} \times \exp -\left(\frac{S}{c}\right)^{k} \quad for \;\; 0 < S < \infty \tag{4.27}$$

A. Wind power model

The output wind power from a wind turbine is a function of wind speed, expressed by the following equation:[48]

$$P_w(\upsilon) = \begin{cases} 0, & \text{for } \nu < \nu_{in} \text{ and } \nu > \nu_{out} \\ P_{wr}\left(\dfrac{\nu - \nu_{in}}{\nu_r - \nu_{in}}\right) & \text{for } \nu_{in} \le \nu \le \nu_r \\ P_{wr} & \text{for } \nu_r \le \nu \le \nu_{out} \end{cases} \tag{4.28}$$

Where ν_{in} , ν_r and ν_{out} are respectively the turbine cut-in, rated and cut-out wind speeds. P_{wr} defines the rated output power of the wind turbine.

B. Wind power probability for different wind speeds

From eq. 4.28, we can note that if ν is less than ν_{in} and above ν_{out} , the power output is zero. Also, the wind turbine produces P_{wr} for the condition $\nu_r \le \nu \le \nu_{out}$. For these discrete zones, the probabilities can be written by the following equations:[107]

$$f_w(P_w)\{P_w = 0\} = 1 - \exp\left[-\left(\frac{\nu_{in}}{\alpha}\right)^{\beta}\right] + \exp\left[-\left(\frac{\nu_{out}}{\alpha}\right)^{\beta}\right] \tag{4.29}$$

$$f_w(p_w)\{p_w = p_{wr}\} = 1 - \exp\left[-\left(\frac{v_r}{\alpha}\right)^{\beta}\right] + \exp\left[-\left(\frac{v_{out}}{\alpha}\right)^{\beta}\right] \tag{4.30}$$

Unlike to the discrete zones, the output wind power is continuous for the condition $v_{in} \le v \le v_r$, Hence the probability for this region is described as follows: [107]

$$f_w(p_w) = \frac{\beta(v_r - v_{in})}{\alpha^{\beta} * P_{wr}}\left[v_{in} + \frac{P_w}{P_{wr}}(v_r - v_{in})\right]^{\beta-1} \exp\left[-\left(\frac{v_{in} + \frac{P_w}{P_{wr}}(v_r - v_{in})}{\alpha}\right)^{\beta}\right] \tag{4.31}$$

Also, the solar irradiance to energy conversion for the PV plant also can be given by

$$P_s(G) = \begin{cases} P_{sr}\left(\dfrac{G^2}{G_{std}R_c}\right) & \text{for } 0 \le G \le R_c \\ P_{sr}\left(\dfrac{G^2}{G_{std}}\right) & \text{for } G \ge R_c \end{cases} \tag{4.32}$$

where G_{std} , is the solar irradiance in standard environment, R_c is a certain irradiance point, P_{sr} is the rated output of the PV power plant.

4.3.3. Proposed optimization algorithms

In this chapter, three meta-heuristics solvers ALO, WOA, and AEO are selected as optimizers to cope with stochastic OPF problem. These optimization techniques are discussed in detail in Chapter 2 Section 2.2. The constraints of stochastic OPF are handled by method superiority of feasible solutions (SF). Adapted IEEE 30-bus test system is also selected for this study as given in section 4.3.1.

4.3.4. Application of AEO algorithm for OPF

The following steps describe the application of the proposed AEO algorithm in solving the OPF problem considering WT and PV generation. Table 4.3 describes the process in detail of applicability of AEO with SF constrain approach for solving OPF problem. The flowchart of proposed algorithm is presented in Figure 2.4.

Table 4.3. AEO algorithm for stochastic OPF

Step 1:	Read data of test system and AEO-SF input Read input data of test system configuration: bus-data, line-data, transformers data, and generation units-data. Dimension of the problem, dim (dim =11 or 19) Number of population, N_P (N_P = 60 considered) Stopping criteria, Maximum number of iterations Minimum and Maximum value of control (decision) variables, in vector like $X_{\min}$ and $X_{\max}$ $X_{\min} = \left[X^{1}_{\min}, X^{2}_{\min}, ..., X^{\dim}_{\min}\right]$ and $X_{\max} = \left[X^{1}_{\max}, X^{2}_{\max}, ..., X^{\dim}_{\max}\right]$
Step 2:	Specify the desired objective function to be optimized
Step 3:	Calculate the forecasted-output power of wind turbine and PV units, as indicated in section 4.3.2
Step 4:	Generate initial population of size N_P individuals uniformly distributed between [$X_{\min}$, $X_{\max}$]
Step 5:	Evaluate objective function, constraint function and constraint violation using Eqs. (4.42) – (4.45) for each individual of generated population
Step 6:	Apply the AEO operators and equations of update to create a new population of individuals' (i.e., Improved solutions of the problem).
Step 7:	In selection phase, individuals for next population are replaced with new individuals if give better value of objective function according to rules of SF method. After each updating process, the new individuals is considered better if it yields lesser constraint violation or zero constraint violation along with smaller fitness value (minimization problem) than the respective old population individual. Otherwise, old population individual is retained.
Step 8:	Repeat steps 5-7 until the stop criteria is reached, i.e., until max_iter reached?
Step 9:	Report the optimal results with curves

The proposed algorithms are developed using MATLAB software, simulation are conducted on a computer with Intel i5 CPU @ 1.90 GHz processor, and 4 GB RAM. Simulation results are discussed in following section.

4.3.5. Simulation Results

To show the effectiveness of the proposed AEO algorithm, it is examined on modified IEEE 30-bus the test system is modified by inserting renewable energy sources. Full data of basic test system with limit of control variables are summarized in Table 3.1, and Table 4.1 shows data of modified IEEE 30-bus. Its corresponding diagram is given in Figure 4.2 above. The

proposed algorithm is described in Chapter 2, section 2.2.2. The input parameters of the algorithm are given in Table 4.4.

Table 4.4. Test-systems description

Parameter	IEEE 30-bus
Dimension of optimization problem (*dim*)	24
Population size	60
Max Iteration	200

4.3.5.1. *OPF study without stochastic wind and solar power*

In order to show the efficiency of the proposed AEO algorithm, the deterministic OPF cases for the original system configuration, i.e., without WT generators and PV units are considered. Five cases are considered herein, with the objective functions mentioned in section above, namely: Case 1– minimization of basic fuel cost; Case 2 – minimization of real power loss; Case 3– Emission; Case 4– minimization of voltage stability index; Case 5– simultaneous of minimization of fuel cost and Valve point effect. The optimal results obtained for each case examined are presented in Table 4.5.

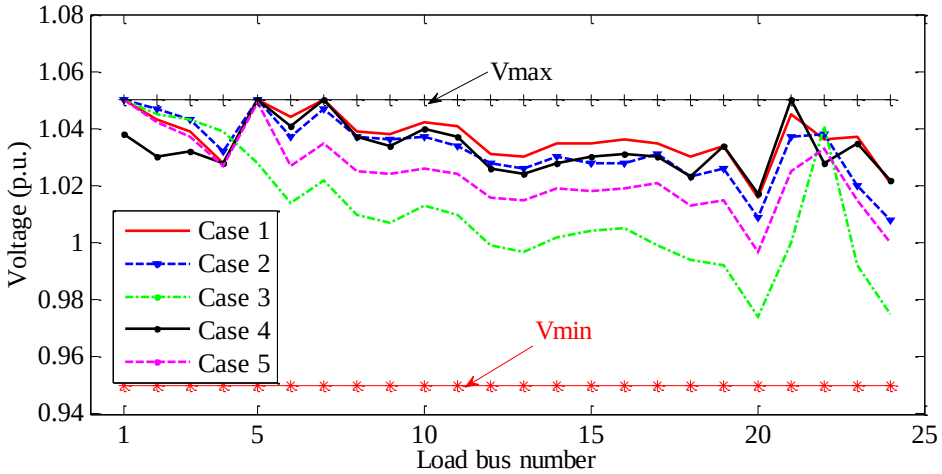

Figure 4.2. Load bus voltage profiles for the best solutions achieved in all cases of 30-bus

According to the figure 4.2 and Table 4.5, it appears clearly that all state or dependent control variables are within the admissible limits. In case 1 of optimization basic fuel cost, AEO algorithm lead to fuel cost of **800.51 $/h**, satisfying all system constraints, especially constraints on generator reactive power and load bus voltage. Some of the recent published papers recorded better results than the proposed method in present study. However, those results reveals violation of voltage bounds [0.95 - 1.05] p.u., which rendering the solutions infeasible.

Table 4.5. Simulation results for best solutions all case studies for IEEE 30-bus

Parameters	Min	Max	Case 1	Case 2	Case 3	Case4	Case 5
PG_1 (MW)	50	200	177.32	51.64	64.35	102.48	193.22
PG_2 (MW)	20	80	48.62	79.79	67.48	58.19	41.78
PG_3 (MW)	15	50	21.39	50	50	45.18	22.13
PG_4 (MW)	10	35	21.29	34.97	35	34.97	10.01
PG_5 (MW)	10	30	11.88	29.95	29.99	24.76	13.79
PG_6 (MW)	12	40	12.01	39.98	40	22.60	12.56
V_1 (p.u.)	0.95	1.10	1.084	1.062	1.071	1.073	1.083
V_2 (p.u.)	0.95	1.10	1.051	1.057	1.065	1.055	1.061
V_5 (p.u.)	0.95	1.10	1.033	1.037	1.051	1.041	1.031
V_8 (p.u.)	0.95	1.10	1.038	1.044	1.043	1.039	1.034
V_{11} (p.u.)	0.95	1.10	1.085	1.067	1.054	1.079	1.097
V_{13} (p.u.)	0.95	1.10	1.054	1.061	1.020	1.029	1.048
T_{11} (p.u.)	0.90	1.10	1.01044	0.98347	1.01299	0.99343	0.99188
T_{12} (p.u.)	0.90	1.10	0.97589	1.02183	1.02684	0.94495	1.07449
T_{15} (p.u.)	0.90	1.10	0.98352	1.01324	0.99092	0.92303	1.00946
T_{36} (p.u.)	0.90	1.10	0.98094	0.97871	1.03189	0.95270	0.99709
Q_{C10} (MVAr)	0	5	0.77891	1.27792	3.39712	2.00442	2.76653
Q_{C12} (MVAr)	0	5	3.75751	3.96474	1.26715	3.37899	1.44351
Q_{C15} (MVAr)	0	5	2.73290	4.70305	2.45466	0.26529	4.26762
Q_{C17} (MVAr)	0	5	4.73146	4.95600	4.20280	2.12006	4.58580
Q_{C20} (MVAr)	0	5	4.26937	4.89976	2.65552	1.45047	4.40507
Q_{C21} (MVAr)	0	5	4.94533	3.26729	4.97072	1.24123	3.03849
Q_{C23} (MVAr)	0	5	3.16956	3.51635	1.04304	3.51498	4.38065
Q_{C24} (MVAr)	0	5	4.90726	4.99316	4.97170	1.26755	4.99775
Q_{C29} (MVAr)	0	5	3.66325	1.08584	4.27144	1.47575	3.31127
Fuel cost ($/h)			**800.5141**	967.5232	944.7075	872.2109	**830.7276**
Emission (t/h)			0.36677	0.20730	**0.20489**	0.23089	0.41552
Loss (MW)			9.0409	**3.1341**	3.4290	4.7808	10.0885
VD (p.u.)			0.88470	0.7828	0.41161	0.79786	0.57932
L-index (max)			0.1389	0.1386	0.15022	**0.13763**	0.14187
Q_{G1} (MVAr)	-20	150	6.07143	-0.11	3.89	23.44787	6.58482
Q_{G2} (MVAr)	-20	60	23.56294	10.03	18.62	5.94833	19.04427
Q_{G5} (MVAr)	-15	62.5	27.44305	24.33	34.42	36.06981	28.04491
Q_{G8} (MVAr)	-15	48.5	30.97491	34.02	25.87	47.76979	26.77113
Q_{G11} (MVAr)	-10	40	18.64563	9.87	14.11	15.74217	25.29394
Q_{G13} (MVAr)	-15	77.7	3.05742	11.45	-0.82	-14.7821	9.89113

These undesirable violations may be due to the use of penalty function method. Optimization of the basic fuel cost in first case lead the maximum power loss and voltage deviation compared with other optimization cases. In **case 2** of minimizing active power losses, the proposed AEO converges to real power loss of 3.1341 MW, but the fuel cost is higher compared with the first case. The high value of voltage deviation in this case can be justified by the need of increasing

voltage at load buses to minimize power losses in the transmission lines. In case 4, the minimum voltage stability indicator is achieved, AEO gives best index of 0.1376, relatively better than the other equivalent algorithms. Study of case 6 reveal the results of minimization of fuel cost considering the valve loading effects, the value of cost being 830.76 $/h obtained by AEO algorithm. In short, the objective of this study is not to show only the superiority of proposed AEO algorithm over other approaches, but to demonstrate strict compliance with the system constraints by the SF technique.

Table 4.6. Comparison results of different algorithms for cases studies of IEEE 30-bus

Case no.	Algorithm	Fuel Cost	Loss (MW)	Emission	L-index (p.u.)
Case 1	AEO	**800.5141**	9.0409	0.36677	0.1389
	AGSO [46]	801.75	–	0.36625	–
	Mod PSO [29]	800.5164	9.0354	0.36624	0.13825
	ARCBBO [108]	800.5159	9.0255	0.3663	0.1385
	SHADE-SR [95]	800.5179	9.0274	0.36625	–
	ICBO [32]	799.0353[a]	8.6132	–	–
	GEM [109]	799.0463 [a]	8.6257	0.3665	0.1264
	DE [110]	799.0827 [a]	8.63	–	1.8505
Case 2	AEO	**872.2109**	**3.1341**	0.20730	0.1386
	Mod PSO [29]	967.6523	3.1031	0.20727	0.13816
	SHADE-SR [95]	967.6635	3.1017	0.20726	0.13868
	ARCBBO [108]	967.6605	3.1009	0.2073	0.1387
	GEM [109]	966.7473[a]	2.8863 a	0.2072	0.1269
Case 3	AEO	944.7075	3.4290	**0.20489**	0.15022
	SHADE-SR [95]	944.3853	3.2358	0.20482	0.13879
	ARCBBO [108]	945.1597	3.2624	0.2048	0.1387
	GEM [109]	943.6358[a]	3.0160	0.2048[a]	0.1269
Case 4	AEO	**872.2109**	4.7808	0.2389	**0.13763**
	SHADE-SR [95]	819.1216	6.6860	0.27316	0.13637
	GEM [109]	816.9095[a]	6.2313	0.2802	0.1257
	DE [110]	915.2172[a]	3.626	–	0.1243
	SKH [111]	814.0100	9.9056	0.3740	0.1366

4.3.5.2. *OPF study with stochastic wind and solar power*

This part of the chapter focuses on application of AEO algorithm to solve optimal power flow incorporating stochastic wind and solar power with conventional power plants in the system. Weibull and lognormal probability-distribution density-functions (PDFs) are used to forecast wind power and solar photovoltaic output, respectively. Original IEEE 30-bus test system is modified by replacing three conventional thermal power plants with renewable energy sources, i.e., two wind farm and solar PV unit.

The wind turbine farm connected at buses #5 and #11 are the collective output of 25 and 20 turbines in the farms, respectively. Each turbine has a rated power of 3 MW. The various wind-speed values are 16 m/s, cut-in wind speed of 3 m/s, and cut-out wind speed of 25 m/s. The PDF parameters for the sources wind and PV power plants are presented in Table 4.7.

Table 4.7. Probability Distribution Function parameters for renewable energy sources

Wind power generators					Solar PV unit		
Wind farm	no. of turbines	P_{wr} (MW)	Weibull PDF parameters	Weibull mean, M_{wbl}	Rated power, (MW)	Lognormal PDF parameters	Lognormal mean
1 (bus5#)	25	75	α = 9, β = 2	v = 7.976 m/s	50	μ =6	*Gs*= 483 W/m^2
2 (bus11#)	20	60	α = 10, β = 2	v = 8.862 m/s	**Bus13#**	σ =0.06	

To calculate the output power generated of PV unit using eq. 4.32, the solar- irradiance at standard test condition (G_{std}) set as 800 W/m^2 and certain irradiance points (R_c) is set to 120 W/m^2. Various cases study is performed for modified IEEE 30-bus system. Results of the case studies with application of AEO, ALO, and WOA algorithms are tabulated and explained in this section. In addition, a general scheme describing the relationships between the scheduled power and the variation of generation costs of wind and solar power. The rest case studies determine the contribution of each generator in the network. In all case study, we set maximum number of iterations ($maxiter = 200$) with a population size of 50 in a single full run. Each case has run 10 times before selecting the best value of the objective function with its corresponding settings control variables.

4.3.5.3. *Scheduled power vs. cost of WT and PV*

The Weibull PDF parameters to this case are presented in Table 4.7. Direct cost coefficients of wind generators are g_1=1.3, g_2 =1.75. Penalty cost-coefficients for not utilizing full produced wind power is assumed as $C_{pw,1}$ = $K_{pw,2}$ = 1.5 and reserve cost coefficient for overestimation is set as $K_{Rw,1}$ = $K_{Rw,2}$ = 3. The programmed power is varied between 0 MW and wind farm nominal power, and the variation of direct, penalty, reserve and total costs are drawn in Figures. 4.3 − 4.5. Total cost is the sum of aforementioned sub-costs corresponding to the scheduled power. From Figure 4.3, we can see that direct cost drawn a linear relationship with scheduled power. As scheduled power increases, necessity of larger spinning-reserve escalates the reserve cost and consequently the overall generation cost. The penalty cost rightly decreases, however at a lower rate, with the increase in scheduled power.

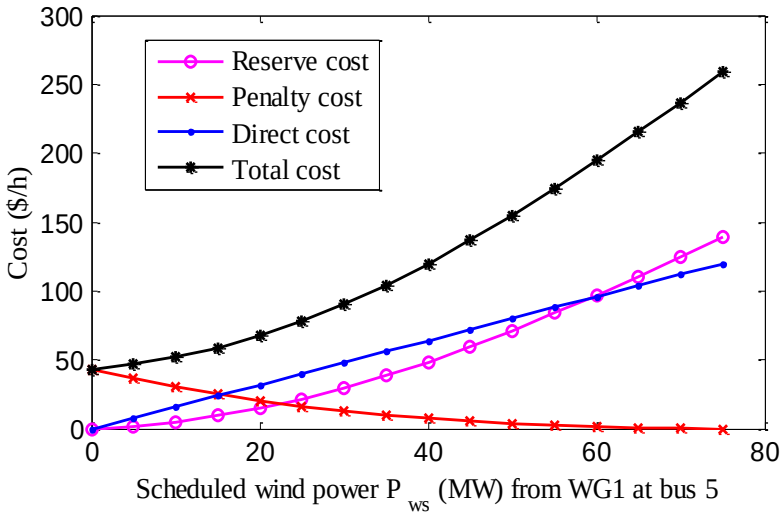

Figure 4.3. Wind power cost variation against programmed-power for first WG

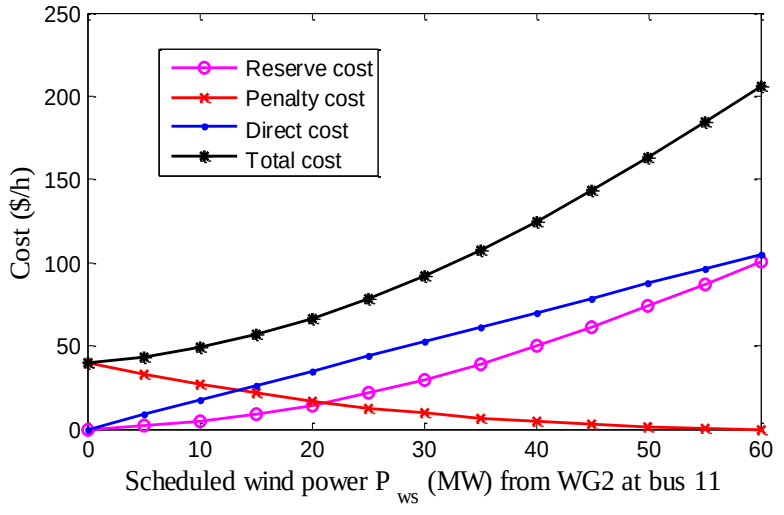

Figure 4.4. Wind power cost variation against programmed-power for second WG

Resemble to wind power, variation of cost for over/under-estimation of solar-power are also plotted vs. scheduled power in Figure 4.5

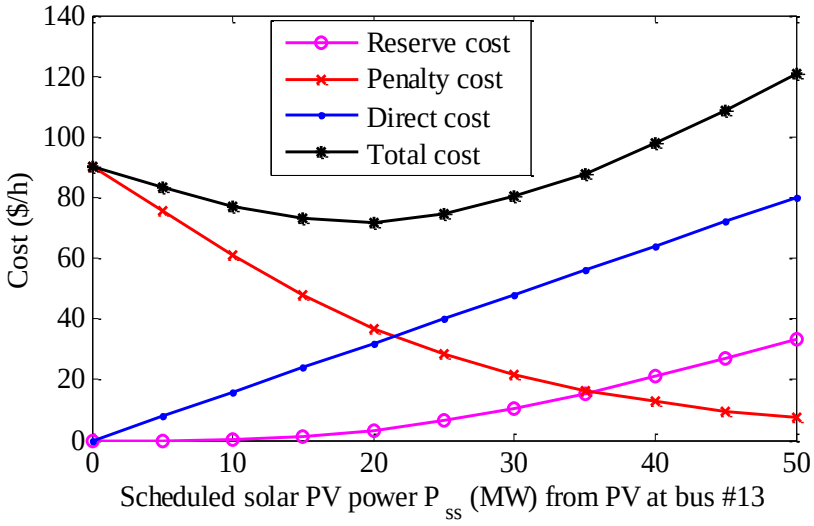

Figure 4.5. Variation of PV power-cost against Lognormal-mean (μ) for the PV unit connected at bus #13

Case 6: Minimization of generation-cost considering intermittent sources

Case 6 performs optimization of the generation schedule for all production units (thermal, WT, and PV) to minimize total generation-cost given in eq. 4.11. Cost coefficients are same to those of first case and PDF parameters are listed in Table 4.7

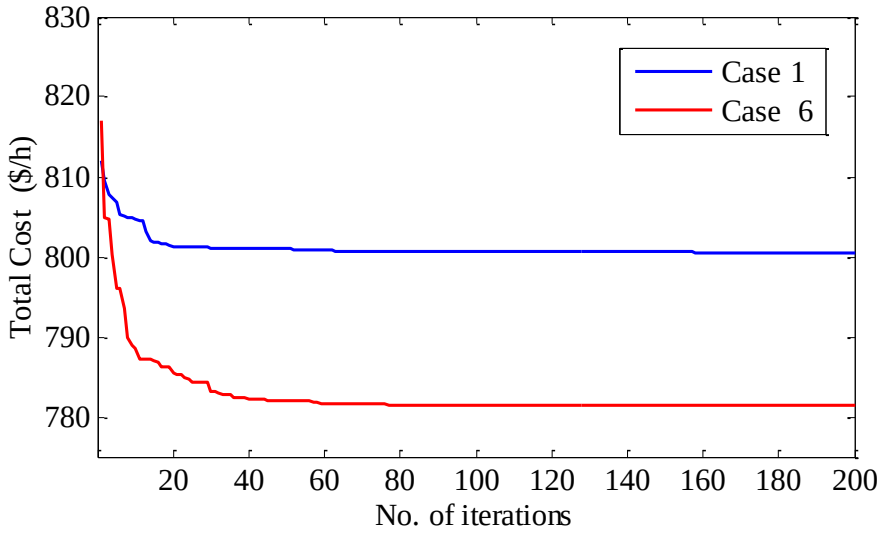

Figure 4.6. Convergence curve of AEO algorithm for Case 1and case 6 of OPF with intermittent source

Table 4.8. Optimal control or state variables for different approaches for case 6, IEEE 30-bus

Parameters	Min	Max	PSO [112]	TLBO [112]	SHADE-SF [95]	JADE [112]	EJADE-SP [112]	NBA	ALO	AEO
P_{TG1} (MW)	50	140	135.014	134.84	134.90	134.90	134.93	134.907	134.907	134. 908
P_{TG2} (MW)	20	80	28.880	29.063	28.564	29.105	29.105	28.13	28.201	27.7985
P_{TG3} (MW)	10	35	12.1994	10.060	10.000	10.000	10.00	12.01	10.554	10.0037
P_{WS1} (MW)	0	75	42.7781	44.045	43.774	44.084	44.148	42.19	41.793	42.9166
P_{WS2} (MW)	0	60	35.5258	36.625	36.949	37.226	36.993	35.54	37.586	35.9806
P_{SS} (MW)	12	50	34.9635	34.582	34.976	33.226	33.840	36.78	36.3535	37.9418
V_1 (p.u.)	0.95	1.10	1.0718	1.0756	1.072	1.0724	1.077	1.083	1.0809	1.075
V_2 (p.u.)	0.95	1.10	0.9973	1.058	1.057	1.0575	1.062	1.061	1.0645	1.058
V_5 (p.u.)	0.95	1.10	1.0870	1.041	1.035	1.0356	1.0381	1.032	1.0442	1.035
V_8 (p.u.)	0.95	1.10	1.0612	1.0353	1.04	1.0398	1.0445	1.027	1.0357	1.038
V_{11} (p.u.)	0.95	1.10	1.0962	1.0874	1.01	1.0998	1.0972	1.075	1.0397	1.100
V_{13} (p.u.)	0.95	1.10	1.0379	1.0359	1.055	1.0543	1.0496	0.983	1.057	1.074
Q_{TG1} (MVAr)	–20	150	19.7425	4.5100	–1.903	-1.8567	-1.8368	25.3384	8.06	5.97209
Q_{TG2} (MVAr)	–20	60	–20	12.044	13.261	13.225	17.078	25.2675	26.1842	15.9173
Q_{TG3} (MVAr)	–15	40	35	29.947	35.101	23.240	20.861	34.3249	34.999	33.7725
Q_{WS1} (MVAr)	–30	35	40	30.734	23.181	35.109	37.264	27.1943	33.4528	25.7527
Q_{WS2} (MVAr)	–25	30	30	27.964	30.00	30.000	28.747	29.0428	11.2807	29.8473
Q_{SS} (MVAr)	–20	25	13.1562	11.860	17.346	17.258	14.291	-2.99593	21.5022	24.4921
Fuel Cost ($/h)			782.340	782.676	782.50	782.35	782.242	784.038	782.811	**781.3979**
Emission (t/h)			–	–	1.762	–	–	1.76171	1.7620	**1.7623**
Loss (MW)			–	–	**5.77**	–	–	6.1668	5.996	**5.8498**
VD (p.u.)			–	–	0.463	–	–		0.4677	**0.5279**
Wind gen cost ($/h)			–	–	–	–	–	447.344	241.752	**239.0989**
Solar gen cost ($/h)			–	–	–	–	–	100.530	99.2848	**104.0397**

The convergence curve of AEO algorithm is illustrated in Figure 4.6. As can be seen from this figure, the optimum cost is achieved in less than 55 iterations. Optimum settings of control variables and corresponding objective values of each algorithm are listed in Table 4.8 above, where the best result has been indicated in boldface. It is worth to note that P_{WS1} and P_{WS2} indicate the scheduled powers from wind generators # W_{G1} and #W_{G2}, respectively. The emission rate is calculated by using the optimal scheduled power of thermal generators, where reserve is assumed an alternate source that does not add to the emission. From Table 4.8, it can be seen that the proposed AEO achieved the smallest cost with **781.3979** $/h, and

outperformed all optimization techniques, PSO (784.3400 $/h), TLBO (782.6767 $/h), SHADE-SF (782.50$/h), JADE, NBA (784.038) and ALO (782.81 $/h).

Based on the results obtained in case 1 of Table 4.5 and Table 4.8, we can state that when renewable energy sources was inserted, the total generation cost decreased from 800.5141 $/h to 781.397 $/h, i.e., around 19 $/h. If every hour can save the cost of 19.11 $, and the operating time per year is supposed as 7500 h, then operating time from the AEO algorithm can save 143378 dollars in total every year. It is obvious that insertion of wind generator and PV unit significantly contributes on the reduction of the total fuel cost compared with the original system configuration (i.e., without RES).

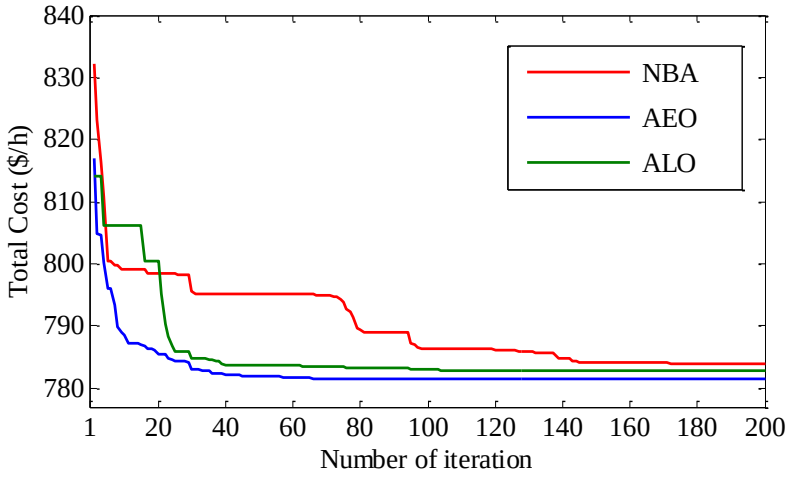

Figure 4.7. Convergence curve of three algorithms for case 6 of OPF with intermittent source

Case 7: Optimized cost against reserve cost

In this case study, all parameters are retained the same as in case 3 except reserve cost-coefficients. These coefficients for both wind generator and solar unit are varied by discrete step of 1 starting from 4 to 6, i.e., $C_{PW,1} = 4$, (case7a), $C_{PW,2} = 5$, (case7b) $C_{PW,3} = 6$, (case7c). The penalty cost-coefficients for all intermittent sources are similar to the case 1. The optimal power scheduled of generators is presented by bar graph in Figure 4.8 and compared with those obtained for the case 6 scheme.

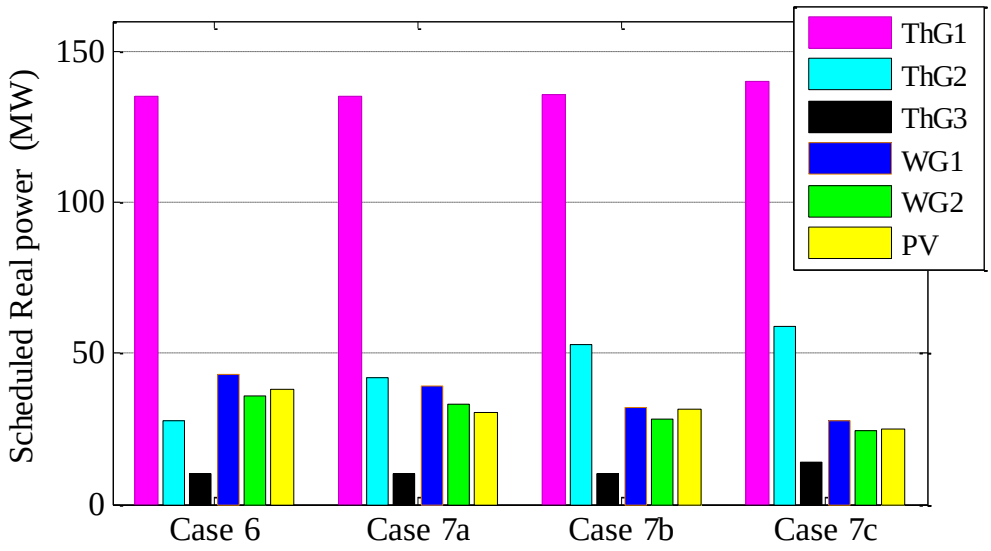

Figure 4.8. Optimal scheduled active power against Reserve cost Coefficient

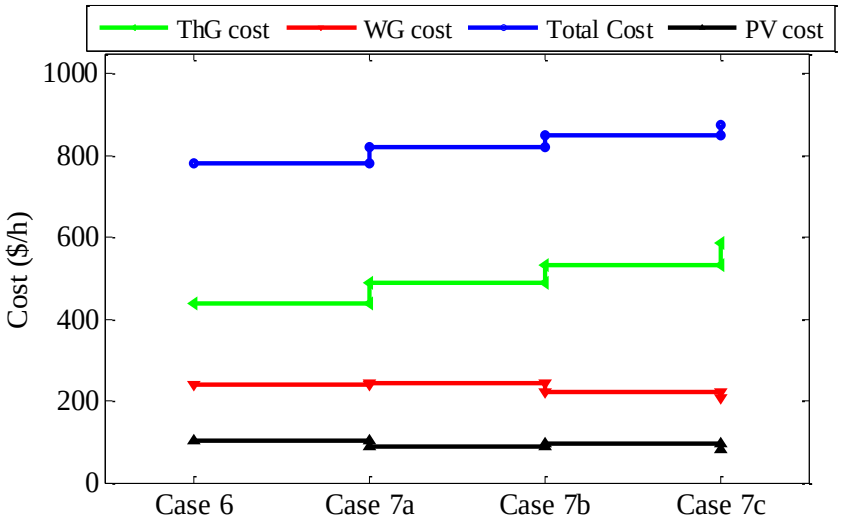

Figure 4.9. Cost curves for change in reserve cost coefficient

When reserve cost coefficient increases, the optimum power scheduled from wind generator and PV power unit decreases as lowering the scheduled power requires a lesser spinning reserve. Thermal power plants compensate lower outputs from the renewable energy sources. Consequently, thermal generator cost increases too as can observed in Fig 4.9. Consequently, thermal power plant cost increases like shown from "ThG cost" profile in Fig 4.9. However, costs of wind power ("WG cost") and PV output ("PV cost") gradually decreases.

Case 8: Minimization of total generation cost considering emission gas

In this case, the total generation cost considering gas emission is minimized. The value of tax rate, C_{tax} is equal to 20 $/tonne [112]. Optimum generation scheduled, generator reactive power, total generation cost and other calculated parameters are tabulated in Table 4.9.

It can be observed that penetration of wind and solar energy is relatively higher with case 8 when emission tax is considered than case 6 without penalty of emission. Hence, the extent of increase in optimum production of renewable energy sources closely depends on the emission volume and the rate of carbon tax imposed. Since the constraint on load bus voltage is also critical as optimum operating voltages of load buses are usually found closely to their bounds. All case studies of this chapter, the minimum and maximum load bus voltage are set into range of 0.95 p.u. and 1.05 p.u,. The voltage profiles of load buses are shown in Figure 4.10 for case 6 for three implemented algorithms.

Table 4.9. Optimal control and state for different algorithms on Case 8

Parameters	PSO [112]	TLBO [112]	ECHT-DE [112]	SHADE-SF [112]	EJADE-SP [112]	NBA	ALO	AEO
P_{TG1} (MW)	124.755	124.5813	123.0251	123.0258	123.0489	123.97	123.86	123.39
P_{TG2} (MW)	28.0839	31.9139	31.7458	31.7454	31.6077	31.09	33.9561	32.6891
P_{TG3} (MW)	12.9998	10.0040	10.0000	10.0000	10.0006	10.28	10.0000	10.0000
P_{WS1} (MW)	44.7650	45.8065	45.3393	45.3395	45.2702	46.85	44.0780	45.8828
P_{WS2} (MW)	36.9547	38.5744	38.1957	38.1948	58.7695	39.14	40.2764	38.6345
P_{SS} (MW)	41.2310	37.8588	40.3707	40.3712	45.0761	37.38	36.6082	38.1087
V_1 (p.u.)	1.0713	1.0737	1.0702	1.0702	1.0259	1.075	1.0742	1.0732
V_2 (p.u.)	1.0529	1.0586	1.0567	1.0567	1.0567	1.059	1.0602	1.0591
V_5 (p.u.)	1.0934	1.0355	1.0355	1.0355	0.9698	1.037	1.0385	1.0374
V_8 (p.u.)	1.0743	1.0405	1.0593	1.0784	1.0046	1.040	1.0388	1.0413
V_{11} (p.u.)	1.0920	1.0845	1.0990	1.0986	1.0343	1.075	1.0941	1.0950
V_{13} (p.u.)	1.0748	1.0351	1.0569	1.0570	1.0101	1.065	1.0617	1.0585
Q_{TG1} (MVAr)	7.6496	2.0806	-2.7444	-2.7873	-3.5178	7.47584	2.58541	2.40079
Q_{TG2} (MVAr)	-1.7011	13.7773	12.1633	12.1791	11.9775	17.07395	20.86979	18.80241
Q_{TG3} (MVAr)	21.8044	40.000	35.1399	35.1227	36.5460	39.79292	34.99969	39.69122
Q_{WS1} (MVAr)	35.0000	22.1815	22.9930	22.9884	22.6192	25.08029	27.30820	25.70393
Q_{WS2} (MVAr)	28.2189	26.5230	30.0000	30.0000	30.0000	22.05586	28.67070	28.80506
Q_{SS} (MVAr)	25.0000	11.1593	18.1392	18.1880	18.0592	22.28975	20.19591	18.77513
Fuel Cost ($/h)	813.343	811.4133	811.2270	811.2270	811.2226	810.6409	810.9903	**810.5886**
Emission (t/h)	–	–	–	–	–	0.91484	0.90854	**0.88465**
Loss (MW)	–	–	–	–	–	5.3040	5.3774	**5.3075**
VD (p.u.)	–	–	–	–	–	0.45389	0.47623	**0.47117**

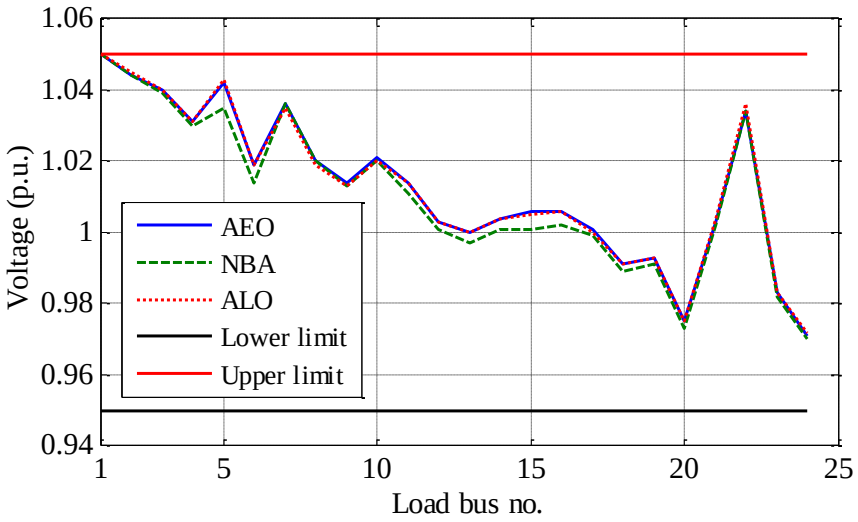

Figure 4.10. Load bus voltage profiles for Case 8

4.3.6. Conclusion

This Chapter proposed a solution approach to optimal power flow problem incorporating stochastic wind and solar power. Probability density function (PDF) was used to model uncertainties of the intermittent renewable energy sources. Different case studies with and without renewable sources are discussed in detail. Total generation cost incorporating different production sources is optimized and the variation in generation cost with change in reserve cost coefficients is studied. The change in PDF parameters of intermittent sources leads to changes in the generation cost following a pattern dedicated by a selected PDF function and associated parameters. Insertion of gas emission in a case study rightly increases the optimum contributions of green energy sources (i.e. RES) and reduces the output of conventional thermal generators. More importantly, power system constraints for all the case studies were fully satisfied by SF constraint handling technique applied of OPF with/without stochastic sources. At the conclusion and in the light of the results obtained we can confirm the superiority and consistency of the proposed AEO technique to find best solutions of a non-linear problem and the suitable choice of SF method of dealing all system constraints imposed.

Chapter 5

DEMANDE SIDE MANAGEMENT IN MICRO-GRID

5.1. Introduction

Recently, demand-side-management (DSM) is considered one of the most solutions for the optimal energy management in smart homes. DSM plays an important role in the smart grid and smart micro-grid through scheduling loads in a smart way return multiple benefits for both consumers and utility. This can be done by managing loads in a smart way while keeping up customer loyalty.

In this chapter, recently published meta-heuristic techniques such as AEO, HHO, MFO, WOA and BAT algorithm are employed to study the optimal power scheduling of home appliances (OSHA). The proposed techniques are used to shift the electricity load from on-peak to off-peak hours according to the load-curve. Moreover, the constraint of starting time and ending time of appliances was considered. To prove the effectiveness and capability of these approaches in solving OSHA problem, they tested on two different electricity pricing schemes: Critical-Peak-Price (CPP) and Real-Time-Price (RTP) and two operational time intervals (OTI) (60 min / 12 min) were considered to evaluate the consumer's demand and behavior of the suggested scheme. Simulation results show that the suggested model schedules the appliances in an optimal way, which leading to electricity-cost reduction and peak average ratio (PAR) curtailment. Hence, the obtained findings confirm the efficiency and effectiveness of the introducing AEO algorithm against remaining ones to relieve the over peaks problem, enhance utility performance, and meet users requirements.

5.2. Overview on strategy of demand side management in micro grid

The growing need for energy demand caused by population growth, and the rapid increase in electronic appliances in the residential areas, drives further research in development of effective strategies of energy management for keeping the balance between supply and demand with an acceptable cost [113], [114]. In addition, extensive and irregular usage of electric appliances leads to obtain an irregular scheme of daily consumption resulting in imbalance electricity load over specific time intervals especially in the On-peak periods and destabilizes the utility. In this context, energy management and optimal scheduling of essential household appliances while minimizing a total electricity cost is very important. In

traditional grid, many public services handle that situation by increasing generation in the same ratio as electricity demand increase in an effort to bridge the gap created between supply and demand. However, these temporary solutions or so-called half-solutions may affect the security constraints of electrical system giving rise to the certain critical situations, for instance, the maximum load-ability problem during the peak hours. Consequently, the total electricity cost increases also due to the tariff-related higher costs applied during on-peak hours.

To manage this situation, the utility has suggested two solutions: (i) Encourage the consumers to adjust their consumption profile by avoiding the maximum usage related of high prices during on-peak hours; (ii) ask the electricity companies to develop to develop effective planning activities to motivate end-users to adjust their level and model of energy usage. However, lack of knowledge into users about how to forecast on-peak hours as well as time varying-prices, has forced public utility to tackle with such problem. It is done by proposing effective scheduling strategies to achieve an acceptable compromise between the minimization of the total electricity costs and waiting time for the operation of each appliance in service. DSM [115,116] is one of the main parts of the Smart Grid (SG) responsible for ensuring balance between the supply and demand sides. It is not only used to reduce the electricity bills for the consumers, but also to help utility companies in preserving reliable electric service with the aim of ensuring users comfort [117,118]. This can be achieved with smart way by reducing the load demand through the Peak-periods.

According to the International Energy Outlook (IEO2016), energy demand is expected to keep rising over the next two decades up to 56% [119]. In other side, about 37% of the global energy consumption is only due to the residential sector. This ratio has attracted considerable attention in most academic researchers for dealing with this consumption level. During the past few years, many demand response (DR) technologies have been developed to cope with increasing demands of power. DSM programs are designed to overcome the energy shortage problems, which are created due to raising demands of electricity. In this context, load management based on demand response (DR) is considered as the most widely DSM strategies used to shift the load on-peak hours to off-peak hours. All these technologies have the same objectives, which are focused on: minimizing electricity consumption costs, minimizing peak to average ratio (PAR), and improvement of user comfort (UC) or (Waiting time).

To determine the optimal solutions for such problems, conventional (deterministic) and non-conventional (meta-heuristic) optimization techniques have been proposed in the literature. […..] The performance of each optimization method depends on the nature of the parameters

associated with the problem; the deterministic-schemes are the best problem optimizers in deterministic environment. In contrast, the meta-heuristic solvers are best suited to find the optimal solutions of problem in stochastic environment. Meta-heuristic techniques have ability to provide optimal solutions and the capability to escape local ones by exploration and exploitation mechanism, avoiding in premature convergence; however, the deterministic techniques make the assumption of certainty, proportionality in order to optimize problem. This reason makes authors prefering to use the nature-inspired optimization techniques for solving aforementioned problem.

5.3. Related works

A huge number of algorithms have been proposed in order to make residential areas smarter, electricity cost minimization as well as energy consumption without affecting the users comfort. These algorithms are inspired from nature, biology and artificial intelligence. In this section, the previous proposed researches are discussed. For instance, in [120], the authors proposed a mixed-integer-linear-programming (MILP) method to optimize the total cost paid by the user by reducing peaks electricity demand in order to reach balance daily load schedule. However, the user comfort was not reduced sufficiently. A scheduling technique based on GA and PSO was proposed in [121] , for home appliances scheduling in an effort to reduce electricity cost and PAR value. Authors worked on multiple pricing signals, ToU, RTP and CPP for total electricity cost optimization. The obtained findings show the efficiency of these approaches. On the other hand, authors in [122], proposed a novel smart load management technique for peak load shaving of Egyptian residential loads considering its daily operation performance and time shifting operation capability. The obtained results confirm the efficiency and effectiveness of proposed methodology to overcome posed problem. In [123], Bharathi et al, examine a benchmark model of DSM by using GA, in an effort to shave the power demand during peak times and electricity bills for residential and commercial users. Although the cost successfully reduced by 21% the waiting time and PAR value were not amply improved. In [124], authors studied the effect of scheduling of power demand on the life span of battery along with energy cost is presented. Optimization results show that established study achieve promising results with high level of robustness against other methodologies. Also, Ihsan Ullah et al. [125] developed a novel appliance scheduling model based on the combination of GA and BPSO algorithms. The model is designed to reduce the total cost of consumed electricity of different household appliances and PAR value under dynamic pricing environment. A load shifting technique was presented in [126], to

schedule household appliances using CSA. Experimental results demonstrate that Peak-load has been decreased by 22% compared with unscheduled case and the load-curve is balanced by user preference for appliances usage. In [119], a hybrid algorithm (GA-BF) was used to adjust the electricity bills of consumer and PAR using the load shifting technique. Authors also succeeded in achieving a favourable trade-off between minimizing the energy cost and the PAR value. In [127] a novel demand management scheme based on the min-max load planning technique was proposed to adjust the PAR value with maximization of the operational comfort level of users. They also worked to define a difficulty faced by users when utility companies proceed to reduce power consumption. The simulation results confirm ability of the technique to shave the Peak-load, the PAR value, and electricity-bills with acceptable comfort levels. In [128], chicken-swarm-optimization (CSO) and enhanced DE techniques with RTP were modeled to minimize electricity bills and to reduce peak average ratio taking into account user comfort. Their results demonstrate that CSO algorithm outperforms enhanced DE technique in terms of electricity-cost-minimization and user comfort. Also in [129], three recent optimization techniques were implemented as comparative study to deal with home−energy management−system, (HEMS). The main objective is to reduce PAR value using two different pricing schemes. The results show that IAPR algorithm reduced the PAR value to a greater degree compared with SA and SSA, were not significantly improved compared with unscheduled case. Elham Shirazi et al. [130] proposed a scheduling technique for an automatic and optimal smart home energy management. The home utilizes electrical and thermal energy as well as the self-storage units. Authors worked in to achieve a best compromise between a total energy cost minimization and the peak demand-load. The graphical results show a significant reduction in electricity costs for multiple scenarios. In [131], SSA was proposed for household appliances management with game theory based pricing strategy, in which every user has different tariff. The authors discussed how to distribute the extra generation charges onto each consumer basing on the electricity load profile. The simulation outcomes confirm the efficiency of proposed model, in which PAR is reduced to 76%, and to minimize user costs. *Abushnaf and Rassau* [132] propose an efficient model for scheduling load demand in residential areas integrated with a grid demand response (DR) program. The problem is formulated as single objective optimization with multi-variables by using genetic algorithm, which aims to minimize the total electricity cost while keeping the energy consumption under a demand limit. The obtained results show that the powerful of the proposed program of which achieved a significant costs-savings for both of consumers and utility. Under the vast exploration of

nature-inspired optimization techniques, and based on the no free lunch theorem, no universal technique has been capable to solve all optimization problems. Hence, there is chance to solve complex issues by suggesting or exploring new meta-heuristic techniques.

In this chapter, novel approach (AEO) techniques along with other approaches are suggested to tackle energy consumption optimization problem in smart residence. It is also considered as an efficient treatment for some limitations of aforementioned techniques in the related work.

The principal-contributions of this chapter are summarized as follow: (1) we have explored and analysed five new algorithms for energy optimization problem i.e., BA [4], MFO [8], WOA [6], HHO [10], and AEO [11]. (2) In addition, for validation of the suggested nature inspired techniques, we applied it in a single home under two operational time intervals (OTI) 60 min and 12 min.

Furthermore, both of non shiftable-appliances and non-interruptible appliances are constrained by starting time and ending time to ensure a maximum comfort level of end users.

On the light of the obtained findings, we have shown that the proposed optimizer outperforms in terms of:

1. Electricity-Cost (EC) minimization and Peak Average Ratio (PAR)-reduction; and
2. Protect users comfort, by improving waiting time of their appliances.
3. AEO based home energy management controller performs better for cost reduction and PAR curtailment compared with others pairs.

In organizing rest of the chapter, Section- 5.4 describes problem description, objectives and mathematical formulation as well as proposed system model. Section- 5.5 covers the Graphical results with the details discussions. Conclusion is given in Section-5.6

5.4. Problem description, objectives and mathematical formulation

Recently, many optimization algorithms have been suggested to deal with HEMS-problem in SG. The vast majority of these approaches have specific control parameters to adjust, which presents the primary factor to influence on their performance, reduce computational-complexity and to avoid getting stuck into the local optimum. In contrast, the remaining ones are commonly the Population-Size and the Max-number of generations. In this context, to selecting the right optimization approach for such problem is also a challenge. Main objectives of SG are electricity-bill minimization, PAR-reduction, User-Comfort-maximization, and optimal load management. In the aforementioned literature, does not exist an inclusive-coverage to the benefits of SG in which some researchers' interest on electricity bills minimization and PAR-reduction, while others ones focus on users comfort

maximization, and optimal load management. In general, the common objective is to lower electricity-bills with maximal satisfaction of users comfort. But, the more importantly is how to achieve a lower electricity bills without compromising users' comfort (maximal satisfaction of users comfort) and reduce the PAR value. In return, there are various pricing tariffs used by utility companies, amongst which the most commonly implemented tariffs are: Critical-Peak-Price (CPP), Time-of-Use (ToU), real-Time-Pricing (RTP), and Day Ahead Pricing (DAP).

5.4.1. Objective function

The main objective behind our scheduling technique is to decrease the total consumer's energy cost with possible peak average ratio enhancement and to protect users comfort by minimizing waiting time in order to avoid their frustration. The objective-function can be defined as: Finding an optimal scheduling of household appliances during each time interval to reduce Electricity-Cost paid by end-users. Each appliance is characterized with only one status is either ON or OFF. The mathematical model for optimization can be defined by eq. 5.1, [133]

$$\min \sum_{t=1}^{T}\left(\sum_{a=1}^{App}\varphi_{app}\times X\left(t\right)\times E_{a,t}^{price}\right) \tag{5.1}$$

Subject to:

$$L\left(t\right)=E_{interru}\left(t\right)+E_{shiftable}\left(t\right)+E_{fixed}\left(t\right), \tag{5.2}$$

$$L\left(t\right)\le\lambda_{th} \tag{5.3}$$

$$L_{total}^{Sched}=L_{total}^{Unsched} \tag{5.4}$$

$$C_{total}^{Sched}<C_{total}^{Unsched} \tag{5.5}$$

$$t_{\alpha}<t<t_{\beta} \tag{5.6}$$

$$X\left(t\right)\in\left[0,1\right]. \tag{5.7}$$

The constraints of the optimization problem can be summarized in the equations, 5.2− 5.7. Equation 5.2 presents the total energy-consumed of all the appliances at the time t. Equation 5.3 illustrates that energy consumed in specified time slot should be must be less than or equal to the predefined. Equation 5.4 indicates that total energy-consumption must rest the same both before and after scheduling. It also guarantees that length-of-operation time of any appliance should not be influenced by scheduling process. Constraint in eq, 5.5 denotes that total cost during 24-h of scheduled- load must be less than the unscheduled-load per day. Equation 5.6 denotes the constraint of starting time and ending time of appliances. Where t_{α}

is earliest starting time of each appliance "a" and t_β the least finishing time of each appliance "a". Equation 5.7 denotes a Boolean variable is used to determine whether the appliance is OFF or ON.

a) Energy consumption

The mathematical form to compute energy consumption is by the following equation:

$$Energy^{consumption} = \sum_{t=1}^{T}\left(\sum_{a=1}^{App}\varphi_{app} \times X\ (t)\right) \tag{5.8}$$

b) Load balancing

The grid stability is necessary to ensure the service continuity and to keep up customer loyalty. Reduction in PAR value leads to maintain the load balancing and to help in reducing electricity cost. It is mathematically calculated by eq. 5.9 [133]

$$PAR = \frac{\max\left(L_{oad}^{Sched}\right)}{avg\left(L_{oad}^{Sched}\right)} \tag{5.9}$$

5.4.2. Proposed system−model

The Figure 5.1 showed the graphical of proposed model. The home is consists of 12 smart-appliances, which they are classified to the nature of energy-consumption pattern. For electricity cost calculation, the RTP and the CPP signals are used. The primary aim is to decrease the total consumer's energy-cost and PAR value as well protect consumer's comfort.

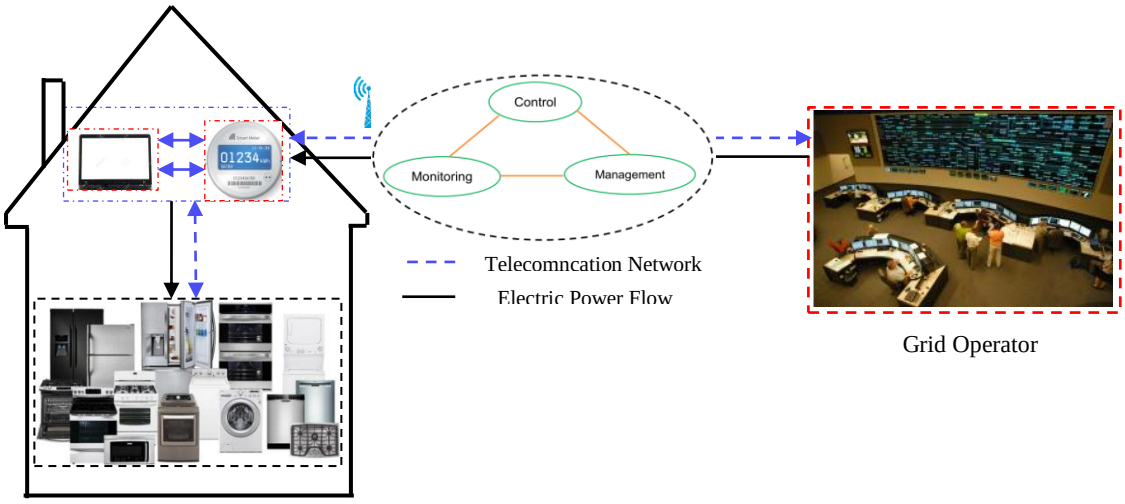

Figure 5.1. An overview of HEMS model

The smart home is directly connected to a grid. The smart meter is used as a bridge between utility company and consumer to permit the electricity utility to communicate the pricing-signals and preventive maintenance-timings. In the present work the appliances are scheduled on period of 24-hour time slots. Since the length operation time (LOT) of some appliances is less than 60 min, a day is divided into120 equal time slots with a range-time of 12 min. Consequently, two kinds of decision are considered: (i) in every 1 hour of time and (ii) in every 12 min.

5.4.3. Mathematical formulation

a) Classification of Load-

According to the patterns of energy-consumption, user-comfort and time of use, appliances are classified into three categories given as follows:

- Non Shiftable−appliances;
- Shiftable appliances;
- Base appliances.

Non shiftable−appliances or interruptible-appliances are those appliances that can be shifted to any time interval and they are also characterized by an interruption during their operation. We indicate set of interruptible-appliances by "IN_{ed}" and their energy-consumption denote with "P_{IN}". For each interrupted-appliance "$in \in IN$", with a factor of power rating "φ_{in}"then total energy-consumption is formulated as follows:

$$E_{in} = \sum_{in \in IN} \left(\sum_{t=1}^{24} \varphi_{in}^{t} \times X_{in}^{app}(t) \right) \tag{5.10}$$

where X_{in}^{app} is the state of each interruptible-appliance in specified time slot "t" and it is written:

$$X_{in}^{app}(t) = \begin{cases} 1 & \text{if Appliance is turn ON,} \\ 0 & \text{if Appliance is turn Off} \end{cases} \tag{5.11}$$

Shiftable-appliances are those which can be easily shifted to another time interval, but can never be interrupted for any length of time within their operation. For instance, washing machine, cloth dryer and dish washer, etc. We denote set of shiftable- appliances by "Sh" and their energy-consumption is represented by "$E_{shiftable}$". If shiftable-appliances $sh \in SH$ have a power rating factor "$\varphi_{Shiftable}$"; the total energy-consumed is given by eq. 5.12:

$$E_{Shiftable} = \sum_{sh \in SH} \left(\sum_{t=1}^{24} \varphi_{Shiftable}^{t} \times X_{Shiftable}^{app}(t) \right) \tag{5.12}$$

where $X^{app}_{Shiftable}$ is the state of each non-interruptible appliance in particular time slot "t" and it is written as:

$$X^{app}_{Shiftable}(t) = \begin{cases} 1 & \text{if appliance is turn ON,} \\ 0 & \text{if appliance is turn Off} \end{cases} \tag{5.13}$$

Fixed-appliances are those working continuously with zero interruption and their operation times are not alterable. We denote fixed-appliances by "F" with $f \in F$ and its consumed power as "φ_{fixed}". Thus, the total power consumption E_{Fixed} in each interval 't' of a day is calculated as:

$$E_{Fixed} = \sum_{f \in F} \left(\sum_{t=1}^{24} \varphi^{t}_{fixed} \times X^{app}_{fixed}(t) \right) \tag{5.14}$$

where X^{app}_{fixed} is the state of each fixed appliance in particular time slot "t" and it is given as:

$$X^{app}_{fixed}(t) = \begin{cases} 1 & \text{if appliance is turn ON,} \\ 0 & \text{if appliance is turn Off} \end{cases} \tag{5.15}$$

Appliances specification used and their characteristics along with LOT are listed in Table 5.1.

Table 5.1. Detail description of appliances used in simulations [134,135]

Appliance Class	Appliance Name	Power rating (kW)	LOT (hours)	Working hours	
Base	Oven	3	3		
	Refrigerator	0.3	24		
	Laptop	0.25	4		
	Desktop PC	0.3	3		
	Lighting	0.5	6		
Interruptible				Time Starts (hour)	Time Ends (hour)
	Vacuum cleaner	1.2	2	09	17
	Water heater	1.5	3	08	23
	Water pump	1.7	4	12	21
	Dish washer	1.2	3	08	22
	Steam Iron	1	6	08	16
Non-Interruptible	Washing Machine	0.7	3	09	17
	Cloth Dryer	0.8	5	08	14

b) Price tariff

Total electricity-cost is calculated based on the price defined by the retailer company. For this intent, various dynamic pricing schemes are used to decrease the total consumer's electricity-cost with possible peak average ratio enhancement and to protect users comfort. Different pricing tariffs are employed in an effort to incite the customers. There are various

pricing tariffs in literature, which are employed to incite the consumers to alter their operational time of electric appliances from 'high-price' hours to 'low-price' hours. RTP is one of the most dynamic price rate tariffs implemented in the world [136]. In RTP pricing model, the signals price is changed for different time intervals (based on the hourly usage of electricity) while rest constant inside every time interval.

CPP: Critical peak events may happen on defined period of time when company of electricity records high market price rate or under emergency conditions that usually happen in hot summer weekdays, characterized by the higher electricity rates. There are two variants of the CPP model: one is grounded on time and duration of peak price which are previously defined and second, depend on the electricity needed to regulate the load in the peak price. The critical hours are often limited and not allowed happen up than 15 times per year. RTP and CPP pricing tariffs are utilized to conduct simulations. Their graphical schemes are shown in Figure 5.2.

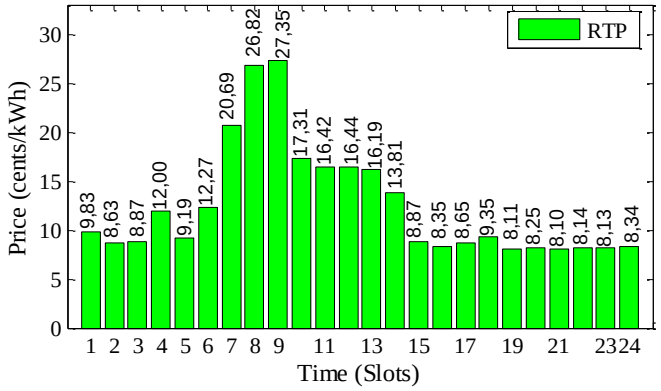

(a)

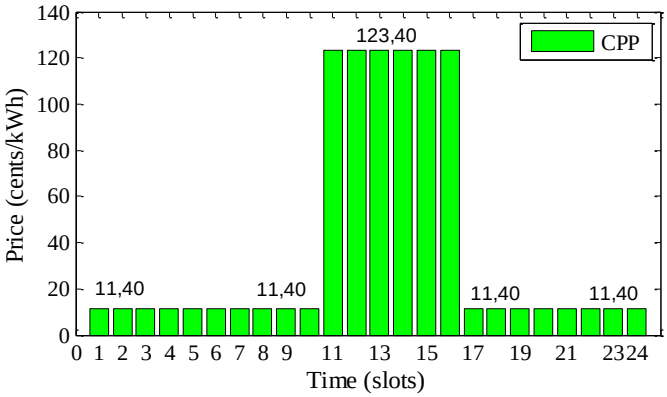

(b)

Figure 5.2. Histogram of pricing tariff: (a) Real time pricing, (b) Critical peak pricing.

Algorithm 1: Pseudo code of the proposed load scheduling using AEO algorithm

Initialization: Generation of the price signal according to the selected scheme. Length of operation time (LOT) of appliances, power ratings of appliances.
Input: Setting variables: PopSize, Max-iter, Dim, lb, ub
Randomly initialize first population (all patterns of appliances)
Evaluate first population
for *hour* = 1 *to* H **do**
Find Electricity cost
Evaluation: Find electricity cost for all of appliances
Select best population, F_{Best} and saved it; Find X_{Best} and $PopF_t$
    for Iter = 1 to Max-Iter **do**
    a (linearly decreased from 1 to 0), and Parameters: param.u, param.**v**, and param.**C**
    Update the Position X1, according to Equation (2.11)
    for i = 3 to PopSize **do**
        if r < 1/3 or **if** 1/3 < r <2/3
        Update the Position Xi, according to Equation**s** (2.16)–(2.18)
        end if
    Evaluate the *ObjFun* for eah Xi
      if $ObjF_i \leq ObjF$ (i − 1) **then**
       replace the previous Position with the new one
      end if
    Find the BestOne so far
    Assign a new position by using Equation (2.1)
    end for
    for i = 1 to PopSize **do**
     Evaluate the *ObjFun* for eah Xi
      if $ObjF_i \leq ObjF$ (i − 1) **then**
         replace the previous Position with the new one
      end if
     Find the best one found so far
    end for
    end for
    Select the best position (solution) achieved so far and memorize it
end for
Return optimum solution (X_{best}) and display graphs of: Cost, load, PAR.

5.5. Simulation-result and discussion,

In this section, an empirical simulation was performed to evaluate the performance of different algorithms in terms of electricity cost minimization, PAR reduction, and improvement the comfort of end-user by reducing the waiting time of appliances. In this work, the smart home consists of twelve kinds of household appliances ($D = 12$), and handled under two operational time intervals (OTI): for one hour (60 min) and for 12 min. All appliances and their power rating with length of operation time (LOT) are given in Table 5.1.

Moreover, for comparison purpose, five heuristic techniques such as BA, MFO, WOA, HHO and AEO are tested to evaluate the proposed scheme by using RTP and CPP tariffs.

The proposed DSM program was developed in MATLAB and our simulations were executed on a Laptop; Intel Core i5 − 4300 CPU 2.50 GHz processor, 4 GB-RAM. Due to the stochastic nature of meta-heuristic optimization techniques, we have taken average results of ten experiments. Simulation results with proper justification are explained in the following sub-sections.

5.5.1. Case I (with operational time intervals of 60 min)

a) Load consumption using RTP

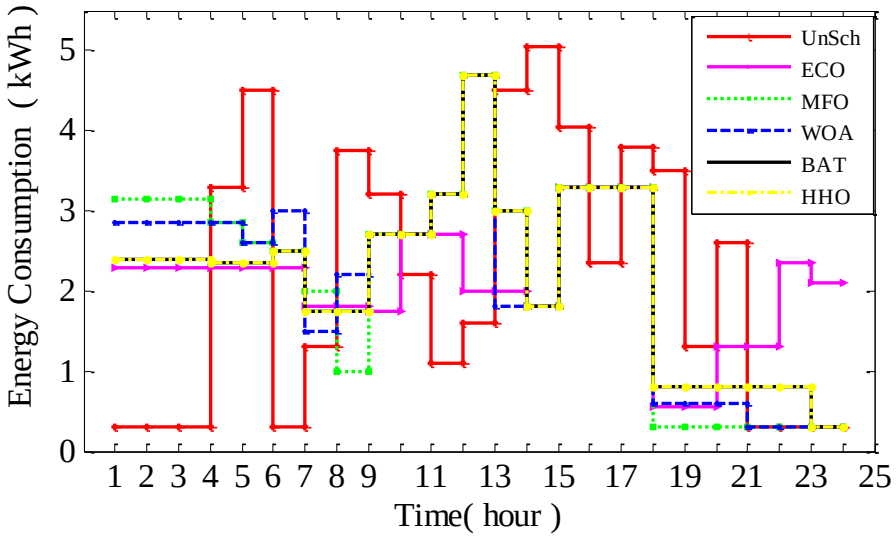

Figure 5.3. Energy consumption profile

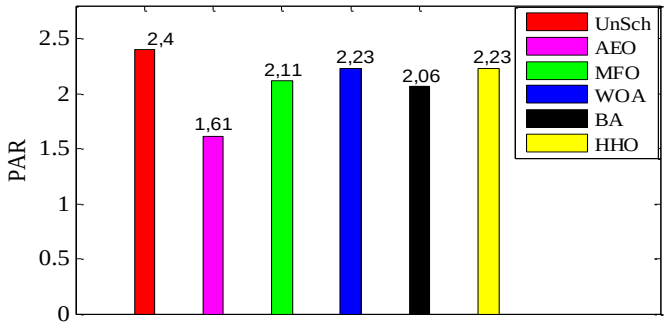

(a)

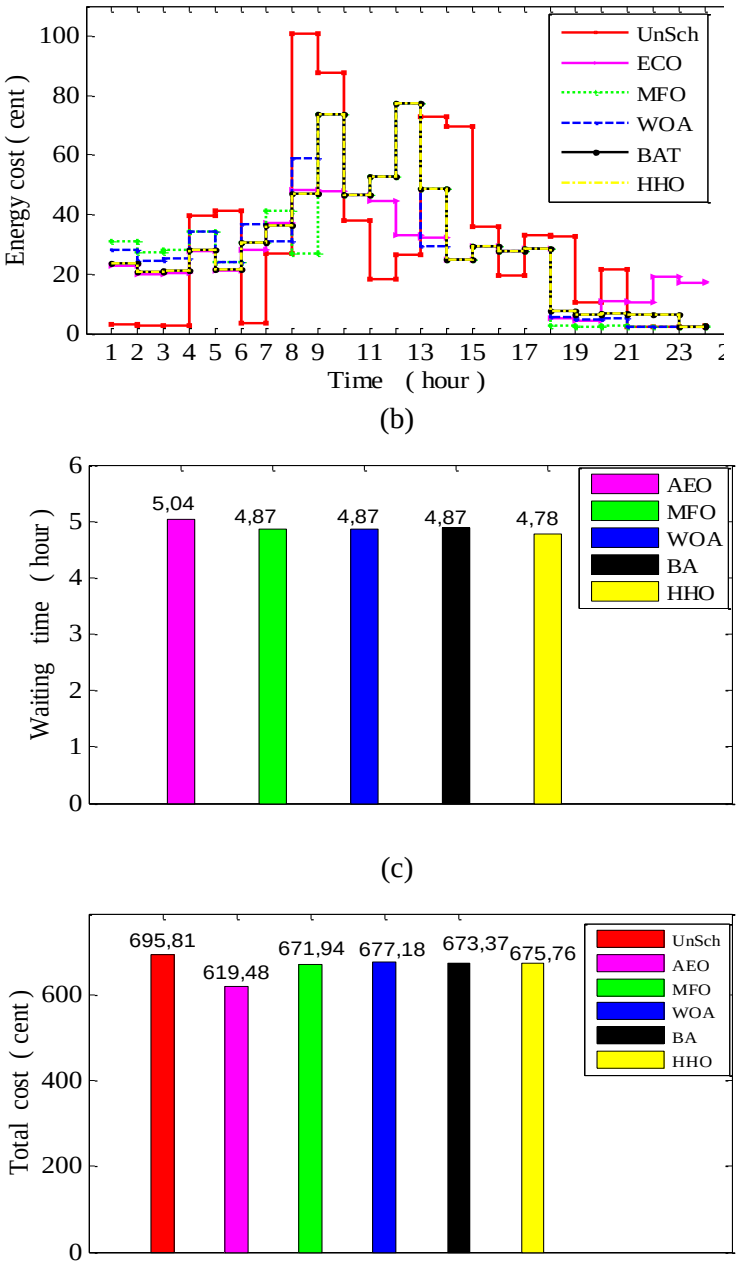

Figure 5.4- Graphical results using RTP tariff for operational time interval of 60 min: (a) Peak to average ratio; (b) Energy cost profile; (c) Average waiting time of electric appliances; (d) Total electricity cost.

5.1.2 Load consumption using CPP

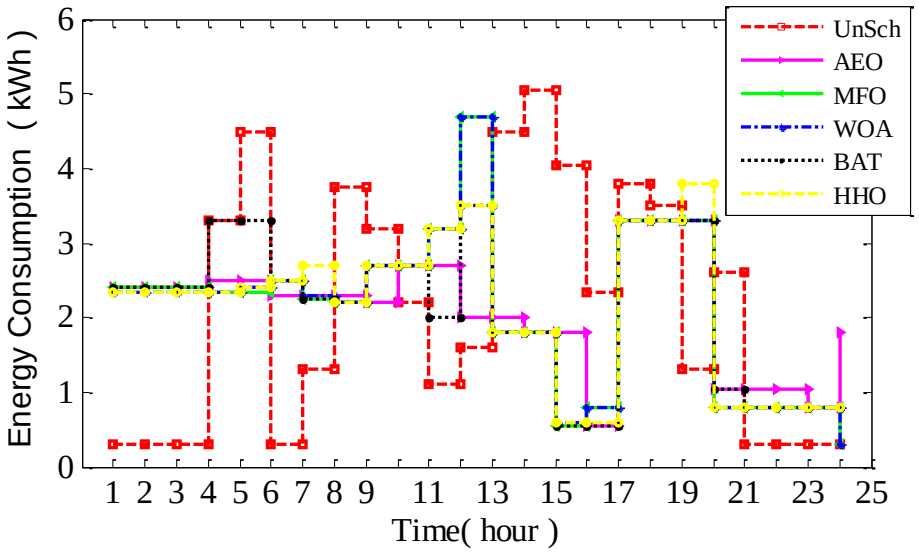

Figure 5.5- Energy consumption profile

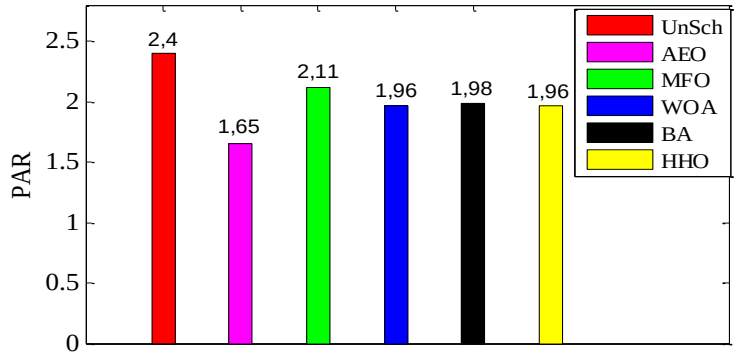

(a)

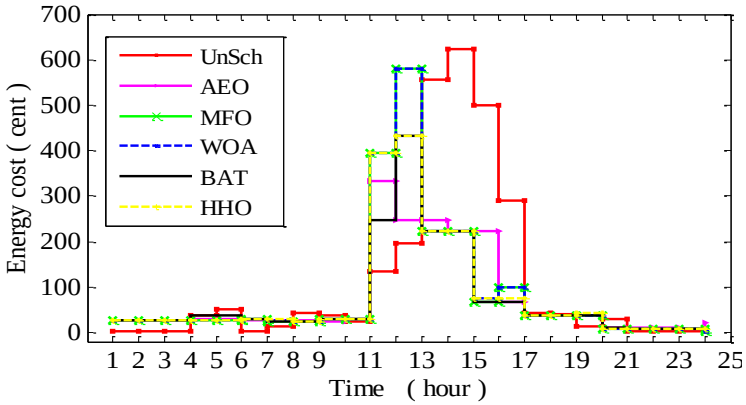

(b)

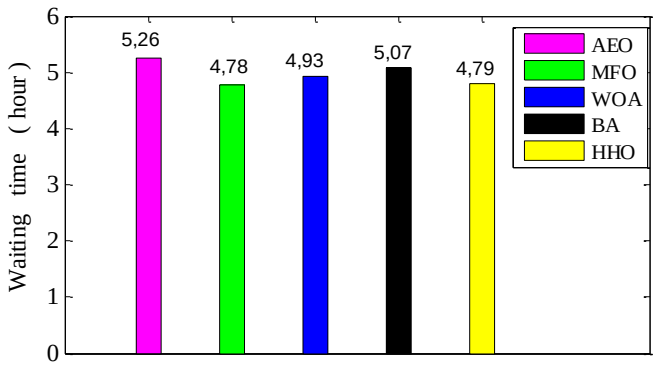

(c)

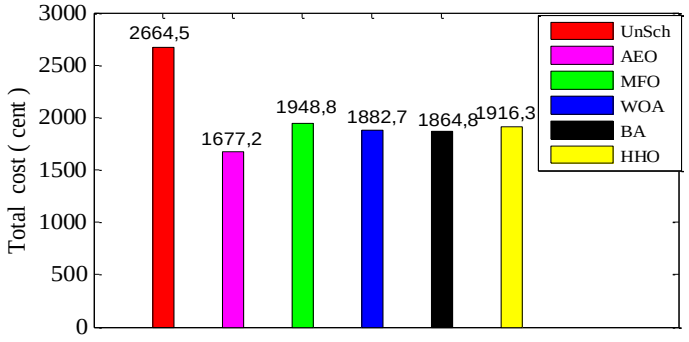

(d)

Figure 5.6– Graphical results using CPP tariff for operational time interval of 60 min; (a) Peak to average ratio; (b) Energy cost profile; (c) Average waiting time of electric appliances; (d) Total electricity cost.

5.5.2. Cost using RTP and CPP

Load consumption patterns using RTP and CPP are shown in figures 5.3 and 5.5 for a 60 min OTI. Figures 5.4, 5.6 show their behaviors to: peaks reduction, electricity cost profile and average waiting times.

In RTP signal, on-peak and shoulder peak hours are within 7 − 10 and 11 − 15 respectively, whereas off-peak hours are set between 1− 6 and 15 – 24, (Figure 5.2). Figure 5.3, shows daily energy consumption scheme of scheduled and unscheduled cases for a 60 min OTI. In unscheduled case, energy consumption is higher during 5 − 6 hour and 13 −16 hours guiding to high cost and PAR. The load profile are almost same between 7 − 24 hours for all algorithms except AEO technique, which shows higher peak values within 12 − 13 hours. This is because these approaches schedules non-interruptible appliances in 13 − 17 hours resulting in decreases PAR values with insignificant reduction in cost electricity. However, the most of interruptible and base appliances are turn ON in 1 − 11 and 19 − 24 hours. Our suggested AEO algorithm shows most successful scheme of energy consumption as compared

to other algorithms. We can also see that AEO has a constant energy consumption profile during 1 − 15 hours except of 2 hours, which maintains a balance between high and low energy consuming devices in parallel to RTP. Non-interruptible appliances are scheduled between 1 − 9 hours with other appliances having lower consumption. In case of unscheduled load, the maximum peak equal to 5.05 kWh while maximum scheduled is 3.3 kWh. Hence, a difference of 1.75 Wh is registered, which leads to reduce PAR. Furthermore, between 9 − 13 hours, AEO consumes less power compared to other approaches which significantly reduces overall cost. Meanwhile, Within 14 − 20 hours, all techniques show the exact same curve, but, after 20-th hour, AEO algorithm show an increase of energy consumption, where energy level pass from 0.6 kWh to 2.35 kWh. Only reason that AEO technique shifts more load in these time slots is the lower electricity prices in end of the day.

Table 5.2. Comparison of cost

Optimization techniques	Cost (S1)	Difference	Savings percentage in cost	Cost (S2)	Difference	Savings percentage in cost
Unscheduled	**695.81**	–	–	**2664.5**	–	–
BA	673.37	22.44	3.22%	1864.8	799.7	30%
MFO	671.94	23.87	3.43%	1948.8	715.7	26.86%
WOA	677.18	18.63	2.67%	1882.7	781.8	29.34%
HHO	675.76	20.05	2.88%	1916.3	748.2	28%
AEO	619.48	76.33	**10.95%**	1677.2	987.3	**37.05%**

S1= RTP, S2= CPP;

In CPP signal, on-peak hours can be observed between 11− 16 hours, and off-peak hours was programmed within 1− 10 and 17− 24 hours (Fig 5.2). Unscheduled and scheduled energy consumption scheme for all implemented algorithms for 60 min OTI based on the CPP signal is shown in Figure 5.6 (b). We can see that for each algorithm, the electricity cost changes according to the consumed energy users load profile during the process of load shifting from on-peak hours to off-peak hours.

In unscheduled case, load profile is higher during 5 − 9 hour and 13−19 hours leading to high cost and PAR. In the case of WOA and MFO algorithms, one peak is created which is 4.7 kWh and 3.8 kWh for HHO where a maximum peak for unscheduled case is registered at 5.05 kWh. However, with BA, and AEO techniques no peak is created during 24 hours. Our proposed AEO algorithm shows the most typical pattern of energy consumption behavior as compared to other algorithms. A constant energy consumption of all implemented algorithms have been envisioned during 1 − 11 hours except of HHO and BA techniques has some

fluctuations on their curves. However, at 12 to13-th hour, each of MFO and WOA are generated a maximum peak, which leading to increases PAR values and electricity cost. In contrast, AEO and HHO algorithms are maintain a balance between high and low energy consuming devices in line to CPP signal. Furthermore, between 11-16 hours where the price reaches its peak value by 123.4 cents/kWh, AEO consumes less power compared to other pairs which significantly reduces overall cost. Furthermore, if we have to calculate the cost of electricity in the critical period for all techniques: is equal to1190.81 cents for BA, 1271.02 cents for AEO, 1338.9 cents for HHO, and 1486.97 cents for each of MFO and WOA. After 17-th hour all optimization techniques generally have the same pattern.

Form Table 5.2, we can see that AEO algorithm has the highest percentage decrement in cost for both RTP and CPP tariff which is equal to 10.95% and 37.05%, respectively. However, WOA shows minimum saving cost, i.e., 2.67% for RTP and 26.86% for CPP with MFO. Simulation results show that AEO algorithm well performed than other optimization techniques in decreasing electricity cost when price of each hour of home is calculated using CPP model. Among all proposed optimization techniques, AEO reduces 37.05% cost.

5.5.3. PAR using RTP and CPP

The reduction of PAR is explained in Table 5.3. It can see that the proposed AEO algorithm surpass the other algorithms for both RTP and CPP signals. Findings in Table 5.3 shows that PAR for AEO technique has decreased 32.9%, on the other hand, BAT - MFO, WOA and HHO decrease 14.16% , 12.1%, 7.1% and 7.1% for RTP, respectively. For CPP tariff, best performance is also achieved of 31.25% by proposed AEO technique, whereas, is equal to 12.1% MFO and 16.6% for WOA, HHO, and 14.5% for BA algorithm. Despite of a minor difference (i.e., 2 ~ 4%), it is observed between RTP and CPP price; AEO algorithm avoids peak formation and keeps the load on the medium level. Table 5.3 presents the comparison PAR for both RTP/CPP signals for a 60 min OTI. From this table it can be easily seen that each algorithm capable of reducing PAR value with respect to load, however, performance of AEO is the better one among to others. AEO algorithm has maximal savings, of which the PAR value is reduced from 2.4 to 1.61 with RTP and to 1.65 by using CPP. The results of both models utilized show that RTP policy is more convenient. Consequently, it is clearly remarked that AEO surpass BA, WOA, MFO, and HHO in every case, as it well performs even with different tariffs.

Table 5.3. Comparison of PAR

Optimization techniques	PAR (S1)	Difference	Savings percentage in PAR	PAR (S2)	Difference	Savings percentage in PAR
Unscheduled	2.4	–	–	2.4	–	–
BA	2.06	0.34	14.16%	1.98	0.42	14.5%
MFO	2.11	0.29	12.1%	2.11	0.29	12.1%
WOA	2.23	0.17	7.1%	1.96	0.40	16.6%
HHO	2.23	0.17	7.1%	1.96	0.40	16.6%
AEO	1.61	0.79	**32.9%**	1.65	0.75	**31.25%**

5.5.4. Waiting Time (users comfort)

The users comfort is defined as the waiting time of appliances. There is always a trade-off between either electricity cost minimization and waiting time of appliances or between PAR and electricity cost minimization [137]. Hence, user must always pay an extra cost in terms of appliances waiting-time when preferring to maximize its comfort. The waiting time in unscheduled case is equal to zero, because appliances are being started on based on the user's demand. Figures 5.7 (c) and 5.9 (c) illustrates average waiting time for both price tariffs. From these graphs, it can be seen that there is no significant difference between waiting time of all suggested algorithms. For RTP signal, the lowest waiting-time is 4.78 hours, which is of HHO algorithm and the highest waiting-time is 5.04 hours is achieved by AEO algorithm, in which the difference between the best and worst waiting time is only 15.6 min. For CPP, the highest average-time is 5 hours 16 min by AEO, and the minimum one is 4 hours 47 min obtained by using MFO. Moreover, it is important to note, that the total load scheduled per day is remained fixed before and after scheduling in all of simulation cases.

5.5.5. Case II: With operational time intervals of 12 min

a) Load consumption using RTP

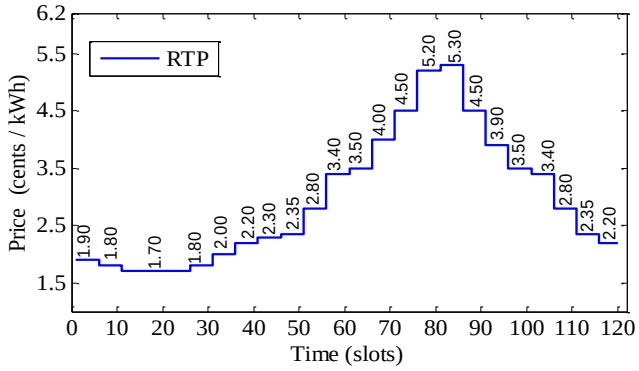

Figure 5.7- - Real time electricity profile [138]

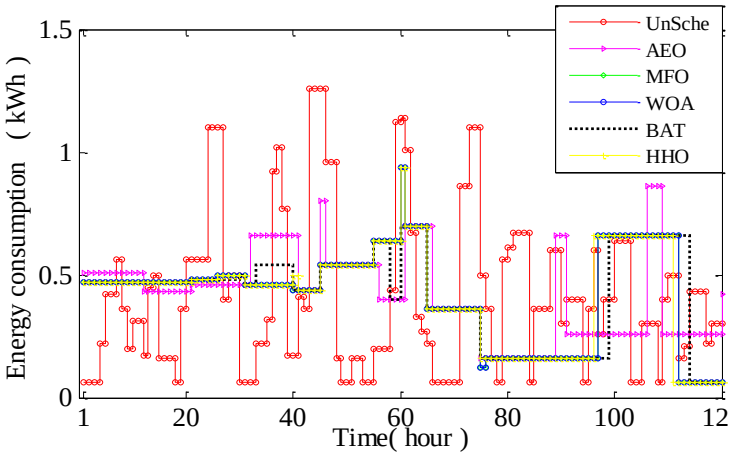

Figure 5.8- Energy consumption profile

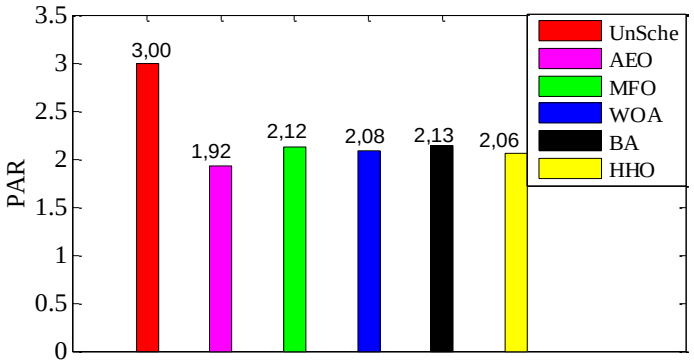

(a)

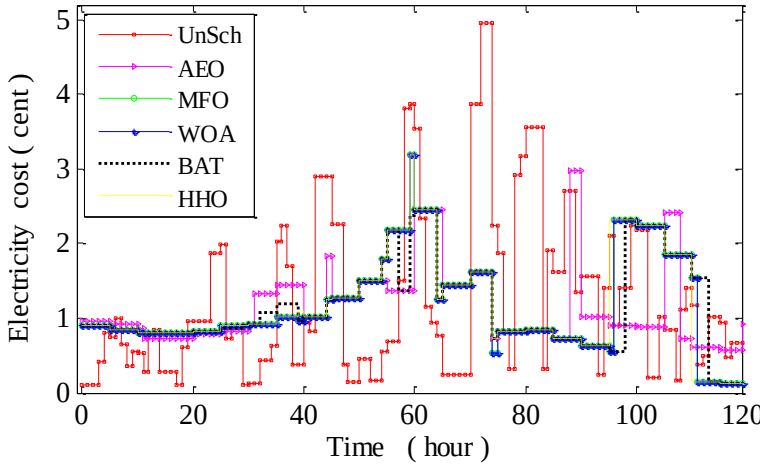

(b)

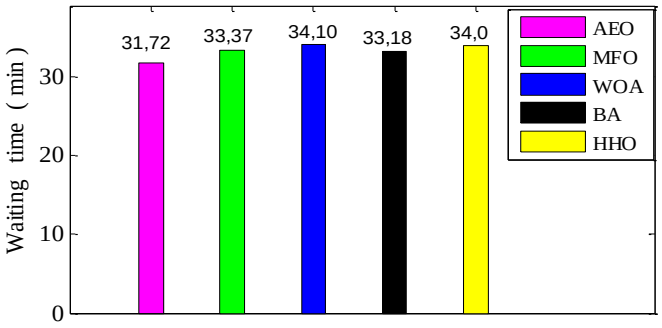

(c)

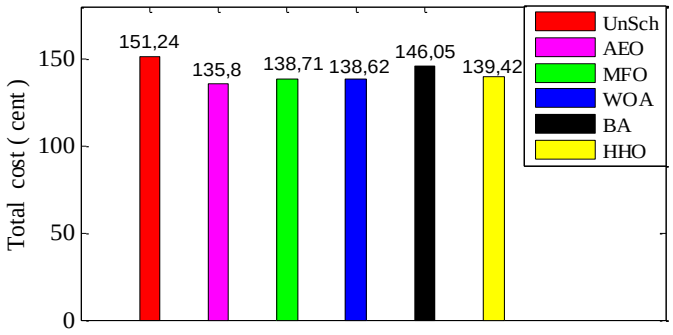

(d)

Figure 5.9 Graphical results using RTP tariff for operational time interval of 12 min: (a) Peak to average ratio; (b) Energy cost profile; (c) Average waiting time of electric appliances; (d) Total cost

Load profile in each time slots of 12 min OTI for RTP tariff is illustrated in Figure 5.8. From this figure, it is clearly that load is shifted to off-peak hours in an effort to attain the objective function of cost minimization. Total electricity cost in unscheduled scenario is 151.24 cents which is reduced to 139.5, 138.7, 138.62, 146, and 135.8 by using HHO, MFO, WOA, BA, and proposed AEO, respectively. So, the proposed AEO algorithm gives maximum reduction in cost which equal to 10.2%, while HHO, MFO, WOA, and BA reduce cost up to 7.87%, 8.28%, 8.34%, and 3.4%, respectively.

The cost paid to the utility company against the consumption aforementioned in Figure 5.8 is given in Figure 5.9 (b). Then, we can see that the curve of electricity price changes according to the daily consumption pattern. Results confirm that the AEO algorithm optimizes better the daily energy use as compared to other pairs by shifting most of the peak load from peak to off-peak periods. Consequently, it is important to point that the proposed control scheme increases the benefit through financial savings, energy savings during the peak demand and posted an optimal schedule for the household appliances.

On the light of our findings, we find that our proposed DSM program based AEO algorithm not only shifts the load from on-peak hours to off-peak hours, but it also examines and guiding the load to that slots having the low-price.

Figure 5.9(a) shows the amount of PAR value for each algorithm. With our proposed AEO technique, the PAR value of the total load is reduced to 36% as compared to unscheduled scenario, whereas, is decreased up to 29.3% for MFO, 29% for BA, 30.6 for WOA and 31.3%

for HHO, respectively. Simulation results show that AEO algorithm well performed than other optimization techniques in reducing PAR value.

Figure 5.9 (c) illustrates average waiting time of all suggested algorithms, respectively. Regarding the total cost paid by end-user, we can see that AEO outperform all other optimization techniques and minimize cost to the lower possible value without compromising user comfort.

In fact, the proposed algorithm significantly outperforms all other suggested optimization techniques both for waiting time of users and for computation of electricity cost. Although, there is a little bit difference into average waiting time between scheduling techniques, but can achieve tangible benefits for protecting users comfort. Comparison of PAR value and waiting time for different scheduling techniques are shown in Table 5.4.

Table 5.4. Comparison of PAR, Cost, and waiting time for different techniques

Optimization Techniques	PAR	Savings percentage in PAR	Cost	Savings percentage in Cost	Waiting time
Unscheduled	3	–	151.24	–	–
BA	2.13	29%	146.05	3.4%	34
MFO	2.12	29.3%	138.71	8.28%	33
WOA	2.08	30.6%	138.62	8.34%	34
HHO	2.06	31.3	139.42	7.87%	34
AEO	1.92	36%	135.8	10.2%	31

5.6. Conclusion

This chapter presented unconventional optimization algorithms for scheduling home−energy−management−system by considering two OTIs and various operational constraints. These approaches are suggested under two pricing schemes RTP and CPP. In addition, two operational time intervals (60 min and 12 min) were considered to evaluate the consumer's demand and behavior of the suggested scheme. The performance of five heuristic algorithms: BA, MFO, WOA, HHO, and novel AEO algorithm were examined to describe the effect of scheduling the appliances on the: electricity-cost, energy-consumption, PAR value, and users-comfort (in terms of waiting-time). Comparison results showed that AEO algorithm can provide both costs and peak demand reduction with acceptable comfort level to consumers.

Simulation results showed that the proposed scheme giving higher reduction in the total

energy cost by about 26% as difference of CPP and RTP for case of 60 min OTI, whereas, in case of 12 min OIT- was reduced up to 10.73%. In terms of PAR reduction, the proposed scheme was also carried out well as compared to WOA, MFO, and BAT algorithms. In general, we can conclude that the proposed AEO algorithm surpass the other optimization techniques in terms of end-users' payments reduction and PAR, however, a trade-off between user comfort and cost was still exists to be addressed.

Chapter 6

CONCLUSION

6.1.1. Summary and Conclusion

This thesis covers some of the optimization problems in modern power system and applications of non-conventional optimization techniques to solve those problems. The first Chapter discusses the importance of meta-heuristic optimization methods and their consistency to solve real and complex problems. Thereafter, main contributions of this thesis are highlighted, followed by outline of the thesis. In the first part of Chapter 2, three nature-inspired optimization algorithms called, Ant lion optimizer and its version multi-objective, artificial ecosystem optimizer and Harris hawks optimization algorithm are presented and adopted for power system optimization problems. Afterwards, an overview on the multi-objective optimization problems is described. Second part dedicated to explain a few constraint handling (CH) methods such as penalty function method (PF) and superiority of feasible solutions (SF), followed by a full definition and importance of OPF and ORPD problems.

The first part of Chapter 3 is focused to study the application of three unconventional optimization approaches to optimal reactive power dispatch problem with various single objectives. Optimization approaches have been successfully applied to find the optimal control variables of the medium-sized and large-scale test systems (IEEE 30-bus, IEEE 118-bus, IEEE 300-bus) as well practical power system DZA 114-bus. The obtained findings proved the efficiency and consistency of suggested optimizer AEO in determining better solutions of ORPD problem vs. existing optimization techniques in the literature. In the second part of Chapter 3, the application of MOALO algorithm to solve large scale multi-objective optimal reactive power dispatch (MOORPD) problem is conducted. The importance of this study overcomes the shortcomes encountered when solving single objective ORPD problem. A critical analysis on the both obtained and reported results was presented, and approved the feasibility of solutions.

The variation in optimal generation cost is studied with the change in reserve cost coefficients and the PDF parameters. The optimization is conducted by using AEO, ALO and NBA algorithms, and the simulation was carried out on the modified IEEE 30-bus test system.

Simulation results prove the capability and superiority of proposed AEO on all optimization techniques for all case studied.

Chapter 5 presents unconventional optimization algorithms for scheduling home−energy−management−system considering two operation interval times (OTIs) and various operational constraints. Two pricing schemes-namely real time price (RTP) and critical peak pricing (CPP) are employed to evaluate the consumer's demand and behavior of the suggested scheme. The optimization of total consumer's energy cost is performed using AEO, HHO, WOA, BA, and MFO algorithms. The graphical results of all implemented algorithms are analyzed and compared. Comparison results showed that AEO algorithm can provide both costs and peak demand reduction with acceptable comfort level to consumers.

The topics of optimization in modern power system are diverse and large. In the future, we plan to carry many more subjects related to the optimization in power systems. Herein, we summarize a brief overview of future works.

6.1.2. Future work

Despite of all efforts made in this marvellous research work to improve modern power system operation, but some short-comes still exists to be addressed. In point of view of future work, some numbers of issues that can be handled are summarized in the following points:

1. We aim to solve multi-objective ORPD problem using meta-heuristics techniques in the cloud computing environments.
2. Besides single and multi-objective ORPD solutions, we propose to extend of integration of renewable energy sources with FACTS device and inclusion of voltage stability of as objective.
3. We propose the integration of storage devices such as batteries (electric vehicles) and pumped hydro in the OPF study considering large-scale power systems. Transient stability analysis of the whole system can also be incorporated for detailed study.
4. Scheduling smart appliances is executed in a single home using some meta-heuristic optimization techniques. As a future work, we propose to extend this study by integration of renewable energy sources with electric vehicles (EVs) as charging/discharging batteries. This variety of production sources in smart micro-grid will facilitate to mitigate energy costs in smart cities. A multi-objective case of home-energy management system (HEMS)

with multiple contradictory objectives will also be studied in the future.

5. The proposed algorithm in this thesis or their improved versions will also be applied to the new formulations of following issues:

- Optimal coordination of directional overcurrent relays;
- Identification and localization of faults in a power transformer winding.

Annexe-

Data of Algerian Electric Grid "MATPOWER format" will be available on any official request from the author.

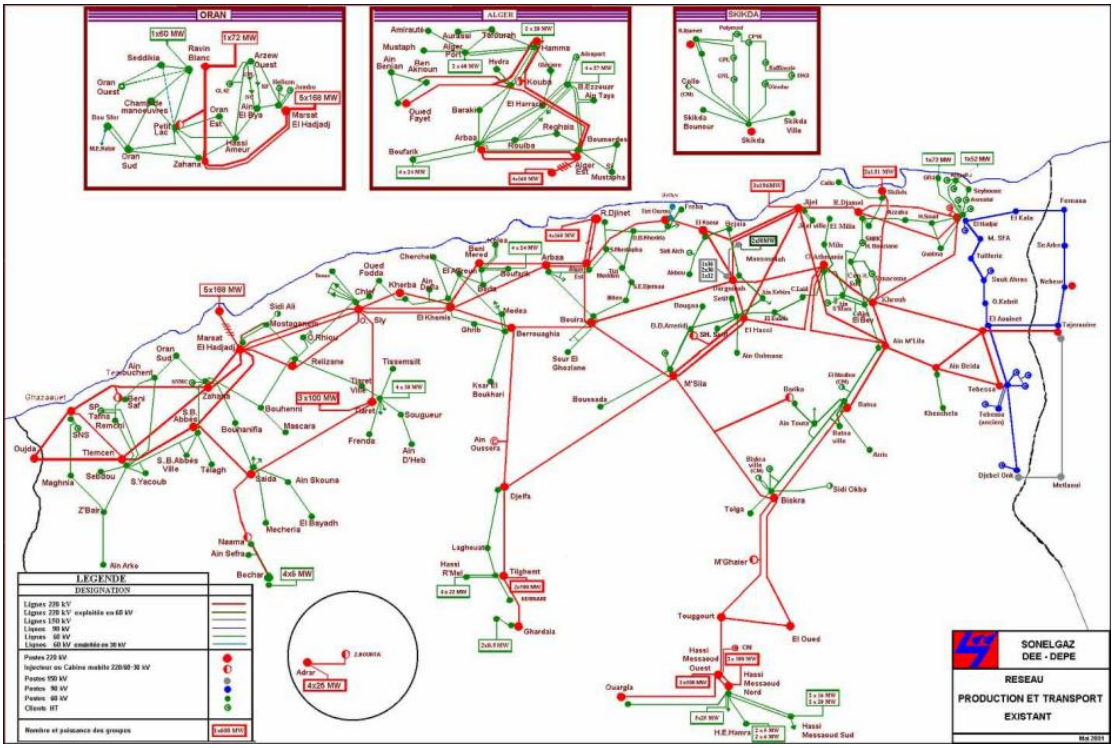

Figure 6.1 Algerian electricity grid Topology- DZA 114-bus

Bibliography

[1] F. Gonzalez-longatt, Advanced Smart Grid Functionalities Based on PowerFactory, UK, 2018. doi:10.1007/978-3-319-50532-9.

[2] G. Guérard, Optimisation de la diffusion de l'énergie dans les Smart Grids, Université de Versailles, 2014.

[3] D. Karaboga, B. Basturk, A powerful and efficient algorithm for numerical function optimization: Artificial bee colony (ABC) algorithm, J. Glob. Optim. 39 (2007) 459–471. doi:10.1007/s10898-007-9149-x.

[4] X. Yang, A New Metaheuristic Bat-Inspired Algorithm, in: Stud. Comput. Intell., Springer Berlin Heidelberg, 2010: pp. 65–74. doi:10.1007/978-3-642-12538-6_6.

[5] X.B. Meng, X.Z. Gao, Y. Liu, H. Zhang, A novel bat algorithm with habitat selection and Doppler effect in echoes for optimization, Expert Syst. Appl. 42 (2015) 6350–6364. doi:10.1016/j.eswa.2015.04.026.

[6] S. Mirjalili, A. Lewis, Advances in Engineering Software The Whale Optimization Algorithm, Adv. Eng. Softw. 95 (2016) 51–67. doi:10.1016/j.advengsoft.2016.01.008.

[7] S. Mirjalili, The ant lion optimizer, Adv. Eng. Softw. 83 (2015) 80–98. doi:10.1016/j.advengsoft.2015.01.010.

[8] S. Mirjalili, Knowledge-Based Systems Moth-flame optimization algorithm : A novel nature-inspired heuristic paradigm, 89 (2015) 228–249. doi:10.1016/j.knosys.2015.07.006.

[9] A.A. Heidari, S. Mirjalili, H. Faris, I. Aljarah, M. Mafarja, H. Chen, Harris Hawks Optimization : Algorithm and Applications, Futur. Gener. Comput. Syst. (2019). doi:10.1016/j.future.2019.02.028.

[10] A. Asghar, S. Mirjalili, H. Faris, I. Aljarah, Harris hawks optimization : Algorithm and applications, Futur. Gener. Comput. Syst. 97 (2019) 849–872. doi:10.1016/j.future.2019.02.028.

[11] W. Zhao, L. Wang, Z. Zhang, Artificial ecosystem-based optimization: a novel nature-inspired meta-heuristic algorithm, Springer London, 2019. doi:10.1007/s00521-019-04452-x.

[12] A.S. Assiri, A.G. Hussien, M. Amin, Ant lion optimization: Variants, hybrids, and applications, IEEE Access. 8 (2020) 77746–77764. doi:10.1109/ACCESS.2020.2990338.

[13] L. Abualigah, M. Shehab, M. Alshinwan, S. Mirjalili, M.A. Elaziz, Ant Lion Optimizer: A Comprehensive Survey of Its Variants and Applications, Arch. Comput. Methods Eng. (2020). doi:10.1007/s11831-020-09420-6.

[14] S. Mouassa, T. Bouktir, A. Salhi, Ant lion optimizer for solving optimal reactive power dispatch problem in power systems, Eng. Sci. Technol. an Int. J. (2017). doi:10.1016/j.jestch.2017.03.006.

[15] S. Mouassa, T. Bouktir, Multi-objective ant lion optimization algorithm to solve large-scale multi-objective optimal reactive power dispatch problem, COMPEL - Int. J. Comput. Math. Electr. Electron. Eng. (2018) COMPEL-05-2018-0208. doi:10.1108/COMPEL-05-2018-0208.

[16] M.. Powell, D., Skolnick, Using genetic algorithms in engineering design opti- mization with non-linear constraints, in: Proc. Fifth Int. Conf. Genet. Algorithms, 1993: pp. 424–431. doi:10.1111/j.1477-9730.1970.tb00984.x.

[17] T.E. Aalberts, Interdisciplinarity on the move: Reading Kratochwil as counter-disciplinarity proper, Millenn. J. Int. Stud. 44 (2016) 242–249. doi:10.1177/0305829815620047.

[18] B. Tessema, G.G. Yen, A self adaptive penalty function based algorithm for constrained optimization, 2006 IEEE Congr. Evol. Comput. CEC 2006. 4 (2006) 246–253.

[19] M.R. AlRashidi, M.E. El-Hawary, Hybrid particle swarm optimization approach for solving the discrete OPF problem considering the valve loading effects, IEEE Trans. Power Syst. 22 (2007) 2030–2038. doi:10.1109/TPWRS.2007.907375.

[20] R. Mallipeddi, P.N. Suganthan, Ensemble of constraint handling techniques, IEEE Trans. Evol. Comput. 14 (2010) 561–579. doi:10.1109/TEVC.2009.2033582.

[21] A.D. Sappa, F. Dornaika, An Edge-Based Approach to Motion Detection Conference, Springer International Publishing, 2019. doi:10.1007/978-3-030-22744-9.

[22] J.A. Joines, C.R. Houck, On the use of non-stationary penalty functions to solve nonlinear constrained optimization problems with GA's, IEEE Conf. Evol. Comput. - Proc. (1994) 579–584. doi:10.1109/icec.1994.349995.

[23] K. Deb, An efficient constraint handling method for genetic algorithms, Comput. Methods Appl. Mech. Eng. 186 (2000) 311–338. doi:10.1016/S0045-7825(99)00389-8.

[24] C.A. Coello Coello, Theoretical and numerical constraint-handling techniques used with evolutionary algorithms: A survey of the state of the art, Comput. Methods Appl. Mech. Eng. 191 (2002) 1245–1287. doi:10.1016/S0045-7825(01)00323-1.

[25] J.A. Momoh, M.E. El-Hawary, R. Adapa, A review of selected optimal power flow literature to 1993 part i: nonlinear and quadratic Programming Approaches, IEEE Trans. Power Syst. 14 (1999) 96–103. doi:10.1109/59.744492.

[26] J.A. Monoh, M.E. Ei-Hawary, R. Adapa, A review of selected optimal power flow literature to 1993 part ii: newton, linear programming and Interior Point Methods, IEEE Trans. Power Syst. 14 (1999) 105–111. doi:10.1109/59.744495.

[27] K.P. Wong, A. Li, M.Y. Law, Development of constrained-genetic-algorithm load-Flow Method, IEE Proc. - Gener. Transm. Distrib. 144 (1997) 91–99. doi:10.1049/ip-gtd:19970847.

[28] J. Yuryevich, Evolutionary programming based optimal power flow algorithm, IEEE Trans. Power Syst. 14 (1999) 1245–1250. doi:10.1109/59.801880.

[29] A.A.A. Mohamed, Y.S. Mohamed, A.A.M. El-Gaafary, A.M. Hemeida, Optimal power flow using moth swarm algorithm, Electr. Power Syst. Res. 142 (2017) 190–206. doi:10.1016/j.epsr.2016.09.025.

[30] W. Bai, I. Eke, K.Y. Lee, An improved artificial bee colony optimization algorithm based on orthogonal learning for optimal power flow problem, Control Eng. Pract. 61 (2017) 163–172. doi:10.1016/j.conengprac.2017.02.010.

[31] A.E. Chaib, H.R.E.H. Bouchekara, R. Mehasni, M.A. Abido, Optimal power flow with emission and non-smooth cost functions using backtracking search optimization algorithm, Int. J. Electr. Power Energy Syst. 81 (2016) 64–77. doi:10.1016/j.ijepes.2016.02.004.

[32] H.R.E.H. Bouchekara, A.E. Chaib, M.A. Abido, R.A. El-Sehiemy, Optimal power flow using an Improved Colliding Bodies Optimization algorithm, Appl. Soft Comput. J. 42 (2016) 119–131. doi:10.1016/j.asoc.2016.01.041.

[33] R. Kouadri, I. Musirin, L. Slimani, T. Bouktir, OPF for large scale power system using ant lion optimization: A case study of the algerian electrical network, IAES Int. J. Artif. Intell. 9 (2020) 252–260. doi:10.11591/ijai.v9.i2.pp252-260.

[34] M. Kaur, N. Narang, An integrated optimization technique for optimal power flow solution, Soft Comput. 24 (2020) 10865–10882. doi:10.1007/s00500-019-04590-3.

[35] W. Warid, H. Hizam, N. Mariun, N.I. Abdul Wahab, A novel quasi-oppositional modified Jaya algorithm for multi-objective optimal power flow solution, Appl. Soft Comput. J. 65 (2018) 360–373. doi:10.1016/j.asoc.2018.01.039.

[36] Warid Warid, Optimal power flow using the AMTPG-Jaya algorithm, Appl. Soft Comput. J. 91 (2020) 106252. doi:10.1016/j.image.2020.115780.

[37] T.T. Nguyen, A high performance social spider optimization algorithm for optimal power flow

solution with single objective optimization, Energy. 171 (2019) 218–240. doi:10.1016/j.energy.2019.01.021.

[38] A.A. El-Fergany, H.M. Hasanien, Salp swarm optimizer to solve optimal power flow comprising voltage stability analysis, Neural Comput. Appl. 32 (2020) 5267–5283. doi:10.1007/s00521-019-04029-8.

[39] R. Dwlrq, H. Dqw, G. Gliihuhqwldo, K. Vhdufk, D. Judylwdwlrqdo, V. Phwkrg, D. Wr, L. Dqg, H. Wkh, V. Txdolw, U. Vhfwlrq, R.I. Wklv, Z. Lv, R. Dv, I. Ri, W.K.H. Srzhu, V.V. Zkloh, P. Wkh, O. Ri, $ssolfdwlrq ri +\eulg 6dos 6zdup 2swlpl]dwlrq 0hwkrg iru 6roylqj 23) 3ureohp, (n.d.).

[40] B. Bentouati, M.S. Javaid, H.R.E.H. Bouchekara, A.A. El-Fergany, Optimizing performance attributes of electric power systems using chaotic salp swarm optimizer, Int. J. Manag. Sci. Eng. Manag. 15 (2020) 165–175. doi:10.1080/17509653.2019.1677197.

[41] M.Z. Islam, N.I.A. Wahab, V. Veerasamy, H. Hizam, N.F. Mailah, J.M. Guerrero, M.N. Mohd Nasir, A Harris Hawks optimization based singleand multi-objective optimal power flow considering environmental emission, Sustain. 12 (2020). doi:10.3390/su12135248.

[42] S. Birogul, Hybrid harris hawk optimization based on differential evolution (HHODE) algorithm for optimal power flow problem, IEEE Access. 7 (2019) 184468–184488. doi:10.1109/ACCESS.2019.2958279.

[43] M. Ghasemi, S. Ghavidel, S. Rahmani, A. Roosta, H. Falah, A novel hybrid algorithm of imperialist competitive algorithm and teaching learning algorithm for optimal power flow problem with non-smooth cost functions, Eng. Appl. Artif. Intell. 29 (2014) 54–69. doi:10.1016/j.engappai.2013.11.003.

[44] P. Jangir, S.A. Parmar, I.N. Trivedi, R.H. Bhesdadiya, A novel hybrid Particle Swarm Optimizer with multi verse optimizer for global numerical optimization and Optimal Reactive Power Dispatch problem, Eng. Sci. Technol. an Int. J. (2016). doi:10.1016/j.jestch.2016.10.007.

[45] H. Pulluri, R. Naresh, V. Sharma, An enhanced self-adaptive differential evolution based solution methodology for multiobjective optimal power flow, Appl. Soft Comput. J. 54 (2017) 229–245. doi:10.1016/j.asoc.2017.01.030.

[46] N. Daryani, M.T. Hagh, S. Teimourzadeh, Adaptive group search optimization algorithm for multi-objective optimal power flow problem, Appl. Soft Comput. J. 38 (2016) 1012–1024. doi:10.1016/j.asoc.2015.10.057.

[47] K. Abaci, V. Yamacli, Differential search algorithm for solving multi-objective optimal power flow problem, Int. J. Electr. Power Energy Syst. 79 (2016) 1–10. doi:10.1016/j.ijepes.2015.12.021.

[48] P.P. Biswas, P.N. Suganthan, R. Mallipeddi, G.A.J. Amaratunga, Optimal power flow solutions using differential evolution algorithm integrated with effective constraint handling techniques, Eng. Appl. Artif. Intell. 68 (2018) 81–100. doi:10.1016/j.engappai.2017.10.019.

[49] E.E. Elattar, Optimal Power Flow of a Power System Incorporating Stochastic Wind Power Based on Modified Moth Swarm Algorithm, IEEE Access. 7 (2019) 89581–89593. doi:10.1109/ACCESS.2019.2927193.

[50] Z. Ullah, S. Wang, J. Radosavljevic, J. Lai, A Solution to the Optimal Power Flow Problem Considering WT and PV Generation, IEEE Access. 7 (2019) 46763–46772. doi:10.1109/ACCESS.2019.2909561.

[51] Y.C. Chang, T.Y. Lee, C.L. Chen, R.M. Jan, Optimal power flow of a wind-thermal generation system, Int. J. Electr. Power Energy Syst. 55 (2014) 312–320. doi:10.1016/j.ijepes.2013.09.028.

[52] C. Mishra, S.P. Singh, J. Rokadia, Optimal power flow in the presence of wind power using modified cuckoo search, IET Gener. Transm. Distrib. 9 (2015) 615–626. doi:10.1049/iet-

gtd.2014.0285.

[53] A.A. Abou El-Ela, A.M. Kinawy, R.A. El-Sehiemy, M.T. Mouwafi, Optimal reactive power dispatch using ant colony optimization algorithm, Electr. Eng. 93 (2011) 103–116. doi:10.1007/s00202-011-0196-4.

[54] T.L. Duong, M.Q. Duong, V.D. Phan, T.T. Nguyen, A. Niccolai, Optimal Reactive Power Flow for Large-Scale Power Systems Using an Effective Metaheuristic Algorithm, J. Electr. Comput. Eng. 2020 (2020). doi:10.1155/2020/6382507.

[55] T.T. Nguyen, D.N. Vo, H. Van Tran, L. Van Dai, Optimal Dispatch of Reactive Power Using Modified Stochastic Fractal Search Algorithm, Complexity. 2019 (2019). doi:10.1155/2019/4670820.

[56] G. Chen, L. Liu, Z. Zhang, S. Huang, Optimal reactive power dispatch by improved GSA-based algorithm with the novel strategies to handle constraints, Appl. Soft Comput. J. 50 (2017) 58–70. doi:10.1016/j.asoc.2016.11.008.

[57] M. Ghasemi, M. Taghizadeh, S. Ghavidel, J. Aghaei, A. Abbasian, Solving optimal reactive power dispatch problem using a novel teaching-learning-based optimization algorithm, Eng. Appl. Artif. Intell. 39 (2015) 100–108. doi:10.1016/j.engappai.2014.12.001.

[58] A.R.J. Ali Asghar Heidari, Rahim Ali Abbaspour, Gaussian bare-bones water cycle algorithm for optimal reactive power dispatch in electrical power systems, Appl. Soft Comput. J. 57 (2017) 657–671. doi:10.1016/j.asoc.2017.04.048.

[59] E. Naderi, H. Narimani, M. Fathi, M.R. Narimani, A Novel Fuzzy Adaptive Configuration of Particle Swarm Optimization to Solve Large-Scale Optimal Reactive Power Dispatch, Appl. Soft Comput. J. (2017). doi:10.1016/j.asoc.2017.01.012.

[60] R. Ng, S. Mei, M. Herwan, Z. Mustaffa, H. Daniyal, Optimal reactive power dispatch solution by loss minimization using moth-flame optimization technique, Appl. Soft Comput. J. 59 (2017) 210–222. doi:10.1016/j.asoc.2017.05.057.

[61] N.H. Khan, Y. Wang, D. Tian, M.A.Z. Raja, R. Jamal, Y. Muhammad, Design of Fractional Particle Swarm Optimization Gravitational Search Algorithm for Optimal Reactive Power Dispatch Problems, IEEE Access. XX (2020) 1–1. doi:10.1109/access.2020.3014211.

[62] D. Gutiérrez, J.M. López, W.M. Villa, Metaheuristic Techniques Applied to the Optimal Reactive Power Dispatch: A Review, IEEE Lat. Am. Trans. 14 (2016) 2253–2263. doi:10.1109/TLA.2016.7530421.

[63] S. Jeyadevi, S. Baskar, C.K. Babulal, M.W. Iruthayarajan, Electrical Power and Energy Systems Solving multiobjective optimal reactive power dispatch using modified NSGA-II, Int. J. Electr. Power Energy Syst. 33 (2011) 219–228. doi:10.1016/j.ijepes.2010.08.017.

[64] S.H. Chen, Gonggui, Lilan Liu, Yanyan Guo, Multi-objective enhanced PSO algorithm for optimizing power losses and voltage deviation in power systems, Int. J. Comput. Math. Electr. Electron. Eng. 35 (2016) 350–372. doi:10.1108/COMPEL-02-2015-0030.

[65] A. Saraswat, A. Saini, Multi-objective optimal reactive power dispatch considering voltage stability in power systems using HFMOEA, Eng. Appl. Artif. Intell. 26 (2013) 390–404. doi:10.1016/j.engappai.2012.06.008.

[66] Y. Zeng, Y. Sun, Solving Multiobjective Optimal Reactive Power Dispatch Using Improved Multiobjective Particle Swarm Optimization, in: Control Decis. Conf. (2014 CCDC), 26th Chinese, IEEE, Changsha, China, 2014: pp. 1010–1015. doi:10.1109/CCDC.2014.6852312.

[67] G. Chen, L. Liu, P. Song, Y. Du, Chaotic improved PSO-based multi-objective optimization for minimization of power losses and L index in power systems, Energy Convers. Manag. 86 (2014) 548–560. doi:10.1016/j.enconman.2014.06.003.

[68] A. Ghasemi, K. Valipour, A. Tohidi, Multi objective optimal reactive power dispatch using a new multi objective strategy, Int. J. Electr. Power Energy Syst. 57 (2014) 318–334. doi:10.1016/j.ijepes.2013.11.049.

[69] R. Liang, J. Wang, Y. Chen, W. Tseng, An enhanced firefly algorithm to multi-objective optimal active / reactive power dispatch with uncertainties consideration, Int. J. Electr. POWER ENERGY Syst. 64 (2015) 1088–1097. doi:10.1016/j.ijepes.2014.09.008.

[70] M.S. Saddique, A.R. Bhatti, S.S. Haroon, M.K. Sattar, S. Amin, I.A. Sajjad, S.S. ul Haq, A.B. Awan, N. Rasheed, Solution to optimal reactive power dispatch in transmission system using meta-heuristic techniques—Status and technological review, Electr. Power Syst. Res. 178 (2020) 106031. doi:10.1016/j.epsr.2019.106031.

[71] A.A.A. El Ela, M.A. Abido, S.R. Spea, Differential evolution algorithm for optimal reactive power dispatch, Electr. Power Syst. Res. 81 (2011) 458–464. doi:10.1016/j.epsr.2010.10.005.

[72] P. Kessel, H. Glavitsch, Estimating the voltage stability of a power system, IEEE Trans. Power Deliv. 1 (1986) 346–354. doi:10.1109/TPWRD.1986.4308013.

[73] M.H. Sulaiman, Z. Mustaffa, M.R. Mohamed, O. Aliman, Using the gray wolf optimizer for solving optimal reactive power dispatch problem, Appl. Soft Comput. J. 32 (2015) 286–292. doi:10.1016/j.asoc.2015.03.041.

[74] Y. Amrane, M. Boudour, M. Belazzoug, A new Optimal reactive power planning based on Differential Search Algorithm, Int. J. Electr. Power Energy Syst. 64 (2015) 551–561. doi:10.1016/j.ijepes.2014.07.060.

[75] A.P. Mazzini, S. Member, E.N. Asada, Solving Control-Constrained Reactive Power Dispatch with Discrete Variables, (2015).

[76] R.D. Zimmerman, C.E. Murillo Sánchez, R.J. Thomas, MATPOWER: Steady-State Operations, Planning, and Analysis Tools for Power Systems Research and Education, Power Syst. IEEE Trans. 26 (2011) 12–19. doi:10.1109/TPWRS.2010.2051168.

[77] A. Rajan, T. Malakar, Optimal reactive power dispatch using hybrid Nelder-Mead simplex based firefly algorithm, Int. J. Electr. Power Energy Syst. 66 (2015) 9–24. doi:10.1016/j.ijepes.2014.10.041.

[78] K.Y. Lee, Y.M. Park, J.L. Ortiz, A United Approach to Optimal Real and Reactive Power Dispatch, IEEE Power Eng. Rev. PER-5 (1985) 42–43. doi:10.1109/MPER.1985.5526580.

[79] S. Duman, Y. Sönmez, U. Güvenç, N. Yörükeren, Optimal reactive power dispatch using a gravitational search algorithm, IET Gener. Transm. Distrib. 6 (2012) 563. doi:10.1049/iet-gtd.2011.0681.

[80] S. Mouassa, T. Bouktir, A. Salhi, Ant lion optimizer for solving optimal reactive power dispatch problem in power systems, Eng. Sci. Technol. an Int. J. 20 (2017). doi:10.1016/j.jestch.2017.03.006.

[81] B. Mandal, P.K. Roy, Optimal reactive power dispatch using quasi-oppositional teaching learning based optimization, Int. J. Electr. Power Energy Syst. 53 (2013) 123–134. doi:10.1016/j.ijepes.2013.04.011.

[82] O.B. Optimization, A. Bhattacharya, Solution of Optimal Reactive Power Flow using, 4 (2010) 26–34.

[83] B. Shaw, V. Mukherjee, S.P. Ghoshal, Solution of reactive power dispatch of power systems by an opposition-based gravitational search algorithm, Int. J. Electr. Power Energy Syst. 55 (2014) 29–40. doi:10.1016/j.ijepes.2013.08.010.

[84] J. Polprasert, W. Ongsakul, V.N. Dieu, Optimal Reactive Power Dispatch Using Improved Pseudo-gradient Search Particle Swarm Optimization, Electr. Power Components Syst. 44 (2016) 518–532. doi:10.1080/15325008.2015.1112449.

[85] E. Yalçın, E. Çam, M.C. Taplamacıoğlu, A new chaos and global competitive ranking ‐ based symbiotic organisms search algorithm for solving reactive power dispatch problem with discrete and continuous control variable, Electr. Eng. 102 (2020) 573–590. doi:10.1007/s00202-019-00895-6.

[86] C. Coffrin, D. Gordon, P. Scott, NESTA, The NICTA Energy System Test Case Archive, ArXiv1411.0359 [Cs]. (2014) 1–26. http://arxiv.org/abs/1411.0359%5Cnhttp://www.arxiv.org/pdf/1411.0359.pdf.

[87] R. Pinto, Stochastic Location of FACTS Devices in Electric Power Transmission Networks, (2013) 86.

[88] A. Rajan, K. Jeevan, T. Malakar, Weighted Elitism Based Ant Lion Optimizer to Solve Optimum VAr Planning Problem, Elsevier B.V., 2017. doi:10.1016/j.asoc.2017.02.010.

[89] K. Deb, Multi-Objective Optimization Using Evolutionary Algorithms : An Introduction, (2011) 1–24.

[90] K. Deb, D.K. Saxena, On Finding Pareto-Optimal Solutions Through Dimensionality Reduction for Certain Large-Dimensional Multi-Objective Optimization Problems EMO for Many Objectives, (n.d.).

[91] S. Dehuri, A.K. Jagadev, M. Panda, T. Advances, Multi-objective Swarm Intelligence: Theoretical Advances and Applications, 1st–2015th ed., Springer-Verlag Berlin Heidelberg, Odisha, India, 2015. doi:10.1007/978-3-662-46309-3.

[92] Y.T. Sakawa M, Yano H, An interactive fuzzy satisficing method for multiobjective linear-programming problems and its application, IEEE Trans Syst, Man Cybern. 4 (1987) 654–661.

[93] H. Singh, L. Srivastava, Recurrent multi-objective differential evolution approach for reactive power management, IET Gener. Transm. Distrib. 10 (2015) 1–13. doi:10.1049/iet-gtd.2015.0648.

[94] J.G. Vlachogiannis, K.Y. Lee, Reactive Power Control based on Particle Swarm Multi-Objective Optimization, Proc. 13th Int. Conf. on, Intell. Syst. Appl. to Power Syst. (2005) 494–498. doi:10.1109/ISAP.2005.1599313.

[95] P.P. Biswas, P.N. Suganthan, G.A.J. Amaratunga, Optimal power flow solutions incorporating stochastic wind and solar power, Energy Convers. Manag. 148 (2017) 1194–1207. doi:10.1016/j.enconman.2017.06.071.

[96] A. Santos, G.R.M. da Costa, Optimal-power-flow solution by Newton's method applied to an augmented Lagrangian function, IEE Proc. Gener. Transm. Distrib. 142 (1995) 33–36. doi:10.1049/ip-gtd:19951586.

[97] M. Bjelogrlic, M.S. Calovic, P. Ristanovic, B.S. Babic, Application of Newton's optimal power flow in voltage/reactive power control, IEEE Trans. Power Syst. 5 (1990) 1447–1454. doi:10.1109/59.99399.

[98] G.X. Luo, A. Semlyen, Hydrothermal optimal power flow based on a combined linear and nonlinear programming methodology, IEEE Trans. Power Syst. 4 (1989) 530–537. doi:10.1109/59.193826.

[99] J.A. Momoh, J.Z. Zhu, Improved interior point method for off problems, IEEE Trans. Power Syst. 14 (1999) 1114–1120. doi:10.1109/59.780938.

[100] V.H. Hinojosa, R. Araya, Modeling a mixed-integer-binary small-population evolutionary particle swarm algorithm for solving the optimal power flow problem in electric power systems, Appl. Soft Comput. 13 (2013) 3839–3852. doi:10.1016/j.asoc.2013.05.005.

[101] R.P. Singh, V. Mukherjee, S.P. Ghoshal, Particle swarm optimization with an aging leader and challengers algorithm for the solution of optimal power flow problem, Appl. Soft Comput. J. 40 (2016) 161–177. doi:10.1016/j.asoc.2015.11.027.

[102] N. Amjady, H. Fatemi, H. Zareipour, Solution of optimal power flow subject to security constraints by a new improved bacterial foraging method, IEEE Trans. Power Syst. 27 (2012) 1311–1323. doi:10.1109/TPWRS.2011.2175455.

[103] H.R.E.H. Bouchekara, M.A. Abido, M. Boucherma, Optimal power flow using Teaching-Learning-Based Optimization technique, Electr. Power Syst. Res. 114 (2014) 49–59.

doi:10.1016/j.epsr.2014.03.032.

[104] E.E. Elattar, S.K. ElSayed, Modified JAYA algorithm for optimal power flow incorporating renewable energy sources considering the cost, emission, power loss and voltage profile improvement, Energy. 178 (2019) 598–609. doi:10.1016/j.energy.2019.04.159.

[105] S. Engelhardt, I. Erlich, C. Feltes, J. Kretschmann, F. Shewarega, Reactive power capability of wind turbines based on doubly fed induction generators, IEEE Trans. Energy Convers. 26 (2011) 364–372. doi:10.1109/TEC.2010.2081365.

[106] R. Albarracin, M. Alonso, Photovoltaic reactive power limits, 12th Int. Conf. Environ. Electr. Eng. EEEIC 2013. (2013) 13–18. doi:10.1109/EEEIC.2013.6549630.

[107] I.U. Khan, N. Javaid, K.A.A. Gamage, C. James Taylor, S. Baig, X. Ma, Heuristic Algorithm Based Optimal Power Flow Model Incorporating Stochastic Renewable Energy Sources, IEEE Access. 8 (2020) 148622–148643. doi:10.1109/ACCESS.2020.3015473.

[108] A. Ramesh Kumar, L. Premalatha, Optimal power flow for a deregulated power system using adaptive real coded biogeography-based optimization, Int. J. Electr. Power Energy Syst. 73 (2015) 393–399. doi:10.1016/j.ijepes.2015.05.011.

[109] H.R.E.H. Bouchekara, A.E. Chaib, M.A. Abido, Multiobjective optimal power flow using a fuzzy based grenade explosion method, Energy Syst. 7 (2016) 699–721. doi:10.1007/s12667-016-0206-8.

[110] R.A. El-Sehiemy, A.M. Shaheen, S.M. Farrag, Solving multi-objective optimal power flow problem via forced initialised differential evolution algorithm, IET Gener. Transm. Distrib. 10 (2016) 1634–1647. doi:10.1049/iet-gtd.2015.0892.

[111] H. Pulluri, R. Naresh, V. Sharma, A solution network based on stud krill herd algorithm for optimal power flow problems, Soft Comput. 22 (2018) 159–176. doi:10.1007/s00500-016-2319-3.

[112] S. Li, W. Gong, L. Wang, X. Yan, C. Hu, Optimal power flow by means of improved adaptive differential evolution, Energy. 198 (2020). doi:10.1016/j.energy.2020.117314.

[113] S.A. Asfaw, Takuro Sato Daniel M. Kammen, Bin Duan, Martin Macuha, Zhenyu Zhou, Jun Wu, Muhammad Tariq, Smart Grid Standards: Specifications, Requirements, and Technologies, First edit, John Wiley & Sons Singapore Pte. Ltd, Chennai, India, 2015. doi:10.1002/9781118653722.

[114] H. Gul, A. Arif, S. Fareed, M. Anwar, A. Naeem, N. Javaid, Classification and Regression Based Methods for Short Term Load and Price Forecasting: A Survey, in: • L.B.• Y.O., F. Amato (Eds.), Adv. Internet, Data Web Technol. 8th Int. Conf. Emerg. Internet, Data Web Technol., Springer Switzerland, Barcelona, Spain, 2020: pp. 416–426. doi:10.1007/978-3-030-39746-3_43.

[115] B.A. Vos, C.T. Officer, Effective Business Models for Demand Response under the Smart Grid Paradigm By Arthur Vos, Chief Technology Officer and VP Comverge, (n.d.) 4244.

[116] Z. Jin, C. Kang, L. Kai, Demand Side Management in China, in: IEEE PES Gen. Meet., IEEE, Providence, RI, USA, 2010: pp. 4–7. doi:10.1109/PES.2010.5589964.

[117] L. Cavalcante, S. Alexandre, R. Aoki, T.S.P. Fernandes, G.L. Torres, Customer targeting optimization system for price - based demand response programs, Int Trans Electr Energ Syst. (2018) 1–14. doi:10.1002/etep.2709.

[118] Z. Wu, H. Tazvinga, X. Xia, Demand side management of photovoltaic-battery hybrid system, Appl. Energy. 148 (2015) 294–304. doi:10.1016/j.apenergy.2015.03.109.

[119] A. Khalid, N. Javaid, A. Mateen, Demand Side Management using Hybrid Bacterial Foraging and Genetic Algorithm Optimization Techniques, in: 10th Int. Conf. Complex, Intelligent, Softw. Intensive Syst. Demand, IEEE, Fukuoka, Japan, 2016: pp. 494–502. doi:10.1109/CISIS.2016.128.

[120] Z. Bradac, V. Kaczmarczyk, P. Fiedler, C. Republic, Optimal Scheduling of Domestic Appliances via MILP, Energies. (2015) 217–232. doi:10.3390/en8010217.

[121] N.J.; N.A.K.; S.R. Mahmood, Anzar, An Optimized Approach for Home Appliances Scheduling in Smart Grid, 19th Int. Multi-Topic Conf. (2016) 1–5. doi:10.1109/INMIC.2016.7840158.

[122] A.M. Elsayed, M.M. Hegab, S.M. Farrag, Smart residential load management technique for distribution systems' performance enhancement and consumers' satisfaction achievement, Int. Trans. Electr. Energy Syst. 29 (2019) 1–23. doi:10.1002/etep.2795.

[123] C.B.D. Rekha, V. Vijayakumar, Genetic Algorithm Based Demand Side Management for Smart Grid, Wirel. Pers. Commun. 93 (2017) 481–502. doi:10.1007/s11277-017-3959-z.

[124] B.K. Sethi, D. Mukherjee, D. Singh, R.K. Misra, S.R. Mohanty, Smart home energy management system under false data injection attack, Int. Trans. Electr. Energy Syst. (2020) 1–20. doi:10.1002/2050-7038.12411.

[125] I. Ullah, N. Javaid, Z.A. Khan, An Incentive-based Optimal Energy Consumption Scheduling Algorithm for Residential Users, Procedia Comput. Sci. 52 (2015) 851–857. doi:10.1016/j.procs.2015.05.142.

[126] C. Recep, I.H. Altas, Scheduling of Domestic Shiftable Loads via Cuckoo Search Optimization Algorithm, in: 4th Int. Istanbul Smart Grid Congr. Fair, IEEE, Istanbul, Turkey, 2016: pp. 16–19. doi:10.1109/SGCF.2016.7492435.

[127] Y. Chen, R.P. Liu, C. Wang, M. De Groot, Z. Zeng, Consumer Operational Comfort Level Based Power Demand Management in the Smart Grid, in: 3rd IEEE PES Innov. Smart Grid Technol. Eur. (ISGT Eur. Berlin, IEEE, Berlin, Germany, 2012: pp. 1–6. doi:10.1109/ISGTEurope.2012.6465829.

[128] Z. Faiz, T. Bilal, M. Awais, S. Gull, Demand Side Management Using Chicken Swarm Optimization, in: Int. Conf. Intell. Netw. Collab. Syst., Springer International Publishing AG 2018, Toronto, Canada, 2018: pp. 155–165. doi:10.1007/978-3-319-65636-6.

[129] S.M. Shuja, N. Javaid, S. Khan, Z.A. Khan, Efficient Scheduling of Smart Home Appliances for Energy Management by Cost and PAR Optimization Algorithm in Smart Grid, in: Work. Int. Conf. Adv. Inf. Netw. Appl., 2019: pp. 398–411. https://link.springer.com/chapter/10.1007%2F978-3-030-15035-8_37.

[130] E. Shirazi, S. Jadid, Optimal Residential Appliance Scheduling Under Dynamic Pricing Scheme via HEMDAS, Energy Build. 93 (2015) 40–49. doi:10.1016/j.enbuild.2015.01.061.

[131] A. Khalid, Z.A. Khan, N. Javaid, Game Theory based Electric Price Tariff and Salp Swarm Algorithm for Demand Side Management, in: Fifth HCT Inf. Technol. Trends, IEEE, Dubai, United Arab Emirates, United Arab Emirates, 2019: pp. 1–5. doi:10.1109/CTIT.2018.8649489.

[132] J. Abushnaf, A. Rassau, An efficient scheme for residential load scheduling integrated with demand side programs and small - scale distributed renewable energy generation and storage, Int Trans Electr Energ Syst. (2018) 1–16. doi:10.1002/etep.2720.

[133] O. Samuel, S. Javaid, N. Javaid, S.H. Ahmed, M.K. Afzal, F. Ishmanov, An efficient power scheduling in smart homes using jaya based optimization with time-of-use and critical peak pricing schemes, Energies. 11 (2018) 1–27. doi:10.3390/en11113155.

[134] S.M. Shuja, N. Javaid, U. Qasim, A.A. Butt, Towards Efficient Scheduling of Smart Appliances for Energy Management by Candidate Solution Updation Algorithm in Smart Grid, in: Int. Conf. Adv. Inf. Netw. Appl., Springer Berlin Heidelberg, 2019: pp. 67–81. https://link.springer.com/chapter/10.1007/978-3-030-15032-7_6.

[135] M. Naz, Z. Iqbal, N. Javaid, Z.A. Khan, W. Abdul, A. Almogren, A. Alamri, Efficient power scheduling in smart homes using hybrid grey Wolf differential evolution optimization technique with real time and critical peak pricing schemes, Energies. 11 (2018) 1–25. doi:10.3390/en11020384.

[136] M. Hashmi, S. Hänninen, K. Mäki, Survey of Smart Grid Concepts , Architectures , and Technological Demonstrations Worldwide, in: IEEE PES Conf. Innov. Smart Grid Technol. Lat. Am. (ISGT LA), IEEE, Medellin, Colombia, 2011: pp. 1–7. doi:10.1109/ISGT-LA.2011.6083192.

[137] Z.A. Khan, A. Khalid, N. Javaid, A. Haseeb, T. Saba, M. Shafiq, Exploiting Nature-Inspired-Based Artificial Intelligence Techniques for Coordinated Day-Ahead Scheduling to Efficiently Manage Energy in Smart Grid, IEEE Access. 7 (2019) 140102–140125. doi:10.1109/ACCESS.2019.2942813.

[138] Z. Zhao, W.C. Lee, Y. Shin, K. Bin Song, An optimal power scheduling method for demand response in home energy management system, IEEE Trans. Smart Grid. 4

ملخص:

نظرًا للتطور السريع لنظام الطاقة الكهربائية في جميع أنحاء العالم استجابة للتطورات التقنية والاقتصادية والبيئية ، غالبًا ما تعمل أنظمة الطاقة الحديثة بالقرب من حدودها القصوى ، مما يؤدي إلى مخاطر عدم استقرار الجهد في الشبكة الكهربائية. من ناحية أخرى ، قد يؤدي التغلغل المفرط لمصادر الطاقة المتجددة في الشبكات الكهربائية إلى العديد من المشكلات وانتهاكات الحد التشغيلي ، مثل زيادة وتقل الجهد ، وفقدان الطاقة النشطة ، والحمل الزائد على خطوط النقل ، وتعطل محطات الطاقة ، ومخاطر عدم استقرار الجهد ، وتضرر راحة المستخدمين. تحدث هذه المشكلات عندما يتجاوز النظام الحد الأقصى للقدرة التشغيلية. في هذه الأطروحة، أولاً ، تم تطوير وتنفيذ العديد من تقنيات التحسين الغير تقليدية للتعامل مع مختلف مشاكل نظام الطاقة، مثل: مشكلة إرسال الطاقة التفاعلية المثلى الفردية منها ومتعددة الأهداف. وبما أن خصائص مشكلة إرسال الطاقة التفاعلية في الطبيعة هي غير خطية وغير محدبة وتتكون أيضًا من مزيج من المتغيرات المنفصلة والمستمرة، فقد قمنا بتطوير بعض الخوارزميات للتعامل مع هده المشكلة بمتغيرات مختلطة في الشبكات الكهربائية واسعة النطاق. بعد ذلك، من أجل ضمان ملائمة الأساليب المقترحة لأنظمة الطاقة الحديثة، قمنا بدراسة مشكلة التدفق الأمثل للطاقة العشوائية مع احتياطيات غير مؤكدة من مصادر الطاقة المتجددة وتطبيقها على عدة سيناريوهات مختلفة. وأخيرًا، تم اقتراح بعض تقنيات التحسين القائمة على إدارة جانب الطلب من أجل تقييم نظام إدارة الطاقة المنزلية. الهدف الرئيسي من هذه الدراسة هو ضبط ذروة الطلب وتقديم إجمالي الطاقة المطلوبة بأقل تكلفة وبجودة عالية، والأهم من ذلك، من أجل توعية المستهلكين بمساهماتهم الفعالة والضرورية في مساعدة مشغل الشبكة للتحكم في التوزيع الامثل للطاقة خاصة أثناء حالات الطوارئ.

كلمات مفتاحية : التدفق الأمثل للطاقة، التخطيط الأمثل للطاقة التفاعلية، تقنيات التحسين الغير تقليدية، تقنيات معالجة القيود، الطاقات المتجددة، تقنية إدارة جانب الطلب

Abstract:

Due to the rapidly developing of electric power system across the world in response to technical, economic and environmental developments, modern power systems often operate proximate to their limits maximal, engendering voltage instability risks in electric grid. On the other hand, excessive penetration of renewable energy sources into electrical grids may lead to many problems and operational limit violations, such as over and under voltages, active power losses and overloading of transmission lines, power plants failure, voltage instability risks and compromising users comfort. These problems happen when the system exceeds maximal operational capability (MOC) limit. In this thesis, firstly, various meta-heuristic optimization techniques have been developed and implemented to deal with different power system problems, such as single and multi-objective optimal reactive power dispatch problem. As the characteristics of ORPD problem in nature are non-linear and non-convex and also are consisting of mix of discrete and continuous variables, some algorithms are developed to deal with discrete ORPD problem in large-scale electric grids. Afterwards, in order to ensure the suitability of the proposed approaches for modern power systems, stochastic optimal power flow (OPF) problem with uncertain reserves from renewable energy sources is studied under different scenarios. Finally, a demand side management (DSM) based meta-heuristic techniques is proposed for home energy management system. The main objective behind this study is to adjust the peak demand and offering the total energy required at minimum cost with high quality. More precisely, in order to make consumers aware of their effective and essential contributions to helping the operator system during emergency cases (requests during peak hours).

Keywords: Optimal reactive power dispatch, Optimal power flow, unconventional optimization techniques, renewable energy sources, constraint handling, Demand side management.

Résumé:

En raison du développement rapide des réseaux électriques à travers le monde en réponse aux développements techniques, économiques et environnementaux, les réseaux électriques modernes fonctionnent souvent à proximité de leurs limites maximales, engendrant des risques d'instabilité de tension dans le réseau électrique. D'autre part, une pénétration excessive des sources d'énergie renouvelables dans les réseaux électriques peut entraîner de nombreux problèmes et violations des limites opérationnelles, telles que les surtensions et sous-tensions, les pertes de puissance active et la surcharge des lignes de transmission, les pannes de centrales électriques, les risques d'instabilité de tension et la compromission du confort des utilisateurs. Ces problèmes surviennent lorsque le système dépasse la limite de capacité opérationnelle maximale (COM). Dans cette thèse, tout d'abord, diverses techniques d'optimisation méta-heuristique ont été développées et mises en œuvre pour traiter différents problèmes de système d'alimentation, tels que le problème de répartition optimale de la puissance réactive à un ou plusieurs objectifs. Comme les caractéristiques du problème ORPD dans la nature sont non linéaires et non convexes et sont également constituées d'un mélange de variables discrètes et continues, certains algorithmes sont développés pour traiter le problème ORPD discret dans les réseaux électriques à grande échelle. Par la suite, afin de garantir l'adéquation des approches proposées pour les systèmes électriques modernes, le problème du flux de puissance optimal stochastique (OPF) avec des réserves incertaines provenant de sources d'énergie renouvelables est étudié dans différents scénarios. Enfin, une technique méta-heuristique basée sur la gestion de la demande (DSM) est proposée pour le système de gestion de l'énergie domestique. L'objectif principal de cette étude est d'ajuster la demande de pointe et d'offrir l'énergie totale requise à un coût minimum avec une qualité élevée. Plus précisément, afin de sensibiliser les consommateurs de leur contribution efficace et indispensable à l'aide au gestionnaire de réseau en cas d'urgence (les demandes durant les heures de point).

Mots clés : Optimisation de l'écoulement de puissance; répartition optimal de la puissance réactive; les méthodes d'optimisation non-conventionnel; technique de traitement des contraintes; sources d'énergie renouvelable; la gestion de la demande.